ANL-6400

ANL-6400

Argonne National Laboratory

AN EXPERIMENTAL INVESTIGATION OF HIGH-FLUX FREE CONVECTION HEAT TRANSFER TO WATER UP TO NEAR-CRITICAL CONDITIONS

by

Vernon Emerson Holt

LEGAL NOTICE

This report was prepared as an account of Government sponsored work. Neither the United States, nor the Commission, nor any person acting on behalf of the Commission:

A. Makes any warranty or representation, expressed or implied, with respect to the accuracy, completeness, or usefulness of the information contained in this report, or that the use of any information, apparatus, method, or process disclosed in this report may not infringe privately owned rights; or

B. Assumes any liabilities with respect to the use of, or for damages resulting from the use of any information, apparatus, method, or process disclosed in this report.

As used in the above, "person acting on behalf of the Commission" includes any employee or contractor of the Commission, or employee of such contractor, to the extent that such employee or contractor of the Commission, or employee of such contractor prepares, disseminates, or provides access to, any information pursuant to his employment or contract with the Commission, or his employment with such contractor.

ANL-6400
Engineering and Equipment
(TID-4500, 16th Ed.,
Amended)
AEC Research and
Development Report

ARGONNE NATIONAL LABORATORY
9700 South Cass Avenue
Argonne, Illinois

AN EXPERIMENTAL INVESTIGATION OF HIGH-FLUX FREE CONVECTION HEAT TRANSFER TO WATER UP TO NEAR-CRITICAL CONDITIONS

by

Vernon Emerson Holt

August 1961

Operated by The University of Chicago
under
Contract W-31-109-eng-38

ACKNOWLEDGEMENT

This report was used as a thesis submitted to the faculty of Purdue University. The guidance and assistance of Professor R. J. Grosh is greatly appreciated.

The financial assistance of The Visking Company and Argonne National Laboratory has made this investigation possible.

The contributions of my colleagues and family are especially appreciated.

TABLE OF CONTENTS

LIST OF FIGURES

LIST OF FIGURES

AN EXPERIMENTAL INVESTIGATION OF HIGH-FLUX FREE CONVECTION HEAT TRANSFER TO WATER UP TO NEAR-CRITICAL CONDITIONS

by

Vernon Emerson Holt

ABSTRACT

The primary purpose of this investigation was to increase the basic knowledge of nucleate and film boiling heat transfer to fluids up to their critical pressures.

An extensive literature survey of the subject indicated a scarcity of consistent data and an absence of proven methods for analysis. This situation led to the design and construction of experimental apparatus suitable for measuring rates of free convection heat transfer and associated temperature differences for fluid conditions up to 4000 psi and 800 F, with provision for visual observation.

The apparatus incorporated a stainless steel system for containing the fluid. Ten-mil-diameter cylindrical and $\frac{1}{8}$-in.-high vertical-plate platinum test sections were placed in the fluid inside a pressure vessel, 5 in. in inside diameter and 21 in. high. The pressure and temperature of the fluid environment were controlled by constant-volume heating of the fluid in the pressure vessel with the aid of seven zones of radiant guard heaters located between the external wall of the pressure vessel and the insulation. Each of these zones was controlled by a differential-thermocouple-sensed circuit that automatically kept the pressure vessel at a prescribed uniform temperature.

Fluid pressure was measured with a dead-weight tester and a 0-4000-psi Heise gauge. Fluid temperature was measured with a calibrated resistance thermometer and Mueller bridge, purchased specifically for that purpose. The heat flux in the test section was obtained from electrical measurements of the direct-current power supplied for Joule heating. The temperature of the test section was measured by means of a resistance thermometer.

The system was outgassed and filled under a vacuum with water that was deionized, degassed, and deionized again. The quality of the water was maintained during an experiment with the aid of a thermal-siphon deionizing loop which was connected to the system.

The results were tabulated and plotted in terms of heat flux and temperature difference between the heated surface and the bulk fluid (water). Nucleate boiling results are included for pressures of 14.7, 1300, 2400, 2800, 2900, 3000, 3100, 3150, and 3180 psia. Film boiling results are included for pressures of 2400, 2800, 2900, 3000, 3100, 3150, and 3180 psia. Results are also included for free convection to water at pressures of 3200, 3250, 3300, 3400, 3625, and 3925 psia.

The nucleate and film boiling results were correlated and compared with other data. At a particular nucleate boiling heat flux, the heat transfer coefficient was observed to increase with pressure up to about 2800 psia. The characteristics associated with transition film boiling vanished above the critical pressure according to the plotted results and the experimental behavior. In fact, for pressures above the critical, a trend toward the characteristics associated with single-phase free convection to a constant-property fluid was observed.

A large convective flow of the fluid and large density gradients accompanied by considerable optical distortion were observed within ±400 psi of the critical pressure. Near the critical pressure, sheets of fluid appeared to be passing the field of observation.

INTRODUCTION

Every macroscopic physical process involves a transfer of energy, and transfer of heat is one of the most important and frequently encountered processes. Heat may be transferred by conduction, convection, and radiation. One, two, or all three processes may be significant in a particular phenomenon; however, high rates of free convection to a fluid undergoing a phase change was the principal consideration of this study.

Convection to a fluid experiencing a change of phase - particularly boiling water - has received considerable attention because some of the highest heat transfer rates with the smallest temperature differences have been achieved by this process. Free convection rates to a saturated liquid undergoing a phase change may be as much as 1000 times greater than corresponding rates without phase change. Superposition of forced convection on free convection boiling may approximately double these rates. Also, the superposition of subcooled boiling conditions may increase these rates as much as one order of magnitude.

The temperature of the heating surface in the latter case must be in excess of the liquid saturation temperature; and thus the temperature drop is considerably increased. This may be undesirable, depending on the application and operating conditions of the system.

Certainly, there are few such important and widely applied physical phenomena that have eluded analysis and promoted confusion to the extent

that heat transfer to boiling liquids has. Relatively few systematic experimental measurements have been made - especially for extensive ranges of pressure, temperature and heat flux. The expense and effort required have been deterring factors. Then, too, nearly every attempt to analyze and predict boiling heat transfer rates has concluded with a twofold apology: 1) suggesting that the analysis presented is being refined and will be more fully developed at some future date, and 2) deploring the scarcity and inconsistency of the available experimental data - especially at pressures greater than one atmosphere.

The inability to understand this physical process adequately has hindered the development of a satisfactory analytical model. Such a process of boiling is complicated by a transient two-phase transfer of mass and energy accompanied by very rapid and intermittent generation of the vapor phase at preferred random locations. The experimental measurements have usually represented time-averaged total values for a large number of the randomly located sites of vapor generation.

Consider the various processes, illustrated in Figure 1, that may be involved in free convection heat transfer from a heated surface to a saturated liquid. The heat transfer rate q" and temperature difference θ in region "a" are in good agreement with the predictions of analyses of single-phase free convection. With increased heat transfer rates, the liquid superheat required to establish the nucleate boiling of region "b" is obtained. The peak nucleate boiling heat flux of region "c," sometimes called the first crisis, is reached when the vapor bubbles begin to coalesce and insulate the heating surface. If the heat flux q" is not reduced after the peak heat flux has been reached, the temperature of the vapor-insulated heating surface will increase to some value in region "f." This temperature often exceeds the melting point of the material, and failure or "burnout" occurs.

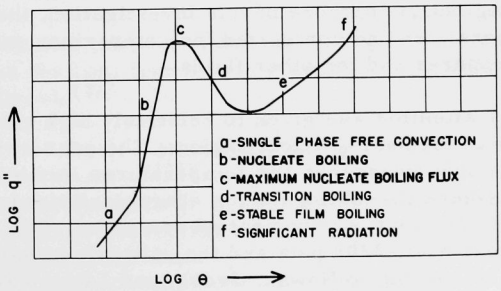

Fig. 1. Representative Curve for Free Convection to a Saturated Liquid.

On the other hand, consider the reduction in heat flux q" in the unstable, elusive transition film boiling region "d." Apparently an increased coalescence of the vapor on the heated surface - with increased temperature difference - causes a decrease in heat flux in this region. The transition from region "d" to "e" indicates complete coverage of the heated surface by a vapor film, and is sometimes called the second crisis. Increased conduction and convection through this vapor film with increased temperature difference result in increased heat flux for the fully developed film boiling of region "e." Region "e" is sometimes described as stable film boiling. Here, the net vapor is generated in the vapor film and is transported into the liquid.

Region "f" in Figure 1, where radiation becomes significant, would undoubtedly terminate with material failure. This failure may be termed the third crisis.

In film boiling, the vapor film surrounding the heat source flows upward in a gravitational field as additional vapor is formed at the liquid-vapor interface. This flow may be either laminar or turbulent, depending on the fluid, geometry, and heat flux. Unlike single-phase fluid flow over a surface, the transition from laminar to turbulent flow in film boiling does not appear to correspond very well with a certain range of the usual Reynolds numbers or Grashof numbers.

The purpose of this investigation was to increase the basic knowledge of boiling, primarily by means of experimental measurements. As influenced by previous considerations, suitable experimental apparatus was designed and constructed for the purpose of investigating free convection nucleate and film boiling heat transfer to saturated water up to near-critical pressures. A considerable effort was made to control uniformly the important parameters that affected the experimental results.

In carrying out the purpose of this investigation, the experimental results were generalized and correlated for comparison with existing data for the lower pressures and for other fluids.

Particular attention was given to relatively high rates of heat transfer to water in the near-critical region. The near-critical region is defined here to include pressures and temperatures immediately above and below the region where the distinguishing characteristics of a two-phase fluid vanish (e.g., the latent heat of vaporization vanishes). The critical pressure of water is approximately 3208 psia and the critical temperature is approximately 705.45 F, according to Nowak, Grosh, and Liley.[73]

Further background and a discussion of some of the previous investigations are included in the subsequent review of the literature.

SURVEY OF THE LITERATURE

The literature searched for pertinent references included Chemical Abstracts, The Engineering Index, Nuclear Science Abstracts, Physics Abstracts, The Monthly List of Russian Accessions, various heat transfer journals, several heat transfer texts, and various dissertations.

Most of the available literature pertaining to two-phase free convection heat transfer is concerned with near-atmospheric pressures. This literature forms an important background for this investigation; but it was not discussed thoroughly here because several good general reviews are available such as those of Drew and Mueller,[23] Jakob,[46] Madsen,[61] Addoms,[1] McAdams,[62] Westwater,[97] and Jicha[47] - in chronological order.

Some of the investigations of forced convection and boiling in a subcooled liquid were considered briefly for illumination and comparison.

The literature was covered primarily in chronological order since many of the articles included a variety of topics.

The evaluation of fluid property is a problem. Some properties - especially surface tension - are greatly influenced by pressure, temperature, and purity. When property evaluation was required, most of the articles didn't indicate the source of the property value, or even the location in the fluid where it was evaluated. Usually, for two-phase conditions the liquid properties are evaluated at the bulk temperature. If the liquid superheat is appreciable, the liquid properties are sometimes evaluated at an average liquid temperature. The vapor properties are usually evaluated at an average vapor temperature - particularly in the case of film boiling. In contrast, the properties are usually evaluated at the average temperature for single-phase conditions.

The choice of a property reference temperature may appreciably affect predictions for heat transfer to a near-critical fluid, as was shown by Fritsch and Grosh.[34]

Nucleate Boiling

The heat transfer rate q" and the heat transfer coefficient h have been measured for free convection boiling from various inclined, vertical, and horizontal test sections with:

1) Joulean heat generation and boiling on the external surface;

2) Joulean heat generation and boiling inside of a tube;

3) condensing vapor heat source inside and boiling outside of a tube;

4) condensing vapor heat source outside and boiling inside of a tube;

5) hot liquid or gas heat source inside and boiling outside of a tube.

Van Camp[92] and Wooldridge[99] list and discuss some of these experiments. These experiments are not equivalent, and must be compared with caution.

Note that Joulean heating should essentially provide a constant heat generation and heat flux from the wall to the fluid. A condensing vapor heat source should essentially provide a constant-source wall temperature - except for problems of temperature distribution in the tube wall. However, a hot gas or liquid heat source would undoubtedly not provide either a constant heat flux or temperature.

One of the first equations developed for predicting boiling heat transfer rates at various pressures was the following, due to Jakob[45] in 1938:

$$\frac{h}{k}\sqrt{\frac{\sigma}{\Delta\rho}} = 31.6\,\frac{\nu_a}{\nu}\left(\frac{\sigma}{\sigma_a}\,\frac{\Delta\rho_a}{\Delta\rho}\,\frac{q''}{\rho_{v_a}\, h_{fg_a}\, w_a}\right)^{0.8} , \qquad (1)$$

where the subscript a refers to atmospheric conditions, and w is the product of the mean diameter d of the vapor bubbles leaving the surface times the frequency. The diameter d is given as $1.034\sqrt{\sigma/\Delta\rho}$. For water w_a is given as 918 ft/hr. Except for the one vapor density, ρ_v, all properties are for the saturated liquid.

This equation is significant for several reasons. From his analysis, Jakob concluded that size or length of heating surface should have little effect on nucleate boiling coefficients. This has been indicated in the succeeding experiments by others, except for small wires. The equivalent of a boiling Nusselt number on the left side of equation (1) that is independent of diameter or length has been very useful to many correlators.

Evaluation of the frequency term is a problem. It is interesting to note that Chang[12,13] has recently submitted a boiling wave theory that included a frequency term.

The concepts presented by Jakob in developing equation (1) have been helpful in many efforts, including the recent correlations of Kutateladze[55] and Nishikawa.[71]

In 1938, Bogart and Johnson[6] reported data for benzene up to 1.1 times the critical pressure and less than one-half the maximum nucleate boiling heat flux for boiling outside of steam-heated tubes. An increase in the heat transfer coefficient h with increased pressure up to near-critical pressures was reported, but extensive fouling and fluid decomposition developed above 65% of the critical pressure.

In 1941 Bonilla and Perry[7] reported results for boiling of water, ethanol, butanol, and acetone. No change in heat transfer coefficient was discerned when the depth of immersion of the heater was increased from 1 in. to 6 in. for fully developed nucleate boiling.

Later (1945), Cichelli and Bonilla[14] obtained extensive nucleate results for boiling heat transfer up to the maximum for five organic compounds at pressures from atmospheric to near the critical, and for water up to 765 psia. Some difficulty was experienced with fouling, and some of the indicated heat transfer coefficients at higher pressures did not increase appreciably as temperature excess increased (at heat fluxes below the maximum for nucleate boiling). The apparatus used in this and the previously mentioned work of Bonilla[7] incorporated as a heating surface a chromium-plated copper disc, several inches in diameter and mounted horizontally at the base of the boiling chamber. The correlation of maximum heat fluxes for the respective per cents of the critical pressures agrees quite well with other measurements and predictions by Kutateladze,[54] Kazakova,[48] and Borishanskii.[8]

Farber and Scorah[28] published results in 1948 for boiling of water with Joulean heated, 0.041-in-diameter nickel, chromel, and tungsten wires at pressures up to 100 psi. A considerable effect due to heater material and pressure was indicated. Gradual discoloration of the water was noted. The test sections were "standardized" by heating them to a red heat and immersing them in water that had not been degassed. An oxide scale formed on the surface. This along with other contamination may explain the high maximum heat fluxes reported; for example, 10^6 BTU/(hr)(sq ft) at 75 psi. Surface temperatures were measured with a thermocouple.

Addoms[1] discusses the works of Braunlich for vacuum pressures and McAdams et al.,[63] for higher pressures, and reported results for the nucleate boiling of water on small horizontal platinum wires up to 2465 psia. Addoms also reported some effect due to increasing the wire diameter from 0.004 to 0.048 in. With smaller wires, generally higher heat transfer coefficients were obtained. The smaller wires apparently were subject to local "hot spots." They failed (reached burnout) at lower heat flux than the larger wires. These comparisons are reasonable because the per cent tolerance of the diameter decreases with decreasing diameter.

Addoms also reported that the peak nucleate boiling heat flux increased with pressure up to about 1200 psia, and the values of the heat transfer coefficient increased with pressure up to and including the highest pressure attained - 2465 psia. Some trouble with fouling - especially at the higher heat fluxes - was encountered, and some of the reported maximum values of heat flux considerably exceeded those reported by Cichelli and Bonilla[14] for a flat plate, and by Kazakova[48] and Kutateladze[54] for small cylinders.

In 1949, Haselden and Peters[40] reported results for condensation and nucleate boiling of oxygen and nitrogen near atmospheric pressure on $\frac{3}{8}$-, $\frac{1}{2}$-, and $\frac{5}{8}$-in.-diameter horizontal and vertical cylinders.

Morgan et al.,[69] in 1949 investigated the effect of adding "Drene" to water. Nucleate boiling heat transfer rates were measured and photographs were taken. One per cent solutions of Drene resulted in much greater heat transfer coefficients than resulted with 0.1 per cent solutions, even though both had nearly the same surface tension. An apparent effective increase in local surface tension was hypothesized as the explanation. However, the photographs indicated an increase in the number of nucleate boiling sites and nuclei accompanied by a decrease in bubble size, similar to the effects of additives and contaminants observed in other experiments with no alteration of the surface tension.

The exact effect of surface tension on nucleate boiling is not clear. In fact, the values of surface tension are not accurately known at various temperatures and pressures, even for most ordinary fluids, including water, and may be greatly affected by the purity of the fluid. Surface tension is discussed here because it is included in several of the correlations and predictions.

Data and predictions about the surface tension of water are presented in Appendix C.

Lowry and Westwater[59] in 1957 reported the effects of additives on nucleate and film boiling of methanol. These additives reduced the surface tension, but some increased and some decreased nucleate boiling heat transfer rates. All increased the film boiling rates. It was suggested that some of the additives behaved as synthetic nuclei.

Zmola[100] in 1950 observed and photographed some of the influences of conditions of the heater surface pressure up to two atmospheres, surface tension, and subcooling on nucleate boiling in water.

In 1950, Kutateladze[54] presented the following equation for predicting the maximum nucleate boiling heat flux:

$$q''_{max} = A h_{fg} (g\rho_v)^{1/2} (\sigma \Delta \rho)^{1/4} \quad , \tag{2}$$

where a is 0.13 to 0.20, depending on the nature of the surface. This prediction presumably applies to all fluids, and is one of the better general predictions of maximum free convection nucleate boiling heat flux. The coefficient A was determined from the experiments of Kutateladze in which graphite plate heaters were used; from the data of Cichella and Bonilla;[14] and from experiments conducted by Kazakova[48] employing Joulean-heated,

vertical nichrome strips (0.196 in. high, 0.0236 in. thick, and about 3 in. long), horizontal platinum wires (0.006 in. in diameter), and nichrome wires (0.012 in. in diameter). Kazakova determined values of the peak heat flux for water up to near-critical pressures. Some difficulty with fouling was experienced.

In 1956, Borishanskii[8] suggested that the coefficient A in equation (2) might be expressed as a function of viscosity, since viscosity is not included in equation (2). The following dimensionless expression was presented:

$$A = 0.13 + 4 \left(\frac{\mu^2 \sqrt{g \Delta \rho}}{\rho \sigma^{3/2}} \right)^{0.4} , \qquad (3)$$

in which the properties are those at the average liquid temperature. The viscosity effect here is usually quite small. Zuber[101] discussed this equation.

In 1952, Kutateladze[55] edited a collection of articles and presented an equation for predicting the maximum heat flux for nucleate boiling at various degrees of liquid subcooling. He also presented the equivalent of the following equation for predicting heat transfer coefficients throughout the range of nucleate boiling with various saturated liquids at various pressures:

$$\frac{h}{k} \sqrt{\frac{\sigma}{\Delta \rho}} = 0.44 \, Pr^{0.35} \left(\frac{10^{-4} q'' P}{h_{fg} \rho_v \nu \Delta \rho} \right)^{0.7} , \qquad (4)$$

in which the units are to be consistent in order to make the equation dimensionless. The coefficient and exponent were evaluated from the data of Cichelli and Bonilla.[14]

Buchberg et al.,[11] in 1951 conducted experiments in an electrically heated, forced-circulation loop to determine the conditions required for boiling and "burnout." A correlation was presented for measured values of excess wall temperature above saturation required to establish boiling conditions with subcooled water flow in a $\frac{1}{4}$-in., vertical stainless steel tube with pressures up to 2,500 psia. Heat fluxes as high as 3.8×10^6 BTU/(hr)(sq ft) were reported for nucleate boiling in turbulent subcooled flow at 2,000 psia.

Various degrees of superheat of the liquid near the heating surface - i.e., excess temperature - are required to establish nucleation, depending on the pressure and nature of the liquid-solid interface. Mead et al.,[65] in 1951 measured the superheat required for glass, stainless steel, and copper surfaces in contact with water up to near-critical pressures. Superheats up

to 110°F were observed at atmospheric pressure. Superheats tended to approach zero as the critical pressure was approached. Dissolved gases in the water were reported to have little effect, but adsorbed gases on the surfaces reduced the required superheat significantly. The studies of Buchberg and Mead are included in reference 89.

Several years later, Bankoff[5] presented arguments for nucleation occurring at a pre-existing vapor- or gas-phase boundary.

Rohsenow[81] developed the following nucleate boiling correlation in 1952:

$$\frac{C\Delta T}{h_{fg} Pr^{1.7}} = 0.013 \left(\frac{q''}{\mu h_{fg}} \frac{\sigma}{\Delta \rho} \right)^{1/3} , \qquad (5)$$

where the properties are those at the liquid saturation temperature. The coefficient and exponents were evaluated from plots of the data of Addoms[1] and of Cichelli and Bonilla.[14] The basic considerations of Jakob[45] were employed in an attempt to obtain a boiling Nusselt number as some function of a boiling Reynolds number and the Prandtl number. The correlation in the above form is one of the easier ones to evaluate, and the predictions are about as good as those obtained with most of the correlations available to date. Some systematic deviation of the correlation from experimental data is evident.

Several attempts have been made to analyze nucleate boiling by means of some type of consideration of bubble dynamics as a first step; however, a comprehensive, workable mathematical model of nucleate boiling has not yet been developed. The various correlations based on a discussion of bubble dynamics for a single bubble warrant a discussion of some of the literature about bubble growth.

Plesset and Zwick[77] in 1952 considered a growing or collapsing spherical vapor bubble surrounded by a liquid, and developed an expression for the temperature difference between the vapor and the bulk of the homogeneous liquid in terms of the heat transferred to the liquid and the temperature gradient at the boundary (essentially the Neuman problem for the sphere). It was concluded that most of the temperature variation would occur in a distance much less than the bubble radius (i.e., a thin thermal boundary layer).

Two years later, in 1954, Plesset and Zwick[77a] published an expression for bubble radius as a function of time; this equation agreed well with experimental measurements for water at atmospheric pressure within the limit of observation. The previously developed expression for the temperature in the vapor bubble was used to find the vapor pressure, assuming a linear relationship, and this vapor pressure

was substituted into the equation of motion developed by Rayleigh.[80] Bubble radius and bubble growth rate were found as functions of time for the initial growth of the bubble and also for bubble sizes in the range of visual observation.

Dergarabedian[18] in 1953 experimentally measured rates of bubble growth at atmospheric pressure in water, and the results compared favorably with the predictions of Plesset and Zwick.

Forster[30] discussed these predictions about bubble growth, and in 1955 Forster and Zuber[31] presented an equation for the prediction of heat transfer coefficients in boiling equivalent to the following expression:

$$\left(\frac{2\pi C_p \sigma}{k}\right)^{1/2}\left(\frac{\rho}{g^{1/3}\Delta\rho}\right)^{3/4}\frac{q''}{\rho_v h_{fg}} = 0.0015\left[\frac{\rho}{\mu}\left(\frac{C_p \rho \sqrt{\pi\alpha}\,\Delta T}{\rho_v h_{fg}}\right)^2\right]^{0.62} Pr^{1/3} \quad . \tag{6}$$

This equation resulted from reasoning that the Nusselt number should be some function of the Reynolds number and Prandtl number, somewhat analogous to established experimental correlations for single-phase forced convection. It was then reasoned that the characteristic length in the Nusselt number should be the bubble radius expressed as a function of time, and that the characteristic velocity in the Reynolds number should be the rate of bubble growth. Various descriptions of the physical phenomena represented by this equation include a "microconvection" in a very thin layer of superheated liquid adjacent to the heating surface. The data of Cichelli and Bonilla about peak heat flux was used to evaluate the exponents and coefficient. The correlation predicts proportionately higher rates of heat transfer than were experimentally measured at heat fluxes less than the maximum; however, this is one of the most "rigorous" developments to date.

Rohsenow et al.,[83] modified equation (6) and presented various coefficients for various fluids, not including water. The data for water still eluded the correlation.

Extensive computation and property determination is involved in the evaluation of equation (6).

Faneuff[27] photographed growing bubbles in 1958 in an attempt to check theories of bubble growth rate and to determine time delays in the formation of vapor. The smallest bubble observed was 10^{-3} cm in diameter. Pulses of power of one microsecond were applied to an 8-mil-diameter nichrome wire in water. One reason for delay in bubble growth was assumed to be the time required to superheat the liquid out to the critical radius required for bubble growth. A second reason for growth delay was taken to be a relaxation time after the bubble has grown much larger than

the critical radius and then grows according to the thermal diffusion through the liquid-vapor interface. It was concluded that good agreement between the predictions and measurements was realized if the average superheat of the liquid adjacent to the heating surface at the time of the initiation of bubble growth was used in the calculations.

Griffith[36] in 1958 developed a mathematical model for predicting rates of bubble growth in boiling by applying the Fourier-Biot law at the liquid-vapor interface in order to estimate the heat transferred to the bubble. This was coupled with the energy equation for the liquid in the immediate vicinity of the bubble. These equations were solved by approximate methods for a range of the parameters and gave quite good agreement with the experimental results of Dergarabedian[18] for water at atmospheric pressure. Predictions of rates of bubble growth were made for higher pressures in terms of fluid properties and temperature differences.

No completely analytical method has been developed for applying the predictions for one bubble to obtain the net rate of heat transfer from a surface on which indefinitely many bubbles are generated.

Westwater and Santangelo[98] in 1955 clarified the picture for transition from nucleate to film boiling by means of photographs of boiling.

Courty and Foust[15] investigated the effects of surface variables in nucleate boiling of ether, n-pentane, and Freon 113 from horizontal copper and nickel plates of various roughnesses at atmospheric pressure. Photographs were taken. Hysteresis up to 25°F was reported for the same nucleate boiling heat flux depending on the initial surface condition and whether heat flux was increasing or decreasing. For polished surfaces, nucleate boiling heat flux increased proportionally to the temperature difference raised to the power 12 to 24 instead of to the usually reported third or fourth power.

Rohsenow and Griffith[82] in 1956 suggested the following correlation for predicting maximum heat flux for nucleate boiling.

$$\frac{q''_{max}}{\rho_v h_{fg}} = 143 \left(\frac{\Delta \rho}{\rho_v} \right)^{0.6} \text{ ft/hr} \quad , \tag{7}$$

where the coefficient and exponent were evaluated from data of Cichelli and Bonilla[14] and of Addoms[1] for various saturated liquids at pressures from a vacuum to near-critical.

Kurihara[53] in 1956 measured nucleate boiling coefficients of various saturated liquids at atmospheric pressure by means of horizontal, copper plate heaters of various degrees of surface roughness.

Mesler and Banchero[67] in 1958 supplemented the Cichelli and Bonilla[14] data with nucleate boiling data for acetone, ethanol, benzene, and Freon 113 up to 515 psia. They compared the results with various correlations and data. The Rohsenow[81] equation reportedly provided the best correlation. The apparatus incorporated a 0.0643-in.-diameter, Joulean heated, stainless steel horizontal tube inside a stainless steel pressure vessel. Rates of heat transfer up to about one-third the maximum were achieved.

Chang[12] in 1957 discussed convection and boiling from the viewpoint of wave theory. He developed relations for the prediction of nucleate boiling heat transfer coefficients in terms of a frequency, contact angle, and an equivalent boiling thermal conductivity that cannot be precisely evaluated with ease. Nucleate boiling, maximum nucleate boiling heat flux, film boiling, minimum film boiling heat flux, and boiling stability are discussed by Chang[12,13] and Zuber.[101]

In 1959, Levy[57] developed the following nucleate boiling correlation:

$$q'' = \frac{kC\rho^2}{\sigma T_{sat}\Delta\rho} \frac{1}{B_L} (\Delta T)^3 \quad , \tag{8}$$

where $1/B_L$ is a variable coefficient defined as a ratio of the actual measured heat flux to a predicted value, and the properties are those of the liquid. The data of Addoms[1] and Cichelli and Bonilla[14] were used to plot a curve for determining $1/B_L$ within a nominal deviation of 100 per cent. Mathematically, the correlation spreads the data over a range of the Y axis that is about 50 per cent greater than the corresponding range of the Rohsenow correlation. This tends to make the data appear to follow the correlation better. The equations applied by Forster and Zuber[31] were applied in the development of the correlation. A constant superheat was assumed to exist in a thin "microconvection" liquid boundary layer adjacent to the heater surface.

Engelberg-Forster and Greif[26] presented this correlation at the same time:

$$q'' = 4.3 \times 10^{-5} \frac{\alpha C\rho T_{sat}}{\sigma^{1/2}(h_{fg}\rho_v)^{3/2}} (CT_s\alpha^{1/2})^{1/4} \quad (\rho/\mu)^{5/8} \, Pr^{1/3} \, \Delta P^2 \quad , \tag{9}$$

where all properties, except the one vapor density, ρ_v, are those of liquid. Various physical descriptions of possible mechanisms of heat and mass transport in nucleate boiling were discussed, including: "microconvection" in the sublayer, roughness and turbulence promotion effects of bubbles, latent heat transport by bubbles (shown by several analysts to be relatively

insignificant), and vapor-liquid exchange or pumping action of the bubbles. It was concluded that the latter mechanism was the most important and the most descriptive of the actual physical phenomena.

The correlation was obtained by considering the equations for bubble growth and various dimensionless groups of properties. In equation (9) the coefficient was obtained from experimental data; the exponent $\frac{1}{3}$ was chosen since in many problems it is $\frac{1}{3}$, and the exponent $\frac{5}{8}$ was obtained from an argument supported by experiments at low pressures. The correlation is in good agreement with various near-atmospheric data at moderate nucleate boiling heat flux, but the predicted rates are somewhat excessive at higher pressures. Throughout the entire range of nucleate boiling, the experimental rates of heat transfer increase more rapidly with increased temperature difference than is indicated by the correlation.

In 1960, Nishikawa and Yamagata[71] published a noteworthy correlation equivalent to the following:

$$\frac{hD}{k} = 0.1\,D\left(f_p^2 f_f \frac{c_p \rho^2}{\sigma k h_{fg} \rho_v}\right)^{1/3} q''^{2/3} \quad , \tag{10}$$

in which all properties are for the liquid except the vapor density ρ_v. The quantity f_p is an experimentally determined pressure factor, and f_f is an experimentally determined "foamability factor" for various surfaces.

In establishing the equation, the stirring effect due to rising bubbles was considered to be the primary convective driving force. The existence of a suitable free convection nucleate boiling correlation of the following form was assumed:

$$Nu = \text{constant} \times (Gr^* Pr)^m \quad , \tag{11}$$

where Gr^* is an equivalent nucleate boiling Grashof number defined in terms of variables that affect the stirring effect of the bubbles, and to some degree representing the ratio of buoyancy force to viscous force.

The coefficient in equation (10) was obtained from experimental data, and the pressure factor f_p was arbitrarily assumed equal to the pressure in atmospheres because of the lack of experimental data for higher pressures. The foamability factor f_f was taken to be unity. When plotted, the experimental data for various fluids extended over a range from 10^5 to 10^6 units. The correlation was also applied to boiling in forced convection and in a subcooled liquid.

Hsu and Schmidt[44] in 1960 attempted to measure local variations in surface temperature during nucleate boiling in water. Surface temperature variations up to 4°F were measured near nucleate boiling sites. In most of the correlations that have been made, the surface temperature was assumed to be constant throughout.

Wallis[96] in 1960 proposed a gas-liquid analogue for nucleate boiling, in which a porous media was used as a generating surface. Air or other gas would be forced through the porous media from one side and developed bubbles in a liquid on the other side. One major problem would be the establishment of the same initial conditions and boundary conditions in both the boiling and bubbling systems. It was assumed that the hydrodynamic and thermal aspects of nucleate boiling could be considered separately.

It was suggested that the analogy would be valid up to and including the peak nucleate boiling heat flux. At this condition in the bubbling system, it is supposed that the gas would cover the bubble-generating surface. No design or experimentation was mentioned.

Some of the nucleate boiling correlations have been applied to boiling liquid metals with some success - primarily near atmospheric pressure.

In 1960, Romie et al.,[84] measured heat transfer rates and temperature differences for a natural-circulation loop with mercury at pressures up to 33 psia and compared their results with other experiments at pressures up to 10 atmospheres.

Film Boiling

One of the early measurements of film boiling heat transfer coefficients was made in 1920 by Pilling and Lynch[76] who provided the data incidental to their investigation of the "quenching power" of water and oil in the quenching of steel. Instrumented cylinders were dipped in water and oil and the temperature recorded as a function of time on a recorder. Knowing the specific heat and dimensions of the steel cylinders and the slopes of the time-temperature curves, Bromley[10] calculated the apparent heat transfer coefficient and found it compared favorably with his experiments.

Bromley[10] in 1950 developed an equation for predicting laminar film boiling coefficients for horizontal cylinders based on the Nusselt[75] theory of film condensation. Bromley's final equation is equivalent to

$$Nu = 0.875\, Pr^{1/4} \left(\frac{h_{fg}}{c_p^{\theta}} + 0.16\, \frac{c_p^{\theta}}{h_{fg}} + 0.8 \right)^{1/4} \left(\frac{\rho \Delta \rho D^3}{4\mu^2} \right)^{1/4} , \qquad (12)$$

where properties are for the vapor at the average temperature, except for the saturated liquid density ρ_L in $\Delta\rho = (\rho_L - \rho)$. In equation (12), D is the diameter of the horizontal heated cylinder, and Nu is the average Nusselt number for a cylinder of diameter D.

This equation was discussed by McFadden[64] and compared with McFadden's integration of the fundamental equations for two pressures. As is mentioned by McFadden, the analysis should apply quite well for laminar film boiling if the assumption that the vapor thickness of the boundary layer be considerably less than the cylinder diameter is satisfied. In addition, if a similarity transformation can be made - subject to limitations discussed by Merk and Prins[66] - one of the independent position variables can be eliminated in a two-dimensional analysis. Then the correspondence between cylinders and vertical plates in laminar free convection as developed by Hermann[41] should apply (i.e., the heat transfer coefficient for a horizontal cylinder is 0.777 times the coefficient for a vertical plate with height equal to diameter).

Applied to vertical plates, the coefficient of equation (12) would then be 1.135.

Bromley's predictions exceed the experimental values at the higher temperature differences, but changing the exponent of the Prandtl number to $\frac{2}{3}$ resulted in considerable improvement - especially for the film boiling results at higher pressure of the present investigation. The use of an exponent larger than $\frac{1}{4}$ has some justification where the boundary layer may be subjected to disturbance from nonuniform external flow along the length of the heated surface as in film boiling.

Bromley conducted extensive experiments with several fluids and various cylinder diameters for atmospheric pressure.

Ellion[25] in 1954 arrived at a coefficient of 1.015 for the application of Bromley's preliminary version of equation (12) to vertical plates.

Kutateladze[55] in 1952 proposed an equation for predicting heat transfer coefficients for free convection laminar film boiling for vertical plates equivalent to the following:

$$\bar{h} = Ak_v \left[\frac{h_{fg}\, \rho_v\, \Delta\rho}{\mu_v\, q''\, x} \left(1 + \frac{c_{p_v}\, \Delta T}{2h_{fg}} \right) \right]^{1/3} , \qquad (13)$$

where $\bar{h}$ is the average coefficient, the properties are for the vapor, ΔT is the temperature difference between the wall and the vapor, and the value of A varies from 0.652 to 1.035 as determined by experimental data up to eleven atmospheres. The inclusion of $\bar{h}$, q", and ΔT in one equation limits the value of the equation. Film boiling in a subcooled liquid is also considered.

Relatively little experimental data about film boiling are available, and most of the experiments have been made in the last ten years at atmospheric pressure for a variety of fluids, including liquid oxygen, nitrogen, organic fluids, and water.

Banchero et al.,[4] measured film boiling coefficients for liquid oxygen boiling on the outside of horizontal cylinders with laminar and turbulent flow conditions at pressures to 500 psia.

Dean and Thompson[17] measured film boiling coefficients for liquid nitrogen in turbulent flow in electrically heated $\frac{3}{16}$-in. tubes up to failure at pressures up to 1.22 times the critical. For these conditions they reported nearly constant heat transfer coefficients throughout the range of fully established film boiling. Tube failure occurred near the tube inlet at supercritical pressures, indicating better heat transfer further along the tube, with pressure dropping toward the critical pressure. Conversely, at subcritical pressures, burnout or tube failure occurred near the outlet, indicating better heat transfer toward the tube inlet, with higher pressures in the direction of the critical pressure.

At supercritical pressures, Dean also reported a gradual change from a stable heat transfer at temperature differences less than 75°F to a less stable film boiling type of heat transfer at higher temperature differences. At temperature differences as high as 1000°F the heat transfer was reported to be equivalent to subcritical pressure film boiling.

Hsu and Westwater[43] measured laminar and turbulent film boiling coefficients for steam-heated vertical tubes, using nitrogen and organic liquids at atmospheric pressure. A correlation is presented in terms of the rate of vapor flow and fluid properties. It was reported that there apparently is not a well-defined region of transition between laminar and turbulent flow in terms of the usual Grashof and Reynolds numbers.

McFadden[64] solved the fundamental boundary-layer equations for free convection stable laminar film boiling for temperature differences of 250, 500, and 1000°F and pressures of 2800 psia and 3100 psia for water under the assumption that properties were variable. Good agreement with constant-property solutions was reported for 2800 psia; however, the prediction under the assumption of constant properties was about 50 per cent too high for 3100 psia, and was expected to diverge even more at higher, near-critical pressures. The temperature profiles were found to be approximately linear - indicating that conduction is the dominant mode of heat transfer for the conditions considered.

Bromley's equation (12) predicts somewhat higher coefficients than McFadden's results. This is reasonable, since the coefficient in Bromley's equation was determined from experiments which probably exhibited a less stable film than McFadden's model.

Chang[13] recently proposed a wave theory for film boiling similar to his treatment of convection and nucleate boiling.[12] For both nucleate and film boiling, Chang's aim was to obtain an expression analogous to those for single-phase free convection, of the form

$$Nu = \text{constant} \times (Pr^* Gr^*)^n \quad , \tag{14}$$

where Pr* and Gr* are some types of film boiling Prandtl number and Grashof number, respectively. Bromley's preliminary equation is taken as the working equation for the actual calculation of film boiling coefficients, and the makeup of Pr* and Gr* follow accordingly.

Chang also proposed the existence of a critical wave length identical with the critical hydrodynamic wave length for stability. By definition, wavelengths longer than this would characterize nucleate boiling, and shorter wavelengths would characterize film boiling. Various discussions of boiling stability have been made from this point of view. Critical or related wavelengths have not been experimentally observed in nucleate or film boiling.

Near-critical Region

Very little information is available for heat transfer to fluids near their critical pressures. This investigation is primarily concerned with free convection, but several investigations for forced flow in tubes are briefly discussed below.

Schmidt, Eckert, and Grigull[87] presented results in 1939 for the total heat transferred to ammonia in a natural-circulation thermal siphon loop operated up to 1.34 times the critical pressure. An apparent thermal conductivity was defined for the specific system as

$$k_{apparent} = \frac{4 q_{total} \ell}{\pi d^2 \theta} \quad , \tag{15}$$

where ℓ was half the total length of the loop, d the inside diameter of the tube, and θ the change of bulk temperature. Insufficient information is available to generalize the results; however, the apparent thermal conductivity increased as much as two-hundred-fold in the near-critical region. Higher rates of heat transfer persisted in the region above the critical pressure compared with those below the critical pressure. Large fluctuations in pressure, temperature, and flow rate were observed in the near-critical region.

Deissler[19] in 1954 developed an analysis of fully developed turbulent flow of air and supercritical water with variable properties in tubes. The predicted local heat transfer coefficients, friction factors, and velocity and temperature distributions were in good agreement with

measurements for air heated to large temperature differences and with Reynolds Numbers greater than 15,000. Predictions were also made for 5,000 psia water.

Goldmann[35] presented an analysis for the same cases.

Doughty and Drake[22] measured free convection heat transfer from an electrically heated, horizontal, 10-mil-diameter platinum wire in Freon 12 at and above the critical pressure of 580 psia and at temperatures from 230 to 260°F. The critical temperature of Freon 12 is 232.7°F. A region of rapid increase in heat transfer coefficient with increased temperature difference was measured for fluid temperatures above and below the critical, similar to a region of nucleate boiling. The measured results for higher temperature differences were similar to those for fully developed film boiling.

The merit of defining a film coefficient as a function of temperature was questioned for regions where such a coefficient changes greatly with temperatures (e.g., in nucleate boiling and near-critical free convection).

An elusive hysteresis was observed, depending on whether heat flux was increasing or decreasing. Larger rates of heat transfer were measured with increasing rates than with decreasing rates.

Heat transfer coefficients measured near the critical state were as much as ten times greater than coefficients for superheated vapor at 283 psia.

The results indicated that supercritical charges will in general provide higher rates of heat transfer than subcritical charges. This is in agreement with the observations of Schmidt and Eckert.[87]

Bringer[9] measured heat transfer rates to carbon dioxide at 1200 psia (1.1 times the critical pressure) for turbulent flow in a 0.18-in.-diameter tube.

Powell[78] measured forced-convection heat transfer rates to oxygen flowing inside a Joulean heated, $\frac{1}{4}$-in.-diameter tube, 6 to 72 in. long, at pressures and temperatures above and below the critical. A decrease in heat transfer rate was reported for the various pressures as bulk temperatures approached the critical temperature. Temperature differences between wall and fluid were mostly in the range from 300 to 1200°F - normally associated with the film boiling type of heat transfer.

Miropolskii and Shitsman[68] measured heat transfer to non-boiling water and superheated steam from 4 to 280 atmospheres in forced flow through tubes about $\frac{1}{3}$ in. in diameter and 5.5 in. long. The proposed general correlation is

$$Nu = 0.023 (Re\ Pr)^{0.8} \quad , \tag{16}$$

with Nu and Re evaluated at the mean film temperature, and Pr evaluated at the wall or in the bulk liquid - whichever gives the smaller value.

Griffith and Sabersky[37] in 1960 photographed free convection heat transfer to Freon 114-A at 550 psia (1.15 times the critical pressure) and for 80 to 350°F (critical temperature is 294°F) with temperature differences up to 400°. High rates of heat transfer were attributed to a bubble-like convective disturbance.

Holman and Boggs[42] measured nonboiling heat transfer to Freon 12 in a closed natural-circulation loop at pressures of 500 to 950 psi and at temperatures from 150 to 400°F (critical pressure and temperature are 596.8 psia and 233.2°F). A correlation involving Nusselt, Grashof, Prandtl, and Reynolds numbers was made.

It was reported that no appreciable increase in the heat transfer coefficient in the critical region was observed, compared with the coefficients for the superheat region. This is explained to be a consequence of the relative importance of convective effects due to increased flow rate with increased heat flux in a natural-circulation loop. The role of buoyancy forces in a natural-circulation loop operated near the critical region was not discussed.

Schmidt[86] heated the lower ends and cooled the upper ends of 2-cm-diameter tubes, 25 cm high, charged with critical volumes of ammonia and carbon dioxide. Equivalent thermal conductivities up to 4000 times that of copper were observed. These high equivalent conductivities decreased rapidly as the temperature increased above the critical.

Fritsch and Grosh[34] in 1961 integrated the fundamental equations for laminar free convection from a vertical, isothermal plate for water in the region above the critical point. Variable specific heat and density were considered. Considerable difference was indicated between variable- and constant-properties results. A generalized correlation of the results was made.

Summary

This survey of the literature has pointed out an absence of consistent experimental data for nucleate and film boiling heat transfer to fluids up to near-critical conditions. This has severely limited the correlations and predictions, since they have, in the end, depended upon experimental data to evaluate coefficients and exponents. These considerations have prompted this investigation.

APPLICABILITY OF THE FUNDAMENTAL EQUATIONS

The heat transferred, the temperature distribution, and the velocity distribution have been predicted for a number of convective heat transfer problems by the application of the fundamental principles of the conservation of mass, momentum, and energy, along with the phenomenological equations and the principles of thermodynamics. The resulting equations were then solved by various means.

Nucleate Boiling

As previously mentioned, nucleate boiling has eluded such analysis because a representative model could not be developed for the mechanism of nucleate boiling, and because the fluid is not continuous - each vapor bubble in the liquid is a singularity. The temperature distribution in a superheated liquid in the vicinity of one growing vapor bubble has been expressed in terms of a Green's function for a sphere integrated over a specified time interval.[30,77] Presumably, the heat transfer could be estimated by summing over all vapor bubbles, but this is not presently feasible and probably would not represent the total heat transferred. The general direction of the various analytical approaches to nucleate boiling does not appear to be pointing toward successful analysis at this time except in an indirect way.

Film Boiling

Stable, free convection, laminar film boiling has been described and the heat transfer has been predicted.[10,64] Deviation of predictions from experiment may be subscribed to the relative lack of stability in the physical process of film boiling.

The fundamental partial differential equations expressing the conservation of mass, momentum, and energy for steady-state, two-dimensional, stable, free convection, laminar boundary layer-type film boiling are as follows[64]:

$$\frac{\partial(\rho u)}{\partial x} + \frac{\partial(\rho v)}{\partial y} = 0 \quad ; \tag{18}$$

$$\rho u \frac{\partial u}{\partial x} + \rho v \frac{\partial u}{\partial y} = g\mu \frac{\partial^2 u}{\partial y^2} - g\left(\frac{\partial P}{\partial x} + G_x\right) \quad ; \tag{19}$$

$$\rho u c_p \frac{\partial T}{\partial x} + \rho v c_p \frac{\partial T}{\partial y} = k \frac{\partial^2 T}{\partial y^2} \quad , \tag{20}$$

where x is the distance along the surface (vertical plate or cylinder) measured from the bottom toward the top. The distance y is measured

perpendicular to and away from the surface, and G_x is the gravitational body force in the x-direction. The heat generation in the vapor has been neglected, flow is considered compressible, specific heat is considered variable, but viscosity and thermal conductivity are considered constant. The boundary conditions are:

1. $T = T_{wall}, \quad y = 0, \quad u = v = 0$;

2. $T = T_{sat}, \quad y = \delta, \quad u = 0$

$$\text{at } y = \delta, \quad q'' = -k \frac{\partial T}{\partial y} = h_{fg} \rho v \quad ,$$

where δ is the unknown thickness of the vapor film boundary layer.

McFadden[64] solved these equations for 2800-psia and 3100-psia water for three temperature differences, considering, first, the properties to be variable and, second, the properties to be constant. The heated wall was considered to be isothermal. Good agreement between variable- and constant-property predictions in the case of water was indicated for pressures less than 2800 psia. In either case, it is noted that in comparing McFadden's predictions with

$$q''_{ave} = (4/3)k \frac{\Delta T}{\delta} \tag{21}$$

(which assumes conduction only), where k is the average vapor film thermal conductivity and δ is the thickness predicted by McFadden for the vapor film boundary layer, the predictions of the above equation are 80 to 95 per cent of those of McFadden.

Therefore, equation (21) should give a simple first approximation to the average stable laminar film boiling boundary layer thickness for various cases not solved by McFadden. Equation (21) may be written for this purpose as

$$\delta_{ave} = k \frac{\Delta T}{q''_{ave}} = \frac{k}{h_{ave}} \quad . \tag{22}$$

This result was useful in the approximate prediction of thermal radiation through an absorbing film boundary layer of vapor.

It may be noted that equation (22) predicts smaller thicknesses for the boundary layer than predicted by McFadden, but experiments have also indicated an effective boundary layer thickness that was somewhat less than McFadden's predictions.

Thermal Radiation

In film boiling with temperature differences greater than 1000°, thermal radiation may be a significant part of the total heat transferred, even with materials of low emissivity, such as platinum. In an attempt to obtain a satisfactory valid method of evaluating simultaneous thermal radiation and conduction, the theoretical analyses of Viskanta[94] and Kellett[49] were investigated.

Heat transfer in media that absorb and scatter thermal radiation has been treated extensively by Viskanta,[94] and an exact formulation was carried out in terms of material constants for simultaneous conduction and radiation in an absorbing grey media between two parallel black planes. An approximate analysis of the same problem was made by Kellett[49] who used the principle of energy conservation within the media. The temperature distribution predicted by Kellett was about one per cent lower than the exact formulation, and the predicted total heat transfer was about 10 per cent lower.

The emissivity, extinction coefficient, and other properties required for evaluating the analyses are not known for water vapor at the relatively high pressures encountered in the present investigation. Available data for these properties[21,62,70] were extrapolated, and predictions were made by means of Kellett's formulation modified to approximately describe radiation and conduction through an absorbing media between platinum at the higher temperature and a black body (assumed to be saturated water) at the lower temperature. Emissivity values used for platinum are given in Appendix C. Computations were made for film boiling conditions as treated in the previous section [equation (22) was used to calculate the vapor thickness] with water pressures from atmospheric to 3100 psia and with heat fluxes up to material failure.

The results indicated that for the thicknesses of the vapor boundary layer associated with film boiling in a normal gravitational field with heating surface heights on the order of one inch, the conduction and thermal radiation may be treated independently, and the heat transfer by radiation is at least 90 per cent of the heat transferred with no absorbing media between the surfaces. For the range of conditions considered, the observations of Viskanta and Kellett supported these conclusions.

In view of these results, the following equation was used to predict the magnitude of thermal radiation in film boiling for comparison with the present experimental investigation:

$$q''_{rad} = 0.1714 \times 10^{-8} \epsilon_{Plat} (T_1^4 - T_2^4) BTU/(hr)(ft^2) \quad , \qquad (23)$$

where the emissivity of the platinum is given in Appendix C, T_1 is the temperature of the platinum surface, and T_2 is the water temperature (in degrees Rankine). Equation (23) assumes the presence of a platinum emitter enclosed by a larger surface that is a black body. Equation (23) has considerable merit because of the exclusion of unknown properties and because it should accurately predict the upper limit of the actual thermal radiation.

DESCRIPTION OF APPARATUS

General

The experimental apparatus was designed to satisfy the following general operating requirements:

1. maintain and contain a constant fluid environment up to 4000 psi and 800°F in a static system;
2. supply and provide for the measurement of heat transfer rates to this fluid up to 3×10^6 BTU/(hr)(ft^2);
3. provide for the measurement of the temperature differences between the heated surface and the fluid that are responsible for the above heat transfer rates;
4. provide suitable means for investigating free convection, nucleate boiling, and film boiling in the contained fluid;
5. provide for visual observation of the heat transfer test section;
6. insure protection of personnel, buildings, and equipment.

The arrangement of the experimental apparatus is shown in Figures 2 and 3.

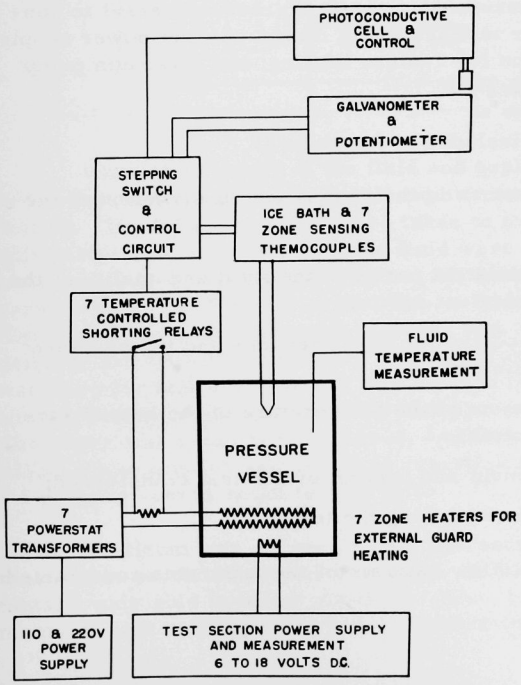

Fig. 2

Block Diagram of Apparatus

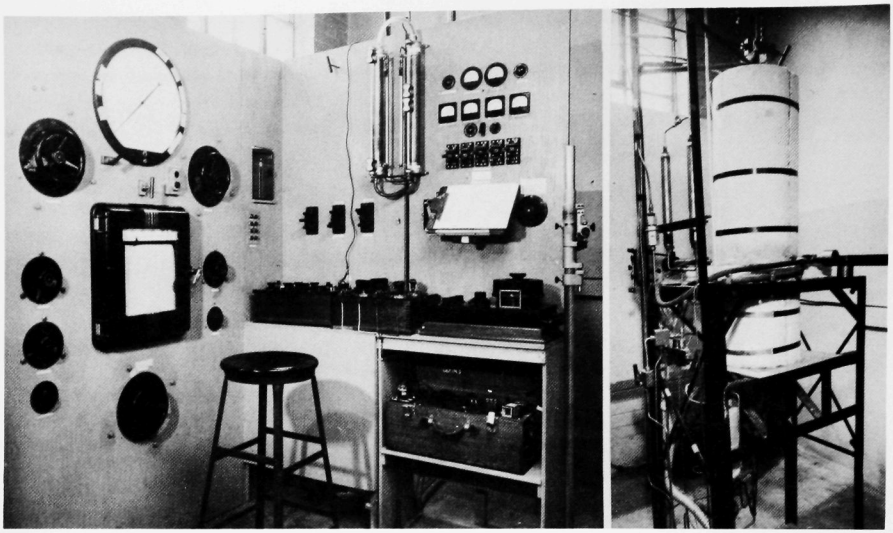

Fig. 3. Photograph of Apparatus

Included are a control and measurement panel; a pressure vessel to contain the fluid and heat transfer test section; a direct-current power supply to the heat transfer test section for Joulean heating; and a vacuum pump for outgassing and filling the system.

A list of equipment is included in Appendix D.

The primary considerations in the design and construction of the apparatus were:

1. maintenance of consistent purity of the fluid and quality of the heated surface of the test section;
2. measurement and control of fluid pressure and temperature within acceptable limits;
3. accurate measurement of the temperature of the heated surface of the test section;
4. accurate measurement and control of the heat transferred;
5. reduction of transients during the tests.

Figure 4 is a schematic flow diagram of the apparatus constructed.

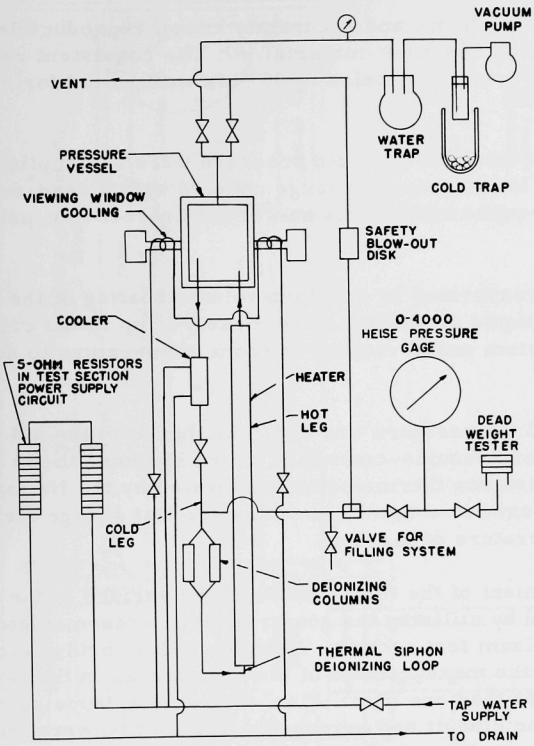

Fig. 4

Flow Diagram

Consistent purity of the fluid and quality of the test section have been very serious problems in all experiments about nucleate and film boiling. The following steps were taken to minimize these problems: The only materials in contact with the fluid were 300 series stainless steels, platinum, silver, quartz, and Teflon. All stainless steel parts were passivated in 135°F nitric acid. Also, a thermal-siphon loop with screen filters and ion-exchange resin columns was incorporated to circulate and deionize the water continuously. Hard-drawn, chemically pure platinum was used for test sections and was cleaned in hot 10 per cent HCl and then annealed at approximately 1400°F at a pressure of several mm Hg absolute. The water was deionized, degassed, and then deionized again shortly before filling the evacuated system. The resistivity of the water exceeded 1.5 megohm-cm at room temperature.

Platinum was chosen for the test sections because it is one of the most noble or stable metals available. In the electromotive series of the metals, only gold is below platinum. Also, platinum meets all the requirements of high melting point-(3227°F), chemical stability, resistance to

oxidation, availability in pure form, and accurately known reproducible properties more closely than any other material.[2] The consistent reproducibility of the electrical resistivity below 2000°F is well suited for resistance thermometry.[2,93]

Measurement and control of the fluid pressure were accomplished with the aid of a 4000-psi Heise pressure gauge coupled with a dead-weight tester which provided for calibration within half of the nearest five-psi scale division.

The system was pressurized by constant-volume heating of the fluid in the system. Saturated liquid conditions were measured up to the critical pressure by filling the system under vacuum at room temperature to about one-third the capacity.

Control of the fluid temperature was accomplished with the aid of a series of differential-thermocouple-controlled guard heaters, shown in Figure 5. A platinum resistance thermometer, calibrated by the National Bureau of Standards, was used in conjunction with a Mueller bridge for measurement of the temperature of the fluid.

Accurate measurement of the temperature of the surface of the test section was facilitated by utilizing the good resistance-thermometer characteristics of the platinum test section. A double Kelvin bridge circuit[99] was employed for the measurement of the resistances in the test section that were much less than one ohm. Also, the voltage drops across a standard resistance in the circuit and across the test section were measured with a potentiometer, as shown in Figure 6, and from these the resistance of the test section could be calculated. The latter method of determining the resistance of test section - for relating to temperature - was easier and usually of comparable accuracy to the former method, especially for film boiling measurements.

Accurate measurement and control of the heat transferred were accomplished with a stable, direct-current power supply, along with standard resistances, standard cells, and a Leeds and Northrup K-2 potentiometer, all calibrated by Mr. D. E. Lipp in the Measurements Laboratory of the Electrical Engineering Department, Purdue University. A DC power supply to the test section was chosen because the power dissipated could be accurately measured. Also, there is some question about related effects with alternating-current Joulean heated test sections. However, the latter was not a decisive factor.

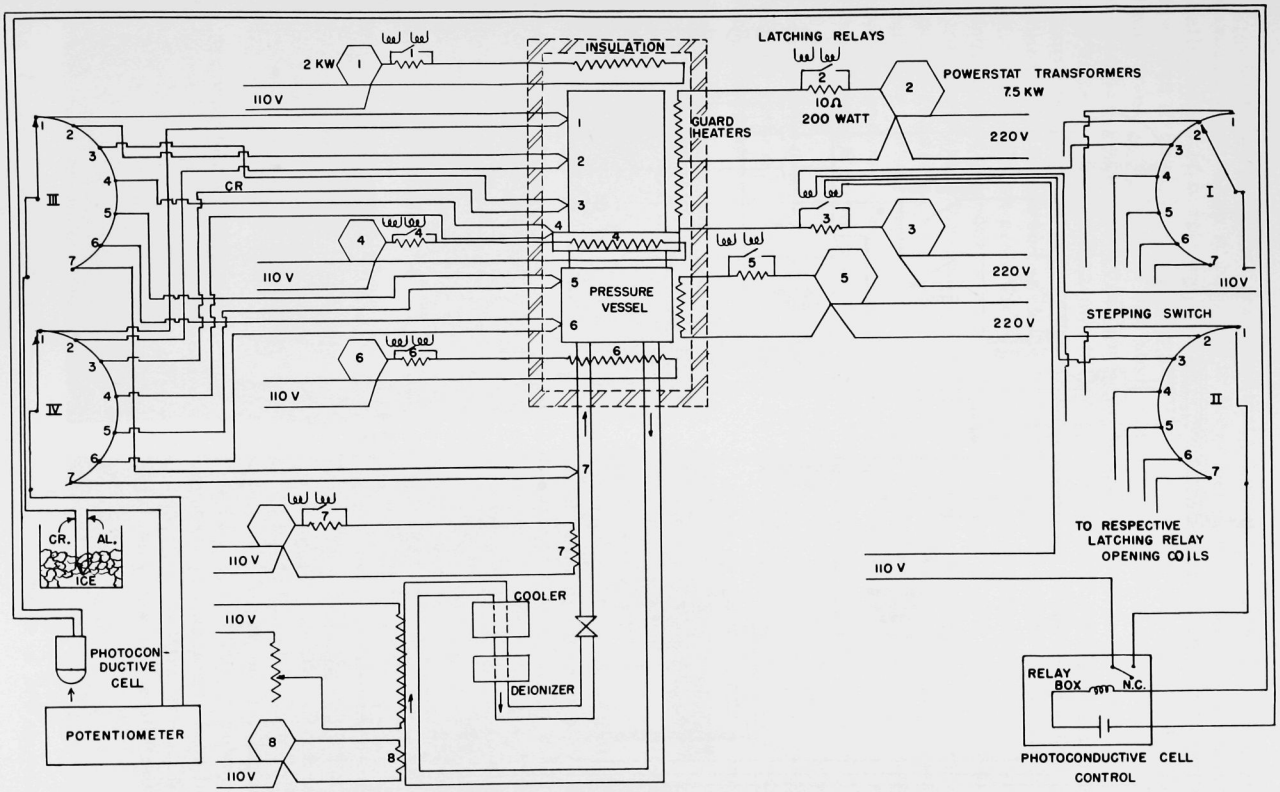

Fig. 5. Temperature-control Circuit

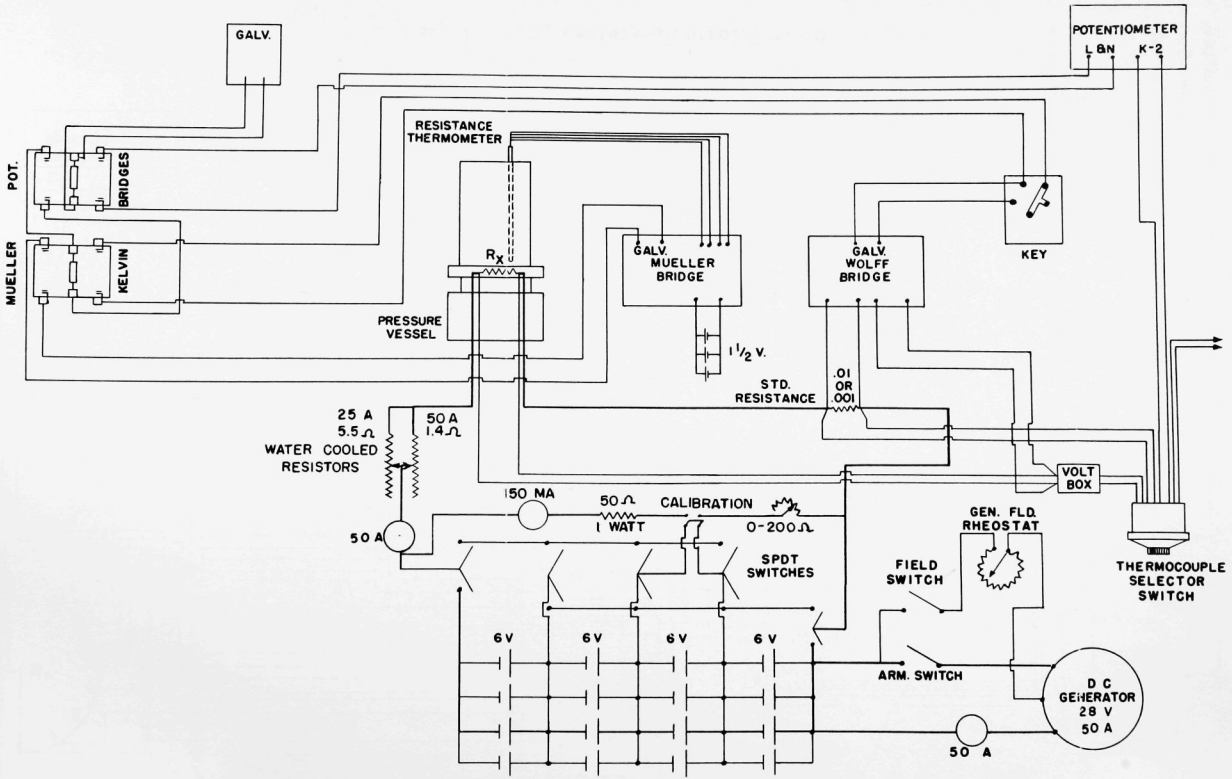

Fig. 6. Measurement Circuit

In order to reduce the transients during the tests, the following measures were taken in addition to those previously mentioned: Four parallel banks of 6-volt automotive-type storage batteries (see Figure 7) were used to provide stable power supplies for the test section up to 50 amp over periods up to one hour with a total drift of less than four per cent (actually, once the conditions reached equilibrium, measurements could be taken in less than one minute). The largest stock stainless steel pressure vessel available from manufacturers (see Figures 8 and 9) was obtained in an effort to essentially provide a semi-infinite fluid environment. Test-section sizes were limited to those required for satisfactory measurements in order to reduce the disturbance of the environment from the total heat transferred from the test section. A special asbestos-magnesia insulating cylinder was made to surround the pressure vessel completely. Also, the guard heater zones were blocked off into isolated spaces to prevent convection of the air from the bottom to the top of the pressure vessel in the space between the insulation and the pressure vessel (see Figure 8). A multipoint temperature recorder continuously reported the outside wall temperatures of the pressure vessel at various locations from the bottom to the top; thus any deviation of an environment guard heater could be quickly detected.

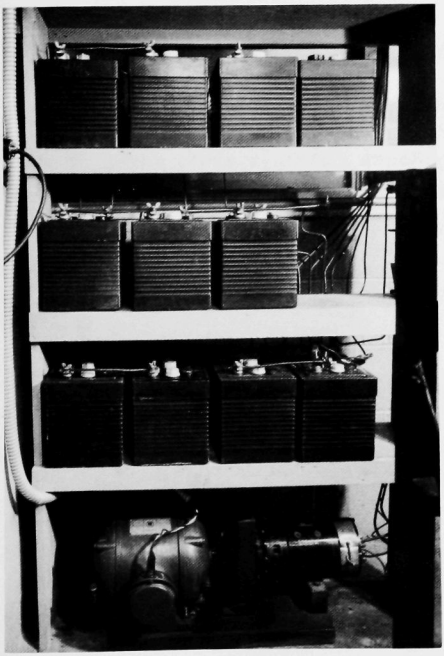

Fig. 7. Test Section Power Supply

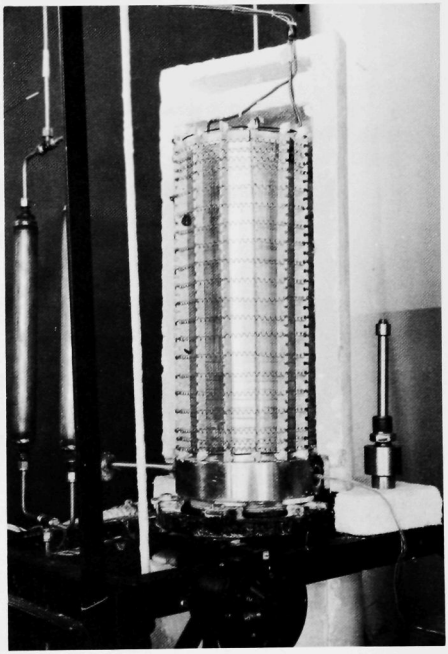

Fig. 8. View of Pressure Vessel

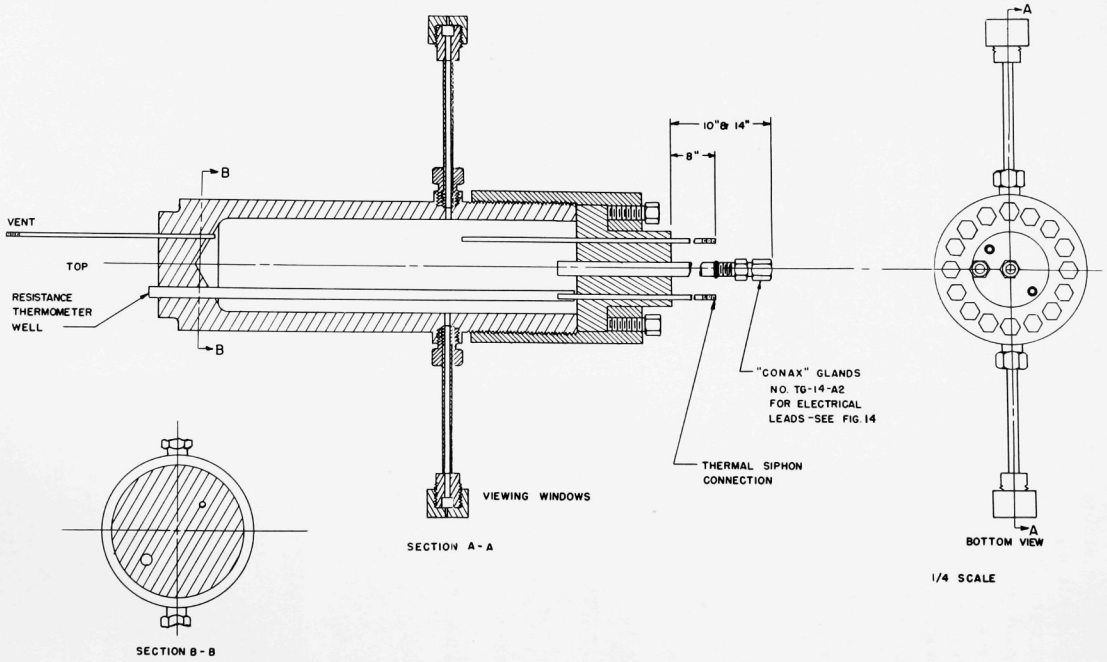

Fig. 9. Modified American Instrument Company No. 41-6130 316 S.S. Reaction Vessel

Detail

A list of equipment is included in Appendix D.

Pressure Vessel

The pressure vessel is sketched in Figure 9 as modified to incorporate viewing windows, a reinforcing ring, and various special connections. The reinforcing ring and the window connections were provided by the supplier according to design codes. The inside dimensions are 5 in. in diameter by 21 in.

The vessel was mounted with the cap and the electrical connections facing downward to facilitate assembly of the pressure vessel and mounting of the test section. It was desirable to locate the test section in the lower third of the vessel to provide an adequate cushion or control volume of vapor at subcritical pressures and yet insure immersion of the test section. Also, the critical pressure and volume correspond to a room-temperature water charge of about one-third the vessel volume. A special vertical lift jack was built to transport and position the 75-lb head and cap for assembly.

Viewing Windows

The viewing window and cold-leg construction are shown in Figure 10. The $\frac{9}{16}$-in.-OD by $\frac{5}{16}$-in.-ID tubing for the cold leg was reamed for loose fit of the clear synthetic sapphire (aluminum oxide crystal) rod with optically polished ends for viewing.

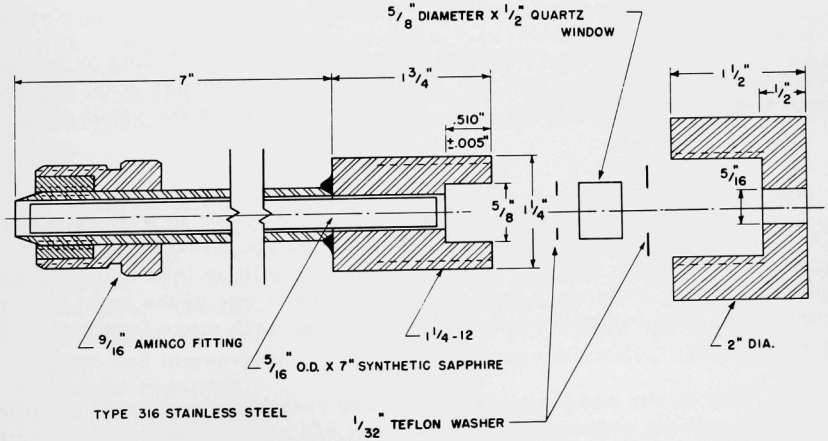

Fig. 10. Viewing Window

The synthetic sapphire rod greatly aided viewing of the test section because the index of refraction and density change with temperature are negligible compared to water. The rod was placed in the region of large temperature change between the fluid in the vessel and the cooler quartz windows and seals. The synthetic sapphire was unaffected by water even up to 3900 psia and 720°F, at which quartz surfaces were quickly etched. The test section was backlighted through one window and viewed through the other.

The test section was visually observed through a prism mounted in line with and outside of the quartz viewing window. This protected the observer in case of window failure. A telescope was also used to provide for better observation, since the test section was viewed through $\frac{5}{16}$-in.-diameter ports. The viewing arrangement is shown in Figure 11. Photographs were taken through the quartz window with the prism removed.

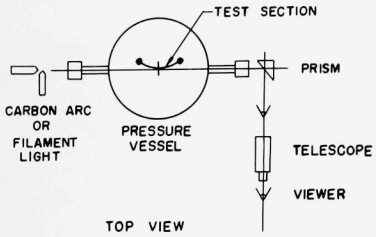

Fig. 11. Viewing Arrangement in Test Section

Attempts to mount synthetic sapphire windows in the heated wall of the pressure vessel were not successful. The windows apparently failed because of the combined thermal stresses and the stresses associated with the forces required to make a nonleaking seal. The failure of these windows with the fluid at 3100 psia and 700°F was a shattering experience, and thereafter window seals were made at the end of cold legs.

Vacuum System

The system was evacuated and outgassed before filling by means of equipment indicated in Figure 4. The vacuum pump, water trap, and vapor cold trap are shown in Figure 12. Dry ice was used in the vapor trap.

Test Section and Leads

The test section and electrical leads are shown in Figures 13 and 14. Quartz tubing was used to insulate the electrical leads in the cold legs. If obtainable, synthetic sapphire tubing would be less soluble than quartz. Silver leads were used because silver is one of the most stable conductors next to platinum and gold, and it is much more feasible economically.

The silver and platinum leads were resistance welded to the platinum with no apparent undesirable effects. The #14 silver wires could readily carry 50 amp. All junctions with the heated platinum test sections were made with platinum leads.

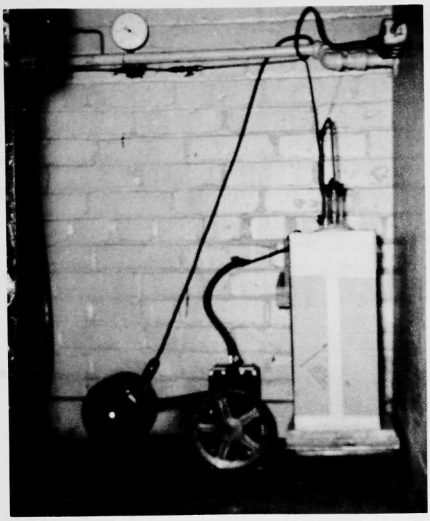

Fig. 12. Vacuum Pump and Cold Trap

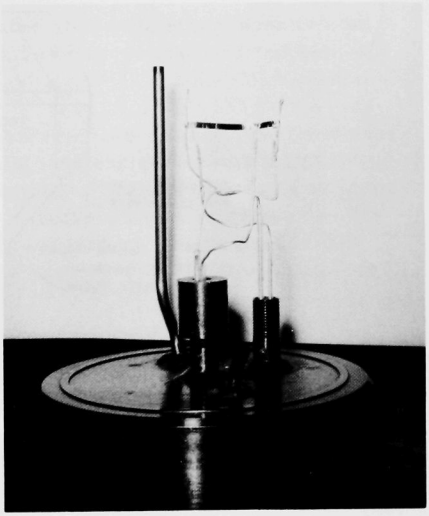

Fig. 13. Test Section

The test section proper is that portion of the heated section between the voltage taps, and measurements and calculations were based on that area. This length was from 1 to 3 in. out of a total length of 2 to 4 in. The end effects were negligible at $\frac{1}{2}$ in. from the end of the heated section.(92,99)

Unsuccessful attempts were made to use a larger $\frac{1}{4}$-in.-diameter test section fabricated from platinum foil bonded to a quartz rod with silver chloride. Also, attempts to use a $\frac{1}{4}$-in.-wide test section made of platinum foil strip stretched around a vertical 2-in.-diameter lava cylinder were not successful because of problems of control and measurement. Apparently, considerable heat was transferred from the lava cylinder to the fluid.

Some difficulty was experienced when mica, ceramic, glass, and lava materials were used in the system. The mica split into thin cleavage planes and flaked. The ceramic materials promoted electrolysis when used as insulators. The ordinary glass dissolved, and there was some powdering of the lava. The lava was stable when fired, but the resulting surfaces were not smooth and impervious. Diamonite was stable, but the surface was not smooth and impervious to water, and it was not readily available in some of the shapes required.

The quartz tubing insulators were dissolved to some extent, but the same tubing lasted for all tests. A special Corning glass was purchased, but has not yet been tried.

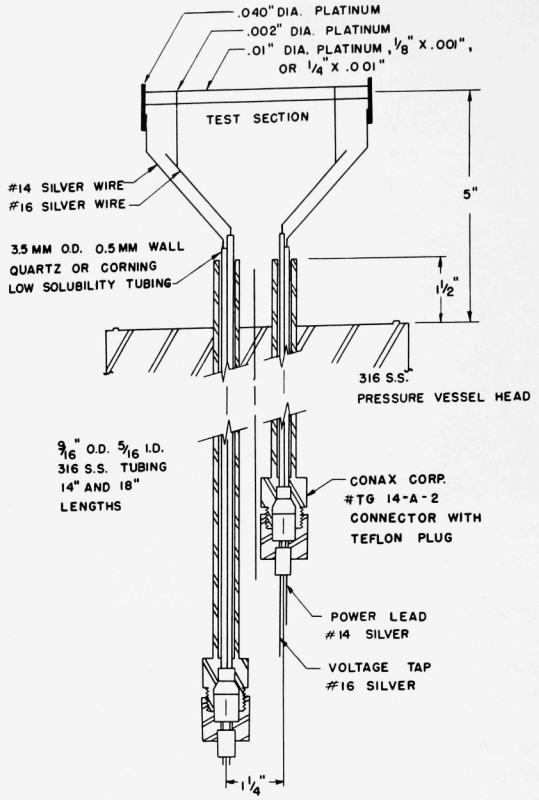

Fig. 14. Test Section Details

Test-section Power Supply and Measurement

The circuit for the measurement of the power supply to the test section is shown in Figure 6. The power supply was designed for selection of zero to 24 volts in six-volt steps. The maximum voltage used was 18. The water-cooled resistors could be adjusted to provide a test-section voltage supply anywhere between the six-volt steps for 1 to 50 amp. The current in the test section was determined by measuring the voltage drop across the standard resistor with the K-2 potentiometer.

A four-contact galvanometer key was constructed for use with the double Kelvin bridge circuit (see Figure 6). This key provided for a wide range of sensitivity for protection of the galvanometer at various degrees

of unbalance. As the key was depressed, the successive contacts cut out galvanometer shunting resistors until the maximum sensitivity of the galvanometer was realized.

The resistances in the test section were also used to determine the temperatures in the test section by treating the test section as a resistance thermometer. The calibration circuit shown in Figure 6 was used to determine the resistance of the test section at various fluid temperatures with negligible heat transfer. For calibration currents up to 100 ma, the calculated temperature difference between the test section and the fluid was less than 0.1°F for all test sections.(92,99)

The power dissipated, and thus the heat generated throughout the length of the test section was determined by multiplying the square of the current by the resistance of the test section. Resistances in the test section much smaller than one ohm were readily measured with the double Kelvin bridge using the Wolff bridge, as shown in Figure 6. However, for measuring larger resistances, it was faster and essentially as accurate to determine the resistance from the current and voltage drop across the test section as measured with the K-2 potentiometer. The resistance ratios obtained from these calibrations agreed, within the limits of observation, with the National Bureau of Standards table of resistance ratio versus temperature supplied with the calibrated resistance thermometer used for measurement of fluid temperature. Thus, the table was used in the determination of both the fluid and surface temperatures.

The resistance of the test section increased with increased heat flux and wall temperature in a constant-temperature fluid environment. The measured resistance of the test section was used in conjunction with the NBS calibration to determine an average temperature in the test section at each heat flux-power level setting.

The variation in the average temperature of the test section for 98 per cent of the length between voltage taps was calculated to be less than one-half of one per cent, based on measurements of variations of the thickness of the test section of less than one-quarter of one per cent. The variations in the thickness of the test section were made by Prof. A. J. Vellinger with the optical comparator in the U. S. Navy Gauge Laboratory, Purdue University. The previous limitation to 98 per cent of the length of the test section resulted from an approximate analysis of the fin cooling effect due to the attachment of the 0.002-in.-diameter voltage taps to the test section (see Figure 14).

The change in width of the test section during a test up to "burnout" could not be detected on the optical comparator (i.e., the change was less than 0.5 per cent); except for the region of failure, the test section remained smooth and bright. For test sections that were not heated to burnout, no deposit was observed at 20 magnifications under a microscope.

The length of the test section between voltage taps was measured with a cathetometer and a steel precision rule. The accuracy of the measured length was within 0.5 per cent.

The resistance ratio (i.e., the measured resistance divided by the reference resistance of the test section at 32°F) was used in obtaining the corresponding temperature from the NBS calibration. This temperature was very sensitive to small errors in length of the test section when this length was used in calculating the reference resistance at 32°F. Instead of using this procedure, the reference resistance for 32°F was obtained from the calibration of the test section at each fluid temperature, as described in Appendix E.

The electrical resistance from the test section to ground was observed to decrease with increasing fluid temperatures. The electrical conductivity of saturated water increases with temperature, but very little information concerning this could be found in the literature. Therefore, the calculations presented in Appendix C were made to obtain an evaluation of the relative conductivity change. The prediction shown in Figure 42 (q.v.) was supported to some extent by measurements of the resistance from the test section to the pressure vessel. For 1300-psia saturated liquid water, this resistance was about one-third the value for atmospheric conditions.

The measured resistance from the test section to pressure vessel was never less than 1000 ohms unless the leads were shorted. Since the resistances of the test sections were on the order of one ohm, the effect of electrical conduction to ground was neglected.

The temperature difference between the heated surface and the bulk fluid is of particular interest in evaluating the heat transfer. The internal temperature distribution across the thickness of the vertical, flat-strip test sections was virtually constant at any one height. However, the mean temperature inside the 10-mil-diameter test sections was as much as two degrees higher than the surface temperature at the highest levels of heat generation, as calculated by the methods described on pages 176-189 of reference 46. This temperature difference was subtracted from the temperature difference obtained from measurements when its effect was noticeable on the graphical plots of the results [at nucleate boiling heat fluxes greater than 5×10^5 BTU/(hr)(ft^2) with 10-mil-diameter test sections]. Such radial temperature variation has often been neglected in Joulean heated rods and tubes of considerably larger sizes than mentioned here, but it may be appreciable.(51)

Fluid Temperature and Pressure

The fluid environment was measured with a Mueller bridge and the NBS-calibrated resistance thermometer, both purchased specifically for this purpose. This equipment was used for the temperature standard. Good agreement was noted between the observed fluid saturation temperature and the corresponding pressure as measured with the Heise gauge and dead-weight tester. The arrangement is shown in Figures 4 and 6.

The resistance thermometer and bridge were checked during the experiments with an equiphase triple-point temperature reference cell, and the indicated temperature was less than 0.001°C above the triple point temperature of 0.01°C.

The temperature difference between the resistance thermometer element in the well shown in Figure 9 and the fluid was calculated to be much less than 0.01°F (with the pressure vessel at equilibrium), considering conduction and convection to room conditions.

Thermocouples were calibrated by placing them in the well with the thermometer and taking readings at fluid temperature equilibrium. The resistance thermometer readings were also used as an indicator for adjusting the automatic controls on the environment guard heaters.

Guard Heaters

Figure 5 is a diagram of the power supply and control for the guard heaters. The pressure vessel was divided into zones with a radiant guard heater for each zone. The photograph in Figure 8 shows the construction of the guard heater. The radiant heaters provided more uniform temperature distribution than was achieved in preliminary trials with strip heaters.

After the pressure vessel was heated to the desired temperature, the powerstat transformers for each guard heater were approximately adjusted to maintain this temperature, and then the control circuit for the guard heater was turned on. This control circuit opened or closed the latching relay that bypasses an adjustable 10-ohm resistor in each guard-heater circuit, and thus decreased or increased the heating of the zone as necessary to maintain the desired vessel temperature throughout.

The signal for opening or closing the latching relays for each zone was obtained from a differential-thermocouple-sensed circuit (see Figures 5 and 15) adjusted so that excess vessel wall temperature would cause a galvanometer light spot to deflect and impinge on a photoconductive cell.

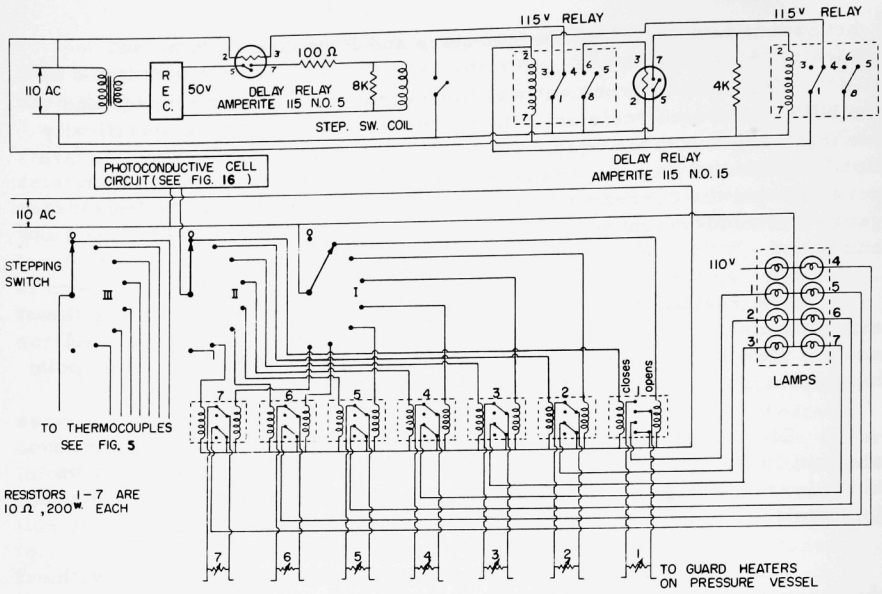

Fig. 15. Control Circuit for Guard Heater

The induced current in the photoconductive cell circuit (Figure 16) will then energize the opening coil on the shorting latching relay, and the power input to the zone heater will be reduced. The reduction in power level of the zone heater when the latching relay is opened may be zero to 25 per cent, depending on the adjustment of the 10-ohm, 200-watt resistor. A reduction of about 10 per cent was selected as a compromise between the temperature fluctuation and the temperature control of a zone.

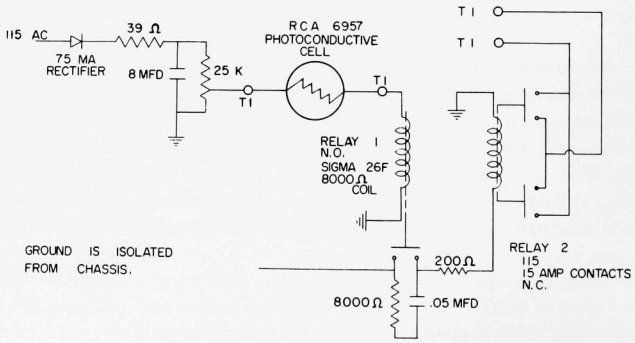

Fig. 16. Photoconductive Cell Circuit

Automatic successive sensing and control of all zones with one potentiometer and photoconductive cell circuit were accomplished with a time-delayed stepping switch circuit, shown in Figures 5 and 15. The time required for one cycle covering all zones was adjusted for about 3 min.

The method of spot welding the chromel-alumel sensing thermocouples to the pressure vessel wall is shown in Figure 17. A capacitor discharge welder was used.

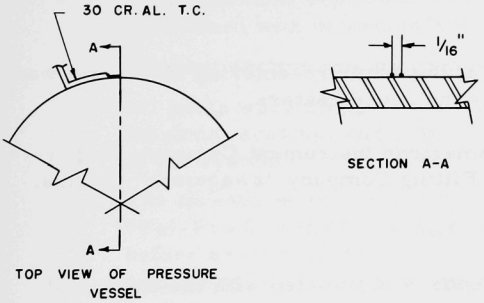

Fig. 17

Thermocouple Junction

Test thermocouples were welded to a short section of stainless steel and placed inside the heated pressure vessel to check the uniformity of the thermocouple readings at various temperatures. Readings were uniform within 0.5 degree. It was assumed that the sensing thermocouples attached to the pressure vessel in each zone would be of comparable uniformity.

The differential thermocouples attached to the pressure vessel for zone control of guard heating were referenced to a pure flaked ice bath, as shown in Figure 5. The flaked ice was obtained from the Chemistry Department. These thermocouples were not used to measure numerical values of temperature. They were used in keeping the zone temperatures uniform and constant so that the fluid temperature indicated by the resistance thermometer did not change from the desired value.

These differential thermocouples were initially referenced to the temperature inside the resistance thermometer well instead of the ice bath. However, with this arrangement the fluid environment temperature tended to drift after being uniformly established.

Deionizing Loop

The thermal-siphon deionizer loop is indicated in Figure 4. Depending on the system pressure, from one to four system volumes of water could be deionized in one hour.

The hot and cold legs are each 8 ft high, and were fabricated from $\frac{1}{4}$-in.-OD, 0.05-in. wall, type 304 stainless steel tubing. The resin columns were fabricated from 12-in. lengths of schedule 80, type 304 stainless steel, 1-in. pipe.

The temperature at the deionizing columns was kept below 150°F to safeguard the Amberlite MB-1 resin (obtained from Enley Products Inc., Brooklyn, New York).

A throttle valve was incorporated in the loop for shut-off and flow control.

The temperature control of the water re-entering the vessel was included in the control circuit for the guard heaters.

All tubing fittings were American Instrument Company "super-pressure" fittings and Crawford Fitting Company "swagelock" fittings.

Safety

A certain aura of catastrophe is associated with the method of constant-volume heating that was used to obtain the desired pressures and temperatures. The system was usually slightly overfilled, and the excess was carefully drained later at near-critical pressures in order to limit the pressure increase and to obtain the desired conditions. No provision was made for adding water to the system at high pressures. A 5000-psi safety rupture disc assembly was incorporated to guard against large pressure increases.

A $\frac{3}{4}$-in. plywood "V" shield opening toward the opposite wall was mounted between the control panel and the pressure vessel. The operator was stationed on the other side of the control panel.

EXPERIMENTAL PROCEDURE

The test section was rebuilt and the pressure vessel was reassembled 14 times during developmental tests, and 11 times during the series of experimental measurements. In preparing for the experimental tests, the following measures were taken:

1. All parts were cleaned with deionized water and a detergent, and rinsed with deionized water.
2. The test section was cleaned with hot hydrochloric acid.
3. All parts were cleaned with carbon tetrachloride, trichloroethylene, acetone, and ether, in that order, before assembly of the system.
4. The threads on the pressure vessel cap were coated with "Fel-Pro C-5 High-Temp" colloidal copper thread lubricant before assembly; the use of low-temperature thread compounds would result in permanent seizure of the cap on the vessel.[58]
5. The system was assembled and evacuated to several millimeters Hg absolute for 6 to 48 hr - usually 48 hr.
6. The pressure vessel was heated to 300-400°F and about one lb water was injected in an effort to aid outgassing by displacing air from the vessel surface.[56,58]
7. The test section was annealed at about 1400°F for 15 min.
8. After 2 to 12 hr of continued evacuation, the cooled system was filled with water that had been deionized, degassed, and then deionized again.
9. After another hour or two of degassing the water, the vacuum line was closed, and the vessel was heated up to the desired temperature and pressure.
10. The pressure gauge was calibrated in the vicinity of the desired pressure and set to read absolute values.
11. After approximate steady-state power adjustment of the guard heaters had been made, the control circuit for the guard heater temperature was energized, and the 8662 potentiometer was adjusted until the fluid temperature remained constant.
12. The Mueller bridge, K-2 potentiometer, and galvanometers were balanced and adjusted.
13. The calibration circuit for the test section was energized, and the test-section resistance and the fluid temperature were measured.

14. After the calibration circuit was opened, the experimental measurements were made, starting with the lower heat fluxes.

15. The following quantities were measured at each heat flux setting after the readings were essentially constant for at least 5 min:

    a. fluid pressure and temperature;
    b. current and resistance of the test section.

The effect of the additional degassing of step 6 was investigated during developmental tests by placing small, brightly polished copper strips in the pressure vessel at pressures to 3300 psia and temperatures to 715°F. Some tarnishing was evident, but was less when the additional degassing of step 6 was included.

The test section was fully annealed before tests because the resistance of platinum decreases noticeably with annealing, and the temperatures in the test section during measurments would provide at least a partial anneal.

The calibration step 13 was performed at each fluid pressure and temperature even for the same test section in order to check the consistency of the method for evaluating the reference test-section resistance of 32°F. The procedure for calibration and measurement is given in Appendix E.

The standard resistors used for measuring current in the test section were changed, when necessary, according to the following schedule:

1. 20-50 amp: 0.001 ohm
2. 1-20 amp: 0.01 ohm
3. 0- 1 amp: 0.1 ohm.

Usually an operator read the test measurements of step 15, which were recorded directly on computer data sheets in floating point decimals by another person. One set of measurements could be taken in less than one minute. The data were reduced to the results that were plotted with the aid of the Purdue University Datatron 204 computer. The method of data reduction is given in Appendix E.

Some hysteresis was observed for increasing and decreasing nucleate boiling heat fluxes. Measurements were usually made with increasing heat flux.

The film boiling measurements with high temperature differences were the last measurements made at each particular pressure. This was done to reduce the effects of any change in the test section at high

temperature. At pressures above 2400 psia, the peak nucleate boiling heat flux was checked again after film boiling measurements. If the observed peak nucleate boiling heat flux had changed for that pressure, the test section had been affected and was replaced. At the end of a particular test, film boiling measurements were usually taken up to failure of the test section.

Some difficulty was experienced in obtaining steady-state heat transfer conditions at high heat flux at near-critical pressures, especially at supercritical pressures. Limited improvement was accomplished by guard-heating reduction, and usually measurements were taken during a period of slight fluid temperature and pressure increase, even with limited test-section size. A sequence of measurements was taken; then the reverse sequence was taken quickly, and the readings were averaged.

At pressures above the critical, some of the fluid was drained from the system in order to provide bulk temperatures corresponding to the maximum specific heat of the fluid. This choice was arbitrary, and it was not the purpose of this investigation to investigate this region thoroughly.

The magnitude of the thermal radiation from the test section at various temperatures was evaluated by evacuating the empty pressure vessel and taking measurements with the pressure vessel first at room temperature and then at approximately 700°F. The conditions approximated net radiation from a heated platinum surface to a black body enclosure, since the enclosure was much larger than the heated surface. Therefore, these measurements should represent the upper limit of the portion of the heat transferred by radiation in the film boiling tests.

RESULTS

The experimental data and results are included in Appendix B. The results are plotted in Figures 18-25 in terms of the heat flux and temperature difference between the fluid and the heated surface. The ordinate scales were staggered by one cycle so that the complete curve for each pressure could be clearly presented to include nucleate and film boiling.

The results for the 10-mil-diameter test sections are plotted in Figures 18-20, and a composite comparison is shown in Figure 21. The results for the $\frac{1}{8}$-in., vertical plate test sections are plotted in Figures 22-24, and a composite comparision is shown in Figure 25.

In both types of test sections, maximum heat transfer coefficients h at constant heat flux q" are indicated in the region of 2800 psia for nucleate boiling of saturated liquid water.

The indicated heat transfer coefficients for the $\frac{1}{8}$-in. vertical plate are generally somewhat less than those for the 10-mil-diameter cylinder for both nucleate and film boiling.

The characteristics associated with transition film boiling were not observed above the critical pressure.

The general characteristics of the curves plotted for the heat transfer rates in the region immediately below the critical pressure are similar to the curves plotted for pressures immediately above the critical.

The results plotted for pressures 300 to 700 psi above the critical pressure indicate a trend toward the characteristics associated with single-phase free convection to those of a constant-property fluid.

The results plotted for pressures above the critical (see Figures 20 and 24) are somewhat surprising. The fluid is supposedly single phase for these conditions, and yet the results indicate a region of rapid increase in the heat transfer coefficient for relatively small increases in the temperature difference. This is similar to the effect observed in nucleate boiling. Also, a region of decreasing heat transfer coefficient with increasing temperature difference was observed at the higher temperature differences. This is similar to the effect observed in film boiling, and was described as film boiling by Doughty and Drake,[22] who reported similar results for supercritical Freon.

The above results are plausible if the variation of properties is considered and it is recalled that the measurements at pressures above the critical were made with bulk fluid temperatures corresponding to the region of maximum specific heat.

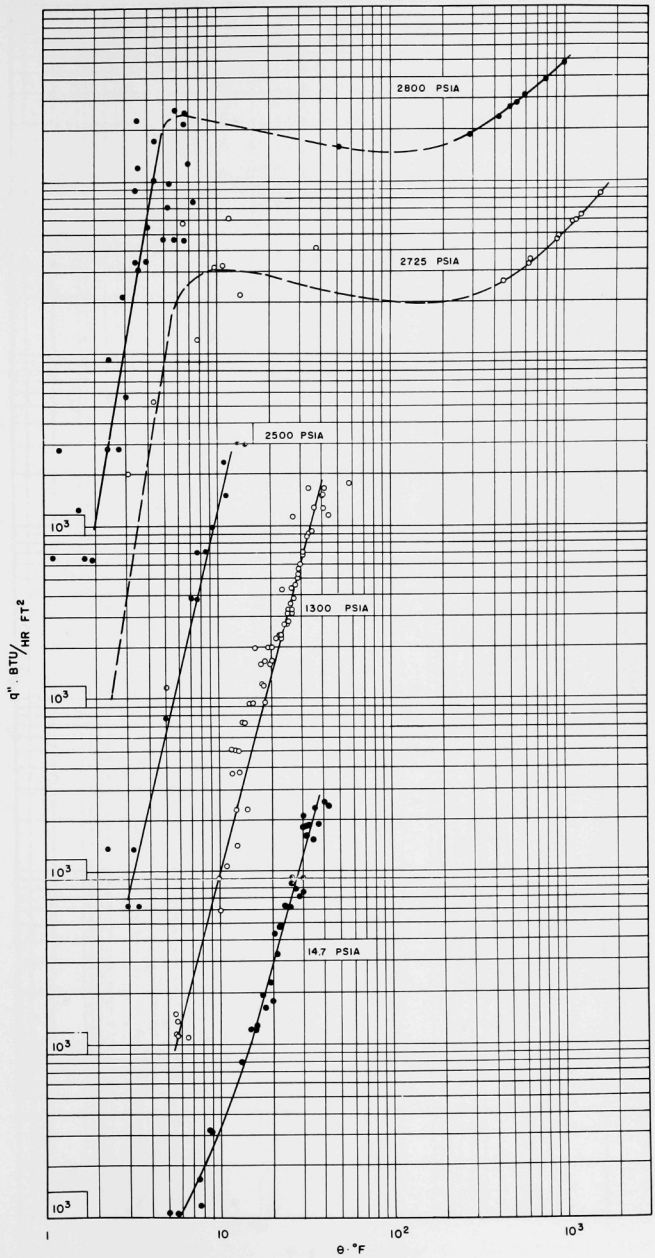

Fig. 18. Experimental Results from 14.7 to 2800 psia for 10-mil-diameter Test Section

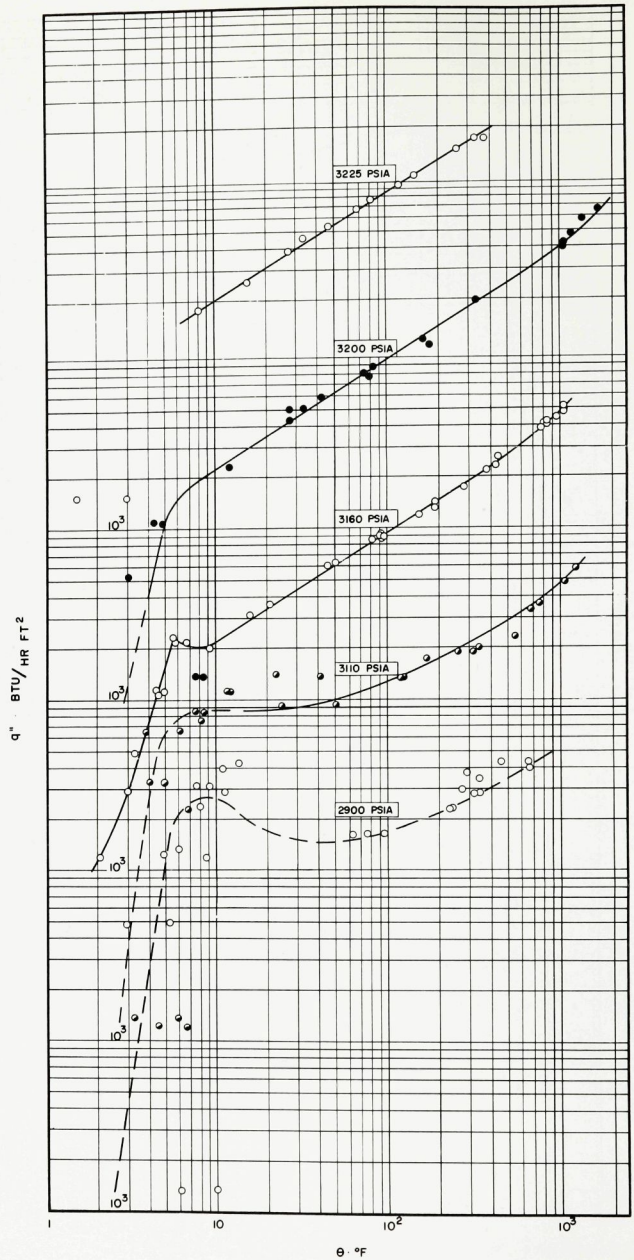

Fig. 19. Experimental Results from 2900 to 3225 psia for 10-mil-diameter Test Section

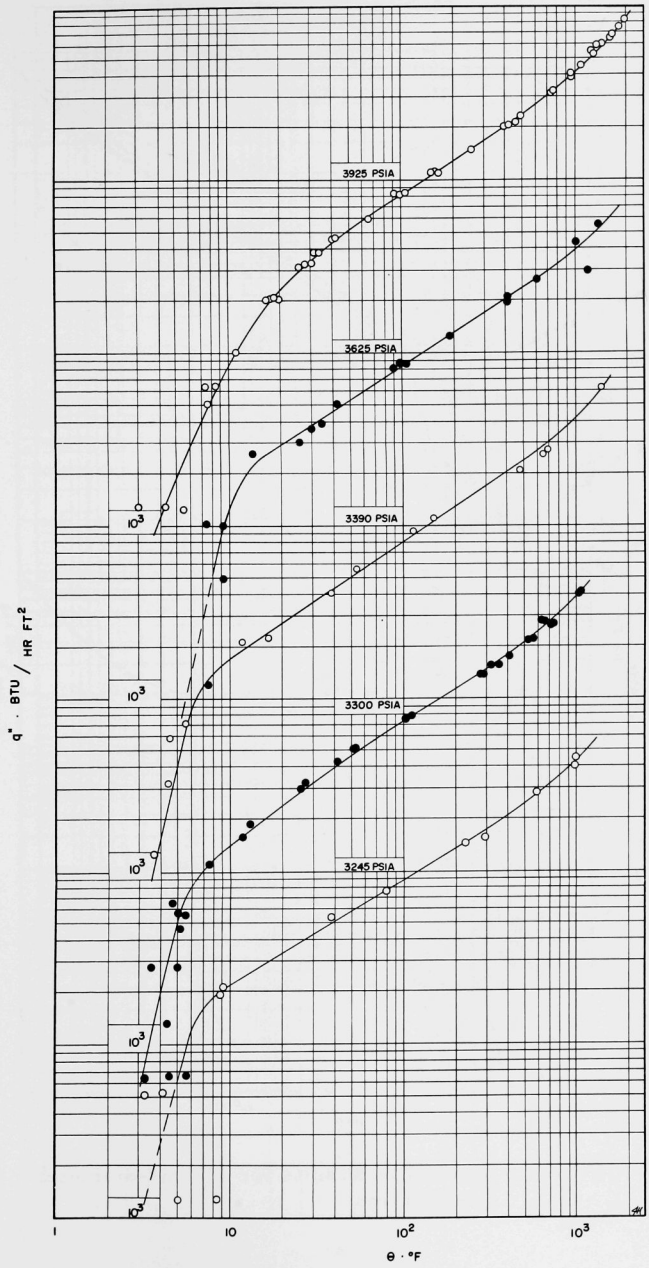

Fig. 20. Experimental Results from 3245 to 3925 psia for 10-mil-diameter Test Section

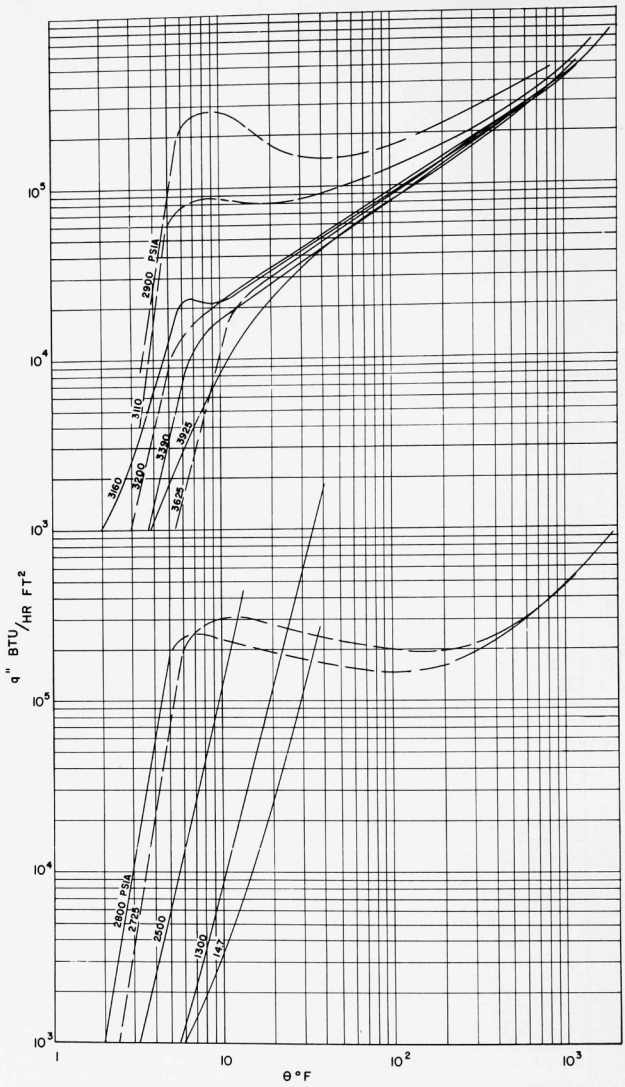

Fig. 21. Composite Results for 10-mil-diameter Test Section

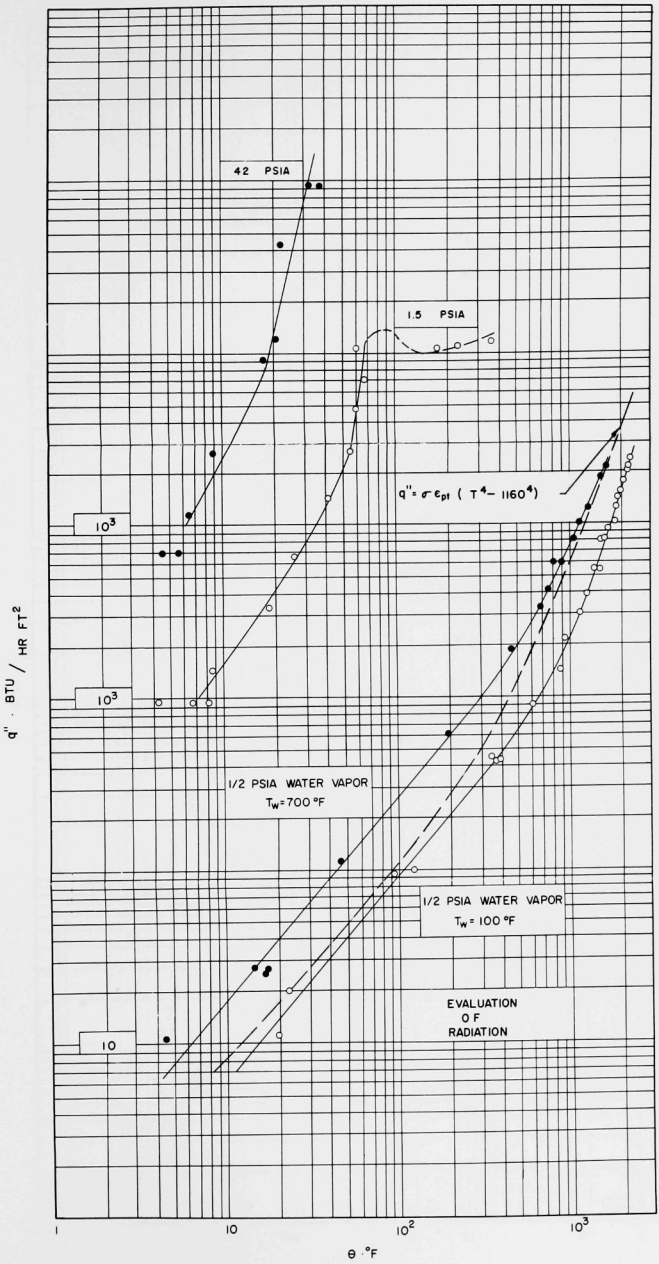

Fig. 22. Experimental Results for Evaluation of Radiation for $\frac{1}{8}$-in., Vertical Plate Test Section

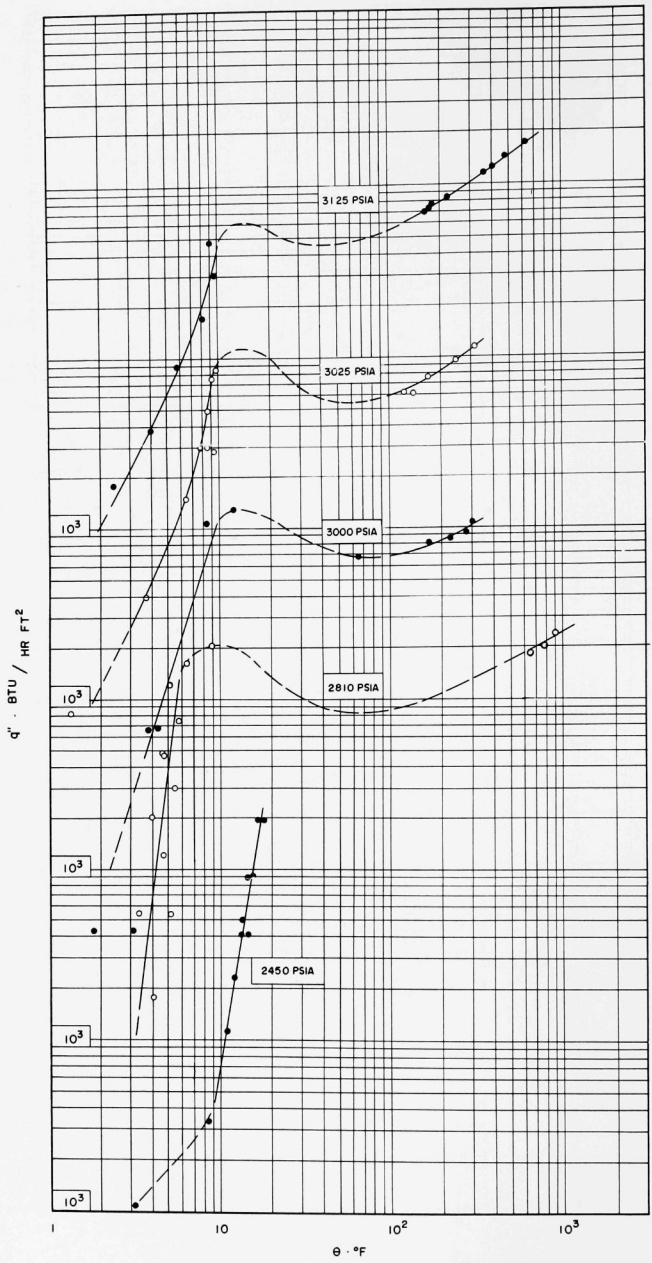

Fig. 23. Experimental Results from 2450 to 3125 psia for $\frac{1}{8}$-in., Vertical Plate

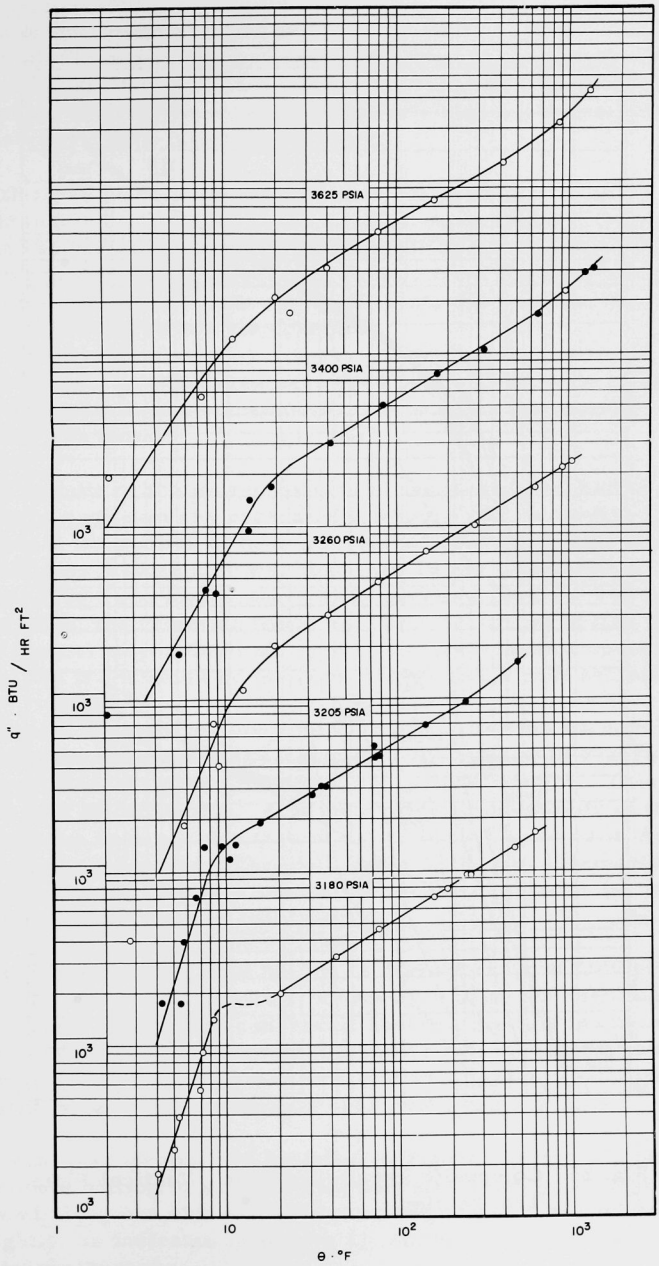

Fig. 24. Experimental Results from 3180 to 3625 psia for $\frac{1}{8}$-in., Vertical Plate Test Section

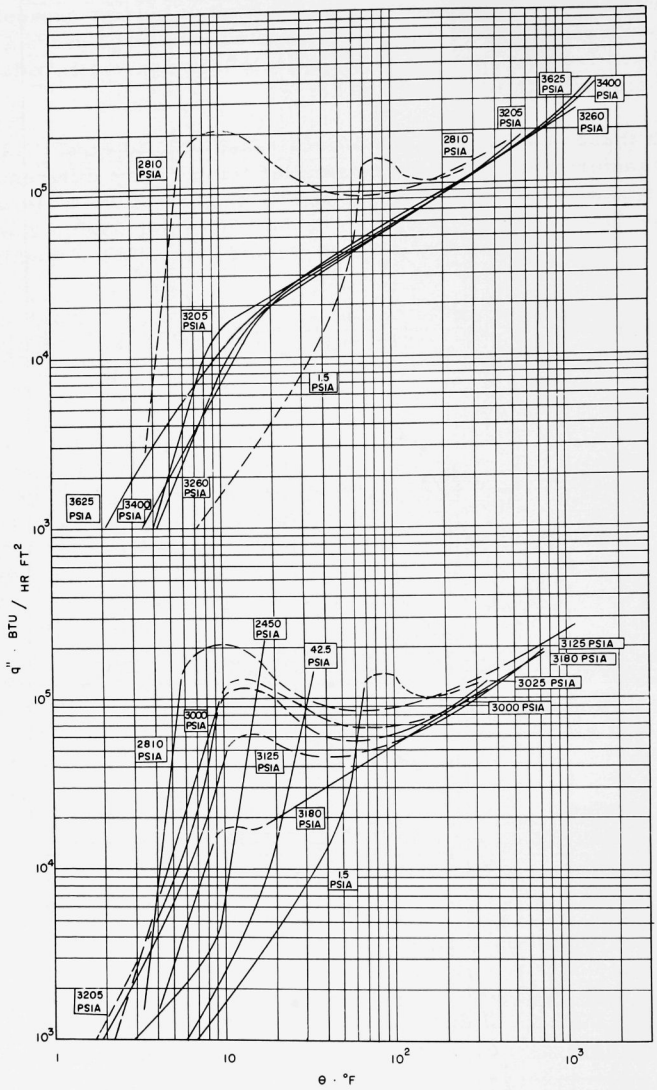

Fig. 25. Composite Results for $\frac{1}{8}$-in., Vertical Plate Test Section

The region of maximum specific heat at near-critical conditions essentially coincides with the region of maximum coefficient of volume expansion β.[72] Also, large values of β are generally associated with large buoyant forces in single-phase free convection, and relatively high convection rates are usually associated with large buoyant forces.

With these conditions in mind, it is reasonable to expect relatively high heat transfer coefficients at the smaller temperature differences with large values of specific heat and β throughout the heated fluid. However, since the specific heat and β decrease rapidly from the maximum with fluid temperature change, the lower coefficients observed for the higher temperature differences are also credible.

The measurements taken near 2400 psia appear to be a little out of line compared with the measurements taken at other pressures. No explanation for this was found.

The results of the measurements of the thermal radiation from the test section in a vacuum are presented in Figure 22. According to these measurements, the portion of heat transferred by radiation for the film boiling conditions investigated was less than 10 per cent of the total heat transferred, even up to temperature differences of 2000°F. For larger heating surfaces, the radiation would be more significant in film boiling because of the corresponding reduction in the heat transfer convection coefficients, as is indicated by the correlations in the next section.

Residual water in the connecting lines limited the vacuum to about $\frac{1}{2}$ psia during the radiation measurements. The results in Figure 22 indicated measured values greater than predicted for radiation. This may have been due in part to convection. Also, the effective emissivity of the test section may have been greater than assumed from Figure 43 in Appendix C for the lower temperatures. The main value of the measurements was to check experimentally the magnitude of the thermal radiation for test-section temperatures greater than 1000°F.

The process of nucleate boiling at pressures up to 3100 psia was photographed with limited success. Above 2800 psia, the associated gradients of fluid density and convection severely limited the observation of the test section, even with low heat transfer rates. This can be appreciated by noting the optical distortion due to very small density gradients in the natural convection of room air over room-heating units.

Several photographs are included in Figures 26 and 27. All pictures are for nucleate boiling to saturated liquid water from $\frac{1}{8}$-in.-high vertical plates viewed along one side and the lower edge. The test sections were curved slightly, as indicated in Figure 11, so the view of the heated surface would not be obstructed.

a. b. c.

Fig. 26. Photographs of Nucleate Boiling

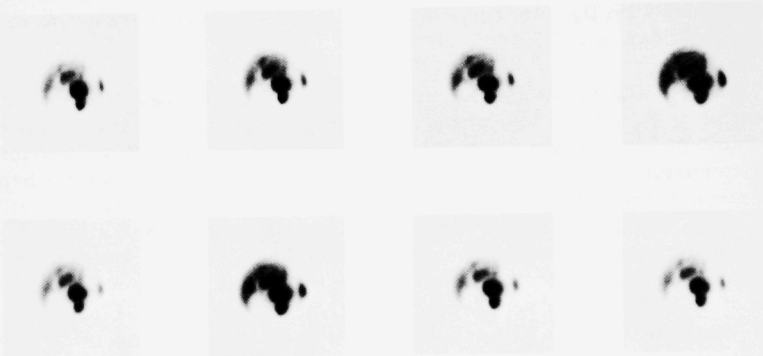

Fig. 27. Photographs for Motion Pictures of Nucleate Boiling

Figure 26a was a 1-sec time exposure for a heat flux of about 10^4 BTU/(hr)(ft^2) to saturated water at 2800 psia. The trace of several rising bubbles can be seen. The picture gives the impression that boiling from only one spot was photographed, but any bubbles along a $\frac{1}{2}$-in. length of the test section were also superposed in the field of view.

All photographs were taken through a $\frac{5}{16}$-in.-diameter port. Some of the distortion common to Figures 26a, b, and c was due to viewing windows.

Figure 26b was taken from a heat flux of about 10^4 BTU/(hr)(ft^2) to saturated water at 2400 psia. Exposure was made by a single strobe-light flash of about $\frac{1}{500}$-sec duration.

Figure 26c was a 1-sec time exposure for a heat flux of about 10^4 BTU/(hr)(ft^2) to saturated water at 2800 psia.

Figure 27 illustrates the rather poor results obtained from the attempts to take motion pictures of nucleate boiling at 2800 psia with a heat flux of about 10^5 BTU/(hr)(ft^2). The test-section arrangement was the same as in Figure 26. After the test section was energized, the field of view became increasingly distorted with time. Figure 27 was made a few seconds after the test section was energized. The bubbles show up as dark spots.

At pressures in the vicinity of the critical, the view of the test section was badly distorted, and sheets of rising fluid appeared to be passing the field of observation.

The nucleate and film boiling results are discussed in more detail in the following correlations and comparisons.

CORRELATION AND COMPARISON OF RESULTS

The experimental results were compared with the predictions of several of the correlations that have been proposed for nucleate and film boiling. The experimental results were also compared with the results of other experiments.

The predictions of the various correlations were compared with the experimental results of several investigations. This was done in an attempt to determine the relative general validity of the various correlations.

Most of the correlations were formulated for data obtained at atmospheric pressure. Two of the more suitable correlations were modified to apply for pressures up to near-critical as well as to near-atmospheric. The modifications were primarily based on the data of this investigation.

A review of the correlations that have been previously proposed is included in the literature survey.

An empirical nucleate boiling correlation is obtained in terms of reduced pressure P/P_c and the reduced heat flux q''/q''_{max}.

Values for the physical properties of water were obtained from references 21, 24, 33, 38, 39, 50, 60, 62, 70, 73, 85, 90, and 95. The properties of platinum were obtained from references 2, 3, 16, 29, 38, and 93. The properties of fluids other than water were obtained from references 38, 70, 79, 88, and 91. The values of surface tension for water that were used in the correlations are given in Appendix C.

The properties were all evaluated for the liquid state unless indicated otherwise. The density and specific heat of the liquid were evaluated at the average temperature of the superheated liquid, assumed to be one-half the temperature difference between the heated surface and the bulk fluid. Other liquid properties were evaluated at saturated liquid conditions.

The subscript v was used to denote vapor properties. The vapor properties were evaluated at the average vapor temperature.

Nucleate Boiling Peak Heat Flux

The correlation of nucleate boiling peak heat due to Rohsenow and Griffith[82] was compared with the data in Figure 28. Deviation is appreciable near the critical pressure.

A correlation for predicting the maximum nucleate boiling heat flux was obtained for the experimental data, and is presented in Figure 29 along with two other correlations which have been applied to several different fluids.

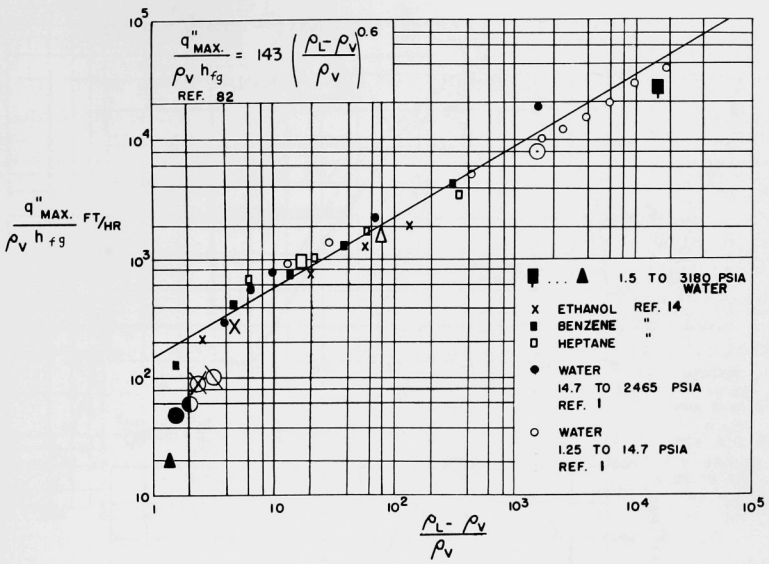

Fig. 28. Peak Nucleate Boiling Heat Flux Correlation of Rohsenow and Griffith(82)

The curves are plotted in the reduced form used by Cichelli and Bonilla(14) for correlating peak heat flux values for various fluids. This is open to some question, but it works quite well.

The equation due to Kutateladze(54) is plotted in Figure 29. This is one of the few nucleate boiling peak heat flux predictions which have been made.

The difficulty and uncertainty in evaluating fluid properties was averted in the correlation obtained to fit the experimental data of this investigation. It was assumed that the peak heat flux could be expressed as a function of the reduced pressure P/P_c. A third-order polynomial was fitted to the data by means of a least-squares polynomial determination program with the Purdue University Datatron 204 Computer. The resulting polynomial is given in Figure 29. The polynomials of higher order obtained offered little if any advantage over the third-order polynomial. The agreement with the other correlations is quite good.

It is not proposed that the polynomial obtained replace the equation due to Kutateladze(54); the polynomial was obtained in order to investigate the feasibility of expressing the peak nucleate boiling heat flux in terms of the reduced pressure for various fluids.

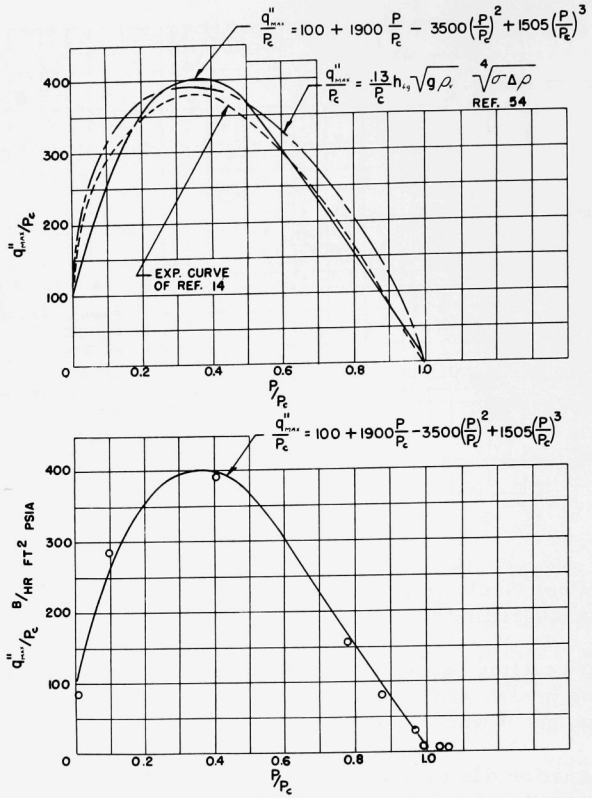

Fig. 29. Peak Nucleate Boiling Heat Flux Correlations of Kutateladze[54]

The polynomial obtained was used as the basis for an approximate qualitative correlation of nucleate boiling in general. This is presented in the next section.

Nucleate Boiling

The correlation due to Rohsenow[81] is compared with the experimental results in the first graph of Figure 30. Only a few representative data points are plotted for each pressure. The data points plotted were taken from values obtained near the peak nucleate boiling heat flux, from values obtained approximately in the middle of the nucleate boiling range, and from values obtained near the lowest nucleate boiling heat fluxes.

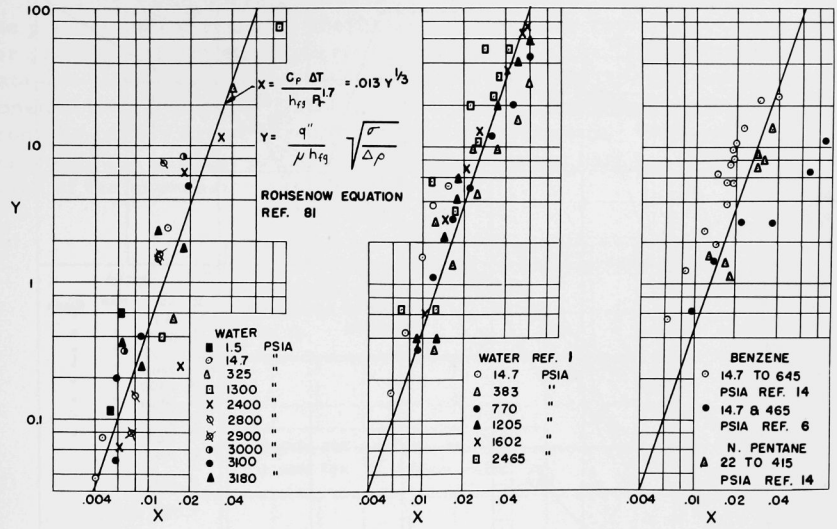

Fig. 30. Nucleate Boiling Correlation

The other two graphs in Figure 30 depict Rohsenow's correlation and other experimental data. Deviations of experiment from prediction are frequently as much as 500 per cent.

The nucleate boiling correlations are usually applied indiscriminately to horizontal surfaces, vertical surfaces, cylinders, and plates. This is done in Figure 30.

Systematic deviations are apparent in the comparison of various data with the Forster-Zuber prediction[31] in Figure 31. Straight lines are drawn to indicate the approximate deviation of the data from the prediction throughout the nucleate boiling region at various pressures. The correlation was originally fitted to the nucleate boiling heat fluxes near the maximum for the various fluids investigated by Cichelli and Bonilla.[14]

The correlation of Nishikawa and Yamagata[71] was modified to include a pressure factor term $P^{0.625}$ (pressure in atmospheres) as indicated in Figure 32. Most of the data are within a deviation of 100 per cent from the modified prediction, including the data of other investigations. This correlation appears to apply to other fluids as well as it applies to water.

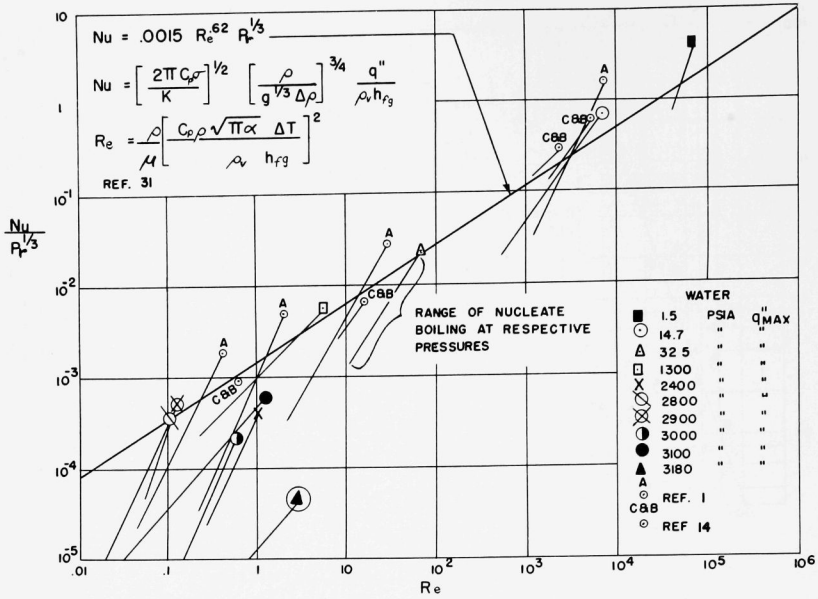

Fig. 31. Nucleate Boiling Correlation of Forster and Zuber(31)

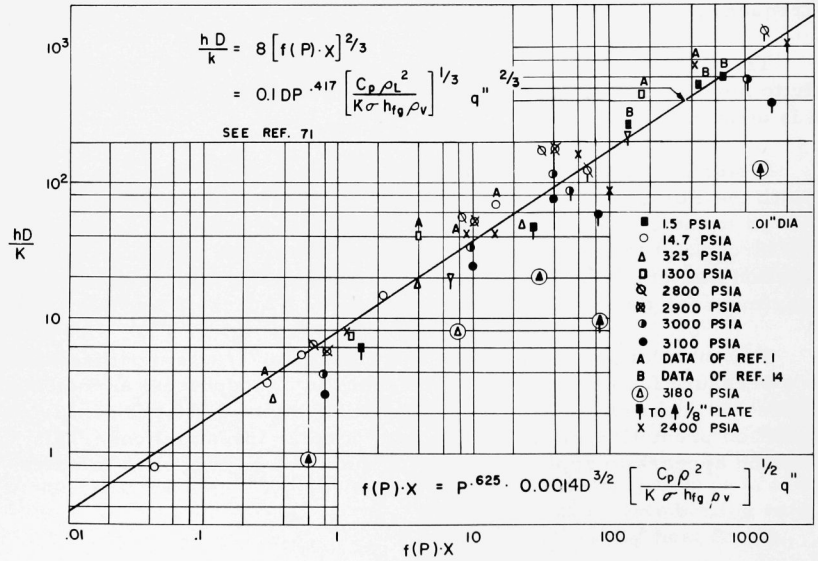

Fig. 32. Nucleate Boiling Correlation of Nishikawa and Yamagata(71)

This same correlation was plotted in Figure 33 in order to compare the predicted heat transfer coefficients with experimentally obtained values for pressures from atmospheric to the critical. The prediction and the data are plotted for a constant heat flux of 10^5 BTU/(hr)(ft^2) and also for a constant heat flux of 10^4 BTU/(hr)(ft^2). The plotted points were obtained from the curves drawn through the experimental data. The prediction fails near the critical pressure because the latent heat h_{fg} in the denominator of the expression approaches zero.

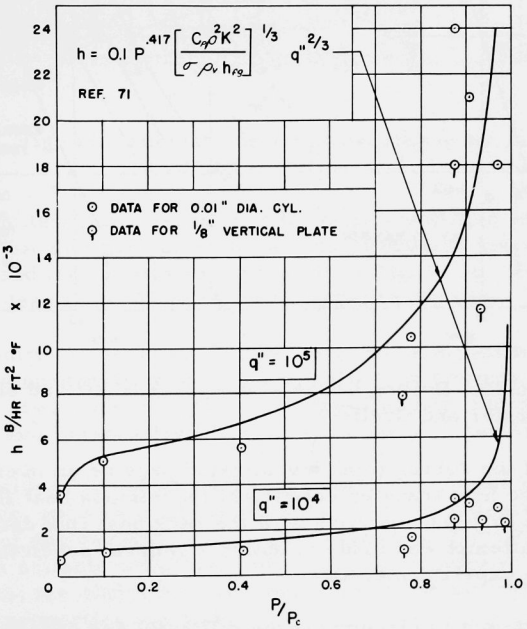

Fig. 33. Heat Transfer Coefficient and the Nucleate Boiling Correlation

The correlation of Levy[57] is compared with the data in Figure 34. Systematic deviations are apparent. The deviation of the prediction from experiment is often as much as 400 per cent for various data. The coefficient B_L was obtained from a plot of experimental data in reference 57.

The correlation of Engelberg-Forster and Greif[26] is subject to even greater deviation. The prediction is much too high for the higher pressures, as indicated in Figure 34.

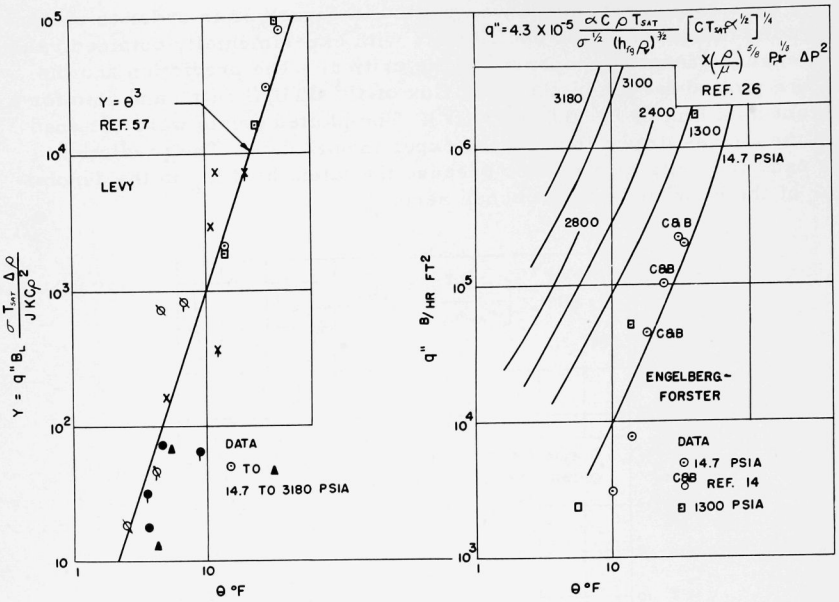

Fig. 34. Nucleate Boiling Correlations of Levy[57] and of Engelberg-Forster and Greif[26]

None of the correlations investigated provide an overall qualitative prediction of the heat transfer coefficient for various heat fluxes at pressures up to the critical. Starting with the peak heat flux data previously discussed, an attempt was made to obtain a general prediction based on the plots of the experimental data.

In an attempt to circumvent the difficulty and uncertainty in evaluating the many fluid properties usually considered pertinent to nucleate boiling, it was assumed that the heat transfer coefficient could be expressed as a polynomial in terms of the following operating variables:

1. reduced pressure P/P_c;
2. reduced heat flux q''/q''_{max}.

The heat transfer coefficients were determined from the plots of experimental data for the various pressures investigated and for values of q''/q''_{max} of 1, $\frac{3}{4}$, $\frac{1}{2}$, $\frac{1}{4}$, and $\frac{1}{50}$. Data from the 10-mil cylinder and the $\frac{1}{8}$-in. vertical plate were both considered. This information obtained from the experimental curves was used along with a least-squares polynomial determination program and the computer to obtain the curves of Figure 35. Polynomials of higher degree than three did not significantly improve the approximation.

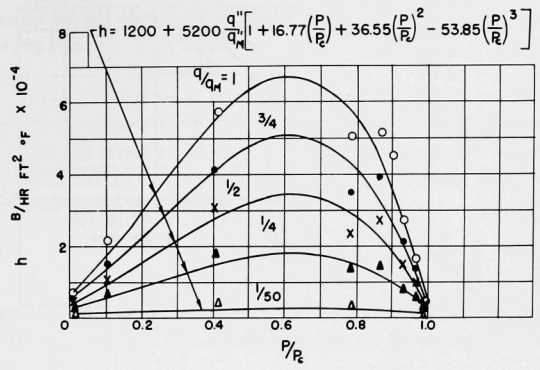

Fig. 35. Nucleate Boiling Correlation by Third-order Polynomial

The same third-degree polynomial was rearranged and plotted in a reduced form for comparison with the data of several investigations for several fluids, and the results are indicated in Figure 36. The deviation is considerably less than 100 per cent for most of the data.

The validity of assuming that the reduced form can be used for various fluids is open to question. It was used here because a similar approach to the prediction of peak nucleate boiling heat flux by Cichelli and Bonilla[14] and Kutateladze[55] was also quite successful.

The consideration of an empirical correlation in terms of the operating parameters, such as by the polynomial that was obtained, is justified by the absence of any suitable theoretical analysis of nucleate boiling and the absence of a suitable empirical correlation applicable to the higher pressures. Also, the difficulties and uncertainties in the evaluation of numerous fluid properties are averted.

In short, it is possible to achieve a closer approximation to the various data with the polynomial than has been achieved by the various correlations.

One limitation of the polynomial in Figure 36 is that q''_{max} must be known in order to establish the heat flux and temperature difference. It is assumed that the correlations of Figure 29 can be used to determine q''_{max}. Also, q''_{max} is one of the most extensively investigated characteristics of boiling.

For design purposes, the polynomial prediction in Figure 36 should be conservative.

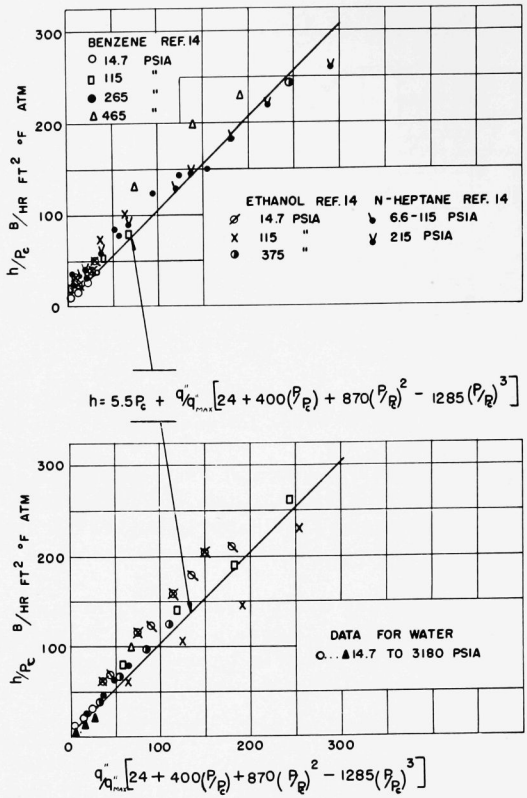

Fig. 36. Nucleate Boiling Correlation by Third-order Polynomial in Reduced Form

A maximum heat transfer coefficient for a particular per cent of the maximum nucleate boiling heat flux is indicated in Figure 35. According to the corresponding equation, this occurred at 62 per cent of the critical pressure, or at about 2000 psia for water.

In comparison, consider the maximum heat transfer coefficient observed for a particular constant heat flux. The experimental results indicated that a maximum heat transfer coefficient for a particular heat flux would be realized at about 87 per cent of the critical pressure, or at about 2800 psia for water, as is indicated in Figures 21, 25, and 33.

The two cases just considered are compatible because the highest value of peak nucleate boiling heat flux was realized at about 40% of the

critical pressure, or at about 1300 psia for water, and the peak heat flux decreased considerably from 1300 psia to the critical pressure.

Another interesting result is indicated in Figures 29 and 35. The peak nucleate boiling heat flux did not approach zero near the critical pressure. A region of heat transfer similar to nucleate boiling was observed at near-critical pressures. This is illustrated more clearly by the logarithmic plots of Figures 21 and 25.

Film Boiling

The film boiling data were compared by the analysis of McFadden[64] and with a modified form of the equation due to Bromley[10] (see Figures 37 and 38).

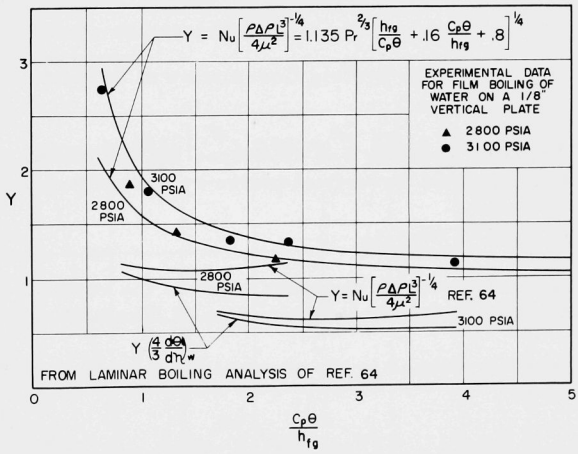

Fig. 37. Film Boiling Correlation of McFadden[64]

Bromley's equation was modified to a Nusselt number dependence on the Prandtl number to the $\frac{2}{3}$ power instead of the $\frac{1}{4}$ power. This has some justification and is discussed in the literature survey of film boiling. The resulting form of the equation as applied to laminar film boiling from vertical plates is as follows:

$$Nu = 1.135\ Pr^{2/3}\left[\frac{\rho\Delta\rho L^3}{4\mu^2}\right]^{1/4}\left[\frac{h_{fg}}{c_p\theta} + 0.16\ \frac{c_p\theta}{h_{fg}} + 0.8\right]^{1/4}, \qquad (24)$$

where all properties are for the average vapor condition except for the saturated liquid density ρ_L used in determining $\Delta\rho = (\rho_L - \rho_v)$.

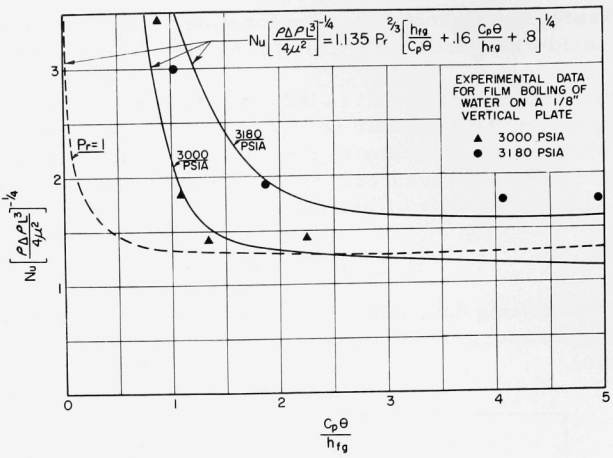

Fig. 38. Film Boiling Correlation of Bromley[10]

The Bromley equation was developed for horizontal cylinders, but was successfully applied to vertical plates by using the relation

$$Nu_{cyl} = 0.777\ Nu_{plate} \tag{25}$$

for horizontal cylinders with diameter equal to the vertical plate height. This was discussed in the literature survey of film boiling.

The Nusselt number is the average for a vertical plate of height L, and is defined as

$$Nu_{ave} = \frac{h_{ave}L}{k} = \frac{4}{3}\left(\frac{\rho_{sat}\ \Delta\rho L^3}{4\mu^2}\right)^{1/4}\left.\frac{d\theta}{d\eta}\right|_w , \tag{26}$$

where the last term is from the analysis of McFadden.[64] Note that the term inside the parentheses differs from the similar term in equation (24) by the use of ρ_{sat} for the vapor instead of the average vapor density.

The two densities are sometimes used interchangeably. The effect of using the average vapor density instead of ρ_{sat} in equation (26) is illustrated in Figure 37, where

$$Y = \frac{4}{3}\left.\frac{d\theta}{d\eta}\right|_w$$

is plotted below the correct curves for the analysis of McFadden.

The experimental data and equation (24) reflect somewhat larger Nusselt numbers than the results of McFadden for the two pressures (see Figure 37). This is reasonable because the experimental conditions were probably less stable than the conditions analyzed.

Several points that were evaluated from the experimental curves for 3000 psia and 3180 psia are plotted for comparison with equation (24) in Figure 38.

The modified Bromley correlation was also compared with other data for film boiling of several fluids from horizontal cylinders (see Figures 39 and 40). The data for the $\frac{3}{4}$-in. cylinder may be for turbulent flow conditions. The increase in Nusselt number with pressure indicated in Figure 40 is much greater than was observed for water or is indicated by the analysis of McFadden. The 0.069-in.-diameter cylinder test section may be too small to satisfy the boundary layer assumptions of the analyses, i.e., that the diameter be much greater than the vapor film boundary layer thickness.

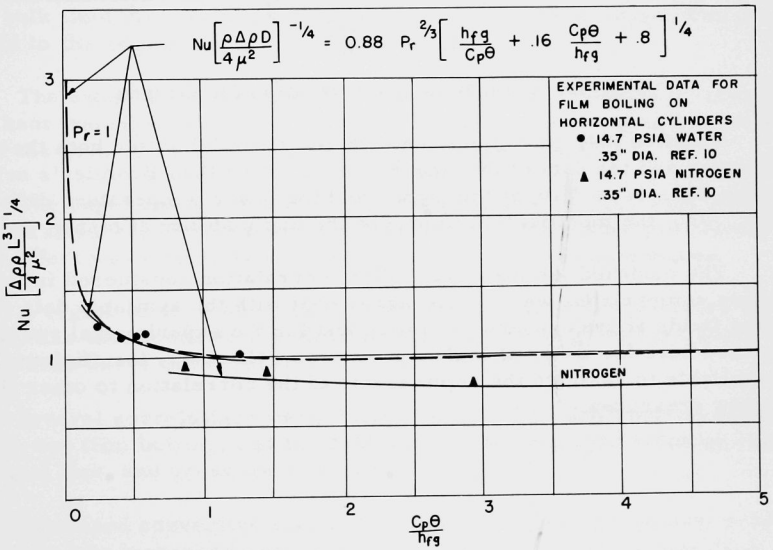

Fig. 39. Film Boiling Correlation for Nitrogen

The experimental data for the 10-mil-diameter cylinder was not included in the previous comparisons because the boundary layer requirements of the analyses were not satisfied (refer to the discussion of this in the literature survey on film boiling). Considerably higher heat transfer rates were obtained with the 10-mil-diameter test section than with the $\frac{1}{8}$-in. vertical plate.

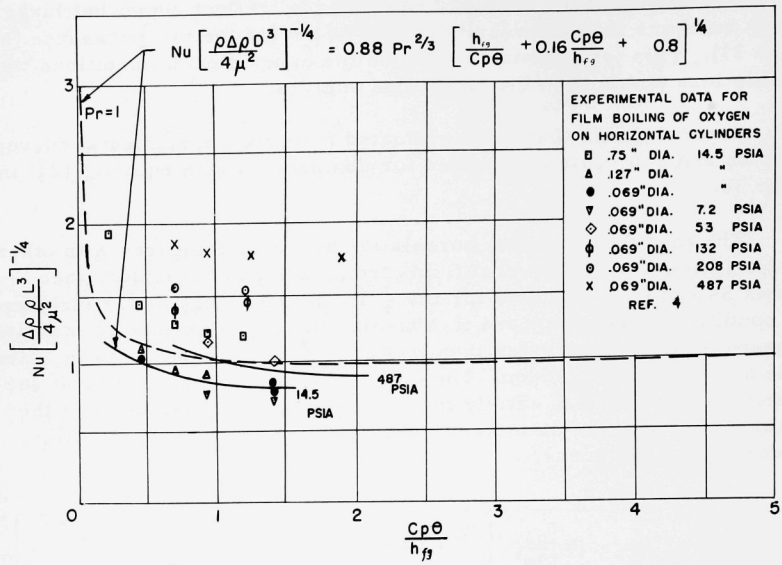

Fig. 40. Film Boiling Correlation for Oxygen

Equation (24), in conjunction with equation (25), fitted both the data of Bromley and the data of this investigation better than Bromley's original equation did - especially at the higher and the lower temperature differences. Also, the modification improved the applicability at higher pressures.

The modified laminar film boiling correlation considered in the previous comparisons was in good agreement with the available data for various fluids at atmospheric pressure and for the experimental results presented here for water at higher pressures. However, insufficient data are available to evaluate the applicability of the correlation to other fluids at higher pressures.

SUMMARY AND CONCLUSIONS

The literature review revealed the nonuniformity and scarcity of the available experimental data for nucleate and film boiling of various fluids at pressures above atmospheric. The absence of adequate methods for the analysis and correlation of nucleate boiling was also indicated by the literature. The use of inaccurately known fluid properties and the frequent extrapolation of very specific experimental results were complicating factors.

Suitable experimental apparatus was designed and constructed for measuring a wide range of rates of free convection heat transfer and for the associated temperatures for fluid pressures from a vacuum to 4000 psia and fluid temperatures up to 800°F.

Free convection nucleate and film boiling in water were experimentally investigated up to near-critical pressures and temperatures. Some high heat flux measurements were taken for free convection to water at pressures above the critical up to 3900 psia. The temperature of the bulk fluid for these measurements was arbitrarily adjusted to correspond to the region of maximum specific heat.

The experimental results for nucleate boiling indicated an increase in the heat transfer coefficient h with increased pressure up to almost 90 per cent of the critical pressure (for a particular heat flux q").

The experimental results for fully developed laminar film boiling indicated an increase in rate of heat transfer with increased pressures, but the effect was diminished at the higher temperature differences.

A region of decreasing heat flux with increasing temperature difference, like that associated with transition film boiling, was not observed at pressures above the critical.

Several correlations were compared with the experimental data for nucleate and film boiling, and the relationship between heat transfer coefficient, heat flux, and pressure was investigated.

Increased convective flow of the fluid and increased density gradients accompanied by increased optical distortion were observed within ±400 psi of the critical pressure. Near the critical pressures, the view of the test section was badly distorted, and sheets of fluid appeared to be passing the field of view.

Incorporation of a pressure accumulator into the system should improve the pressure control, particularly for pressures above the critical.

REFERENCES

1. Addoms, J. N., Sc.D. Thesis in Chem. Eng., M.I.T., (1948).
2. American Institute of Physics, Temperature: Its Measurement and Control in Science and Industry, Vol. I, Reinhold Pub. Corp., New York (1941); also Vol. II (1955).
3. American Society for Metals, Metals Handbook, American Society for Metals Pub. Co., Cleveland, O. (1948).
4. Banchero, J. I., G. E. Barker, and R. H. Boll, A.I.Ch.E. Chem. Eng. Prog. Symp. Series, 51(17), 21 (1955).
5. Bankoff, S. G., Trans. of the Amer. Soc. of Mech. Engrs., 79(4), 735 (1957).
6. Bogart, N. T., and A. L. Johnson, S. M. Thesis in Chem. Eng., M.I.T. (1938).
7. Bonilla, C. F., and C. W. Perry, Trans. Am. Inst. Chem. Engrs., 37, 685 (1941).
8. Borishanskii, V. M., Soviet Phys. - Technical Physics, 1(2), 438 (1956).
9. Bringer, R. P., and J. M. Smith, Journal of the Am. Inst. of Chem. Engrs., 3 49 (1957).
10. Bromley, L. A., Chem. Eng. Prog. 46 221 (1950). Also Ind. and Eng. Chem., 44(12) 2968 (1952) and 45(12), 2646 (1953).
11. Buchberg, H., F. Romie, R. Lipkis, and M. Greenfield, Heat Transfer and Fluid Mech. Inst., Stanford, Calif. (1951), p. 177.
12. Chang, Y. P., Trans. of the Am. Soc. of Mech. Engrs., 79, 1501 (1957).
13. Chang, Y. P., Trans. of the Am. Soc. of Mech. Engrs., Series C, Heat Transfer Journal, 81(1), 1 (1959).
14. Cichelli, M. T., and C. F. Bonilla, Trans. Am. Inst. Chem. Engrs., 41, 755 (1945).
15. Courty, C. and A. S. Foust, A.I.Ch.E. Chem. Eng. Prog. Symp. 51(17) 1 (1955).
16. Davisson, C. and J. R. Weeks, Jr., J. Opt. Soc. Am., 8 581 (1924).
17. Dean, L. E. and L. M. Thompson, Study of Heat Transfer to Liquid Nitrogen, A.S.M.E. paper 56-SA-4.
18. Dergarabedian, P., Trans. of the Am. Soc. of Mech. Engrs., J. of App. Mech., 20(4), 537 (Dec 1953).
19. Deissler, R. G., Trans. of the Am. Soc. of Mech. Engrs., 76(1), 73 (1954).
20. Donald, M. B. and F. Haslam, Chem. Eng. Sci., 8(3-4), 287 (1958).

21. Dorsey, N. E., Properties of Ordinary Water-Substance, Reinhold Pub. Corp., New York (1940).

22. Doughty, D. L. and R. M. Drake, Trans. of the Am. Soc. of Mech. Engrs., 78, 1843 (1956).

23. Drew, T. B., and A. C. Mueller, Trans. of the Am. Inst. of Chem. Engrs., 33, 449 (1937).

24. Eckert, E. R. G. and R. M. Drake, Jr., Heat and Mass Transfer, 2nd ed., McGraw-Hill Book Co., Inc., New York (1959).

25. Ellion, M. E., A Study of the Mechanism of Boiling Heat Transfer, Memo. No. 20-28, Jet. Prop. Lab., Calif. Inst. of Tech. (1954).

26. Engelberg-Forster, K. and R. Greif, Trans. of the Am. Soc. of Mech. Engrs., Series C, Heat Transfer Journal, 81(1), 43 (1959).

27. Faneuff, C. E., E. A. McLean, and V. E. Scherrer, Journal of App. Phys., 29,80 (1958).

28. Farber, E. A., and R. L. Scorah, Trans. of the Am. Soc. of Mech. Engrs., 70, 369 (May 1948).

29. Foote, P. D., N.B.S. Bul. 11, Sci. Paper 243, p. 607 (1914). Also, Acad. Sci. 5, 1 (1914).

30. Forster, H. K., Journal of App. Phys., 25, 1067 (1954).

31. Forster, H. K., and N. Zuber, Journal of the Am. Inst. of Chem. Engrs., 1, 531 (1955).

32. Frederking, T. H. K., Journal of the Am. Inst. Chem. Engrs., 5, 403 (1959).

33. Fritsch, C. A. and R. J. Grosh, ANL-6238 (Oct 1960)

34. Fritsch, C. A., and R. J. Grosh, Free Convective Heat Transfer to a Supercritical Fluid, ASME HT paper (1961).

35. Goldman, K., A.I.Ch.E. Chem. Eng. Prog. Symp. Series No. 11, 105 (1954).

36. Griffith, P. Trans. of the Am. Soc. of Mech. Engrs., 80, 721 (1958).

37. Griffith, J. D. and R. H. Sabersky, Am. Rocket Soc. Journal, 30, 289 (1960).

38. Handbook of Chemistry and Physics, 40th ed., Chem. Rubber Pub. Co., Cleveland, Ohio (1958).

39. Harned, H. S. and B. B. Owen, The Physical Chemistry of Electrolytic Solutions, 3rd ed., Reinhold Pub. Corp., New York (1958).

40. Haselden, G. G., and J. I. Peters, Trans. of the Inst. of Chem. Engrs. (British), 27, 201 (1949).

41. Hermann, R., Heat Transfer by Free Convection from Horizontal Cylinders in Diatomic Gases, NACA TM 1366 Translation (1936).

42. Holmon, J. P. and J. H. Boggs, Trans. of the Am. Soc. of Mech. Engrs., Series C, Heat Transfer Journal, 82(3), 221 (1960).

43. Hsu, Y. Y. and J. W. Westwater, Journal of the Am. Inst. of Chem. Engrs., 4(1), 58 (1958).

44. Hsu, S. T. and F. W. Schmidt, A.S.M.E. paper 60-HT-32.

45. Jakob, M., Fifth Int. Cong. for App. Mech., Cambridge, Mass., John Wiley and Sons, Inc., New York (1938).

46. Jakob, M., Heat Transfer, John Wiley and Sons, New York (1949) Vol. I.

47. Jicha, J. J., and E. J. Lemanski, Nucleate Boiling Literature Search, AEC MND-1062 and MND-1062-1 (Apr 1957).

48. Kazakova, E. A., included in reference 54.

49. Kellett, B. S., J. Opt. Soc. Am. 42, 339 (1952).

50. Keenan, J. H., and F. G. Keyes, Thermodynamic Properties of Steam, John Wiley and Sons, New York (1936).

51. Kreith, F. and M. Summerfield, Trans. of the Am. Soc. of Mech. Engrs., 71, 805-15 (1949).

52. Kucherov, R. Y. and L. E. Rikenglaz, Soviet Phys.-Journal of Exp. and Th. Phys., 37(1), 88 (1960).

53. Kurihara, H. M., Ph.D. thesis in Chem. Eng., Purdue University (1956).

54. Kutateladze, S. S., Zhurn. Tekh. Fiz., 20(11), 1389 (1950).

55. Kutateladze, S. S., Heat Transfer in Condensation and Boiling, AEC tr 3405 (1952), and 2nd ed. AEC tr 3770 (1953).

56. Leidenfrost, W., Prof. of Mech. Eng., Purdue University, personal communication.

57. Levy, S., Trans. of the Am. Soc. of Mech. Engrs., Series C, Heat Transfer Journal, 81(1), 37 (1959).

58. Liley, P. E., Assist. Prof. of Mech. Eng., Purdue University, personal communication.

59. Lowry, A. J., and J. W. Westwater, Ind. and Eng. Chem. 49, 1445 (1957).

60. Macleod, D. B., Trans. Faraday Soc., 19, 38 (1923).

61. Madsen, D. H., M. S. thesis in Mech. Eng., Purdue University (1948).

62. McAdams, W. H., Heat Transmission, 3rd ed., McGraw-Hill Book Co., Inc., New York (1954).

63. McAdams, W. H., J. N. Addoms, P. M. Rinaldo, and R. S. Day, Chem. Eng. Prog., 44, 639 (1948).

64. McFadden, P. W. and R. J. Grosh, ANL-6064 (Oct 1959).

65. Mead, B. R., F. E. Romie, and A. G. Guibert, Heat Transfer and Fluid Mech. Inst., Stanford, Calif. (1951), p. 209.

66. Merk, H. J., and J. A. Prins, App. Sci. Res. (Holland), Section A, 4(1), 11 (1953); and 5(3), 195 (1954).

67. Mesler, R. B. and J. T. Banchero, Journal of the Am. Inst. of Chem. Engrs., 4(1), 102 (1958).

68. Miropolski, L. and M. E. Shitsman, Soviet Physics-Technical Physics, 2(10), 2196 (1957).

69. Morgan, A. I., L. A. Bromley, and C. R. Wilke, Ind. and Eng. Chem., 41, 2767 (1949).

70. National Research Council, International Critical Tables, McGraw-Hill Book Co., Inc., New York (1933).

71. Nishikawa, K. and K. Yamagata, Int. Journal of Heat and Mass Transfer, 1, No. 2/3 (Aug 1960).

72. Nowak, E. S., Graduate Assistant, Purdue University, personal communication regarding ANL-6064 and related work.

73. Nowak, E. S., R. J. Grosh, and P. E. Liley, Trans. Am. Soc. of Mech. Engrs., Series C, Heat Transfer Journal, 83(1), 1, 14 (1961).

74. Nukiyama, S., Journal of the Soc. of Mech. Engrs. (Japan), Vol. 37, No. 206, p. 367 (1934).

75. Nusselt, W., Zeit. Ver. deut. Ing., 60, 541 (1916).

76. Pilling, N. B., and T. D. Lynch, Trans. Am. Inst. of Min. and Met. Engrs., 62, 665 (1920).

77. Plesset, M. S., and S. A. Zwick, J. Appl. Phys., 23, 95 (1952).

77a. Plesset, M. S., and S. A. Zwick, J. Appl. Phys., 25, 493 (1954).

78. Powell, W. B., Jet Propulsion, 27, 776 (1957).

79. Properties of Materials at Low Temperatures, Phase I, N.B.S. Cryogenic Eng. Lab., Denver, Colo. (Dec 1959).

80. Rayleigh, Lord, Phil. Mag., 34, 94 (1917).

81. Rohsenow, W. M., Trans. of the Am. Soc. of Mech. Engrs., 74 (1952).

82. Rohsenow, W., and P. Griffith, A.I.Ch.E. Chem. Eng. Prog. Symp. Series, 52(18), 47 (1956).

83. Rohsenow, W. M., P. Griffith, and P. J. Berenson, Trans. of the Am. Soc. of Mech. Engrs., 80, 716 (1958).

84. Romie, F. E., S. W. Brovarsy and W. H. Giedt, Trans. of the Am. Soc. of Mech. Engrs., Series C, Heat Transfer Journal, 82(4), 387 (1960).

85. Sato, K., Journal of Chem. Eng. (Japan), 18, 266 (1954).

86. Schmidt, E., Int. Journal of Heat and Mass Transfer, 1(1), 92 (1960).

87. Schmidt, E., E. R. G. Eckert, and U. Grigull, Heat Transfer by Liquids near the Critical State, A.A.F. Translation 527 (1939).

88. Scott, R. B., Cryogenic Engineering, D. van Nostrand Co., Inc., Princeton, N. J. (1960).

89. Studies in Boiling Heat Transfer, COO-24 (AEC), Univ. of Calif., L. A. (March 1951).

90. Tables of Thermodynamic Properties of Water and Water Vapor, Moscow - Leningrad (1952). Translated by G. V. Krenikoff, Westinghouse Elect. Corp. (1954).

91. U.S. Dept. of Commerce, Tables of Thermal Properties of Gases, N.B.S. Circular 564, U.S. Gov't Printing Office, Washington, D.C.

92. Van Camp, W. M., Ph.D. thesis in Mech. Eng., Purdue University (1952).

93. Vines, R. F., The Platinum Metals and Their Alloys, Int. Nickel Co., Inc., New York (1941).

94. Viskanta, R., ANL-6170 (May 1960).

95. Volyak, L. D., Teploenergetika, 5(7), 33 (July 1958).

96. Wallis, G. B., Nuclear Power, 5(52), 99 (1960).

97. Westwater, J. W., Advances in Chemical Engineering, Academic Press Inc., (1958), Vols. I and II.

98. Westwater, J. W., and J. G. Santangelo, Ind. Eng. Chem., 47, 1605 (1955).

99. Wooldridge, C. B., Ph.D. thesis in Eng. Sci., Purdue University (1958).

100. Zmola, P. C., Ph.D. thesis in Mech. Eng., Purdue University (1950).

101. Zuber, N., Trans. of the Am. Soc. of Mech. Engrs., 80, 711 (1958).

APPENDIX A

NOMENCLATURE

A	Heat transfer surface area or a constant if so noted	ft^2
A_x	Cross-section area	ft^2
C	Specific heat	BTU/(lb)(°F)
C_p	Specific heat at constant pressure	BTU/(lb)(°F)
D	Diameter	ft
Gr	Grashof number	dimensionless
g	Acceleration due to gravity	4.17×10^8 ft/hr^2
h	Heat transfer coefficient	BTU/(hr)(ft^2)(°F)
h_{fg}	Latent heat of vaporization	BTU/lb
I	Electric current	amp
J	Mechanical equivalent of heat	778(ft)(lb)/BTU
L, l	Length	ft
Nu	Nusselt number hD/k	dimensionless
P	Pressure	lb/ft^2 or atmospheres
Pr	Prandtl number $C_p\mu/k$	dimensionless
q	Heat transferred	BTU/hr
q"	Heat transfer rate per unit area	BTU/(hr)(ft^2)
R	Resistance	ohms
Re	Reynolds number vD/ν	dimensionless
T	Temperature	°F or °R
t	Temperature or time in seconds as noted	°C
u	Velocity in x-direction	ft/sec
v	Velocity in y-direction	ft/sec
V	Voltage potential	volts
x	Coordinate along a surface	ft
y	Coordinate perpendicular to a surface	ft

α	Thermal diffusivity $k/\rho C_p$	ft^2/hr
β	Coefficient of volume expansion	$°R^{-1}$
Δ	Difference	
$\Delta\rho$	Difference between the liquid density and the vapor density ($\rho_L - \rho_v$)	lb/ft^3
δ	Boundary layer thickness	ft
ϵ	Emissivity	dimensionless
θ	Temperature difference between surface and fluid ($T_w - T_\infty$)	°F
μ	Absolute viscosity	lb/(ft)(hr)
ν	Kinematic viscosity	ft^2/hr
ρ	Density	lb/ft^3
σ	Surface tension	lb/ft

$\left[\frac{d\theta}{d\eta}\right]_w$ Temperature gradient at the heat transfer surface wall where η is the dimensionless independent variable used in the similarity transformation of reference 64, and θ is the dimensionless temperature in reference 64.

Subscripts

L	Liquid
S, sat	Saturated conditions
T	Total
v	Vapor
w	Wall or heated surface
∞	Bulk fluid condition

APPENDIX B

TABULATION OF DATA AND RESULTS

The data were tabulated in two sections. The first section is for the 10-mil-diameter test sections and the second section is for the $\frac{1}{8}$-in. vertical plate test sections. The following observed data were tabulated:

1) fluid pressure P (psia);

2) resistance R_T, of the thermometer used for determining fluid temperature;

3) voltage drop ΔV_x across the test section;

4) voltage drop ΔV_R across the standard resistance in the circuit.

Also, the computer results for heat flux q", fluid temperature T_∞, and temperature difference θ are tabulated.

Data for 10-mil-diameter Test Sections

Observed Data				Computed Results		
P	R_T	$\Delta V_x/20$	ΔV_R	T_∞	θ	q" x 10^{-4}
14.6	35.592	0.009646	0.009814	212.1	5.2	.105
	35.575	0.043	0.04268	211.8	17.5	1..99
	35.550	0.04466	0.04454	211.2	19.2	2.21
	35.562	0.06455	0.06365	211.6	20.9	4.38
	35.570	0.0651	0.06467	211.9	21.8	4.66
	35.582	0.0655	0.0649	212	22.1	4.8
	35.563	0.07477	0.07383	211.7	25.5	6.14
	35.570	0.0895	0.0792	211.9	28.8	7.3
	35.590	0.0905	0.07972	212.5	30	7.46
	35.597	0.1212	0.1186	212.1	33.8	15.7
	35.634	0.1287	0.1252	212.9	37	18.6
	35.635	0.1372	0.1341	213	42.8	23.8
	35.637	0.1385	0.1348	213.1	40	25.5
	35.637	0.137	0.1338	213.1	35.5	23.2
	35.64	0.13611	0.1333	213	30	20.2
	35.634	0.1277	0.12505	212.9	29.8	18
	35.635	0.1279	0.1255	212.9	30.1	18.2
	35.562	0.1280	0.1257	211.55	31.7	18.5
	35.57	0.1290	0.11806	211.9	32	15.8
	35.590	0.07537	0.0746	212.1	23.8	6.26

Data for 10-mil-diameter Test Sections (Cont'd.)

Observed Data				Computed Results		
P	R_T	$\Delta V_{x/20}$	ΔV_R	T_∞	θ	q" x 10^{-4}
	35.580	0.0887	0.081	212	27.5	7.8
	35.580	0.08915	0.0856	212	26	8.4
	35.581	0.0899	0.0888	211.9	26.2	9.1
	35.580	0.08989	0.08874	211.9	30	9
	35.638	0.0677	0.06005	212.9	20.6	4.22
	35.682	0.0396	0.0392	213.7	18	1.6
	35.550	0.03978	0.03968	211.7	20	1.76
	35.640	0.0365	0.03237	213	15	1.20
	35.660	0.0365	0.03237	213.3	16.2	1.2
	35.550	0.03378	0.03385	211.7	16	1.27
	35.550	0.02628	0.02644	211.7	15.4	0.77
	35.592	0.0169	0.01716	212.1	9	0.322
	35.597	0.01689	0.01715	212.2	8.6	0.32
	35.552	0.0095	0.00967	211.5	5.6	0.102
	35.601	0.0097	0.00985	212.3	7.7	0.116
	35.548	0.01194	0.01213	211.7	7.5	0.161
Test-section Length: 2.8125 in.						
320	46.970	0.03343	0.02556	423.2	11.25	0.915
320	46.975	0.06115	0.04464	423.4	12.7	2.85
325	47.031	0.0455	0.03383	424.2	22.5	1.62
322½	47.005	0.1574	0.1129	423.6	24.7	18.5
322½	47.010	0.2245	0.1601	423.8	27.9	37.4
322½	47.007	0.2347	0.1665	423.6	34.4	40.8
325	47.02	0.2521	0.1792	424	34.2	47.2
322½	47.005	0.2625	0.1842	423.6	43.5	50.46
Test-section Length: 3.0 in.						
1300	55.033	0.01256	0.00808	577.4	5.4	0.1129
	55.027	0.01256	0.008075	577.3	5.5	0.1323
	55.025	0.01408	0.009284	577.2	5.57	0.1454
	55.0225	0.02843	0.018684	577.2	9.91	0.5909
1295	55.0115	0.03535	0.02322	577	9.9	0.913
1290	55.0045	0.04382	0.02873	576.7	12.25	1.400
	54.960	0.01224	0.00808	576.0	5.62	0.1102
1285	54.957	0.012235	0.00807	575.9	6.56	0.1098
	54.957	0.0381	0.02503	575.9	10.86	1.061
1290	54.965	0.05544	0.0363	576.1	14.31	2.239

Data for 10-mil-diameter Test Sections (Cont'd.)

Observed Data				Computed Results		
P	R_T	$\Delta V_{x/20}$	ΔV_R	T_∞	θ	q" x 10^{-4}
	54.968	0.05532	0.03268	576.1	12.33	2.233
	54.969	0.07097	0.04651	576.1	13.1	3.672
	54.973	0.0709	0.04652	576.5	11.9	3.669
	54.98	0.08265	0.0542	576.4	12.35	4.983
	54.996	0.08263	0.0542	576.7	11.7	4.983
	54.997	0.08263	0.0542	576.7	12.7	4.982
	54.997	0.099265	0.06502	576.7	13.3	7.18
	54.995	0.09923	0.06498	576.7	13.6	7.173
	54.994	0.112475	0.07353	576.7	15.34	9.20
	54.994	0.11249	0.07357	576.7	15	9.206
	54.995	0.11257	0.0736	576.7	18.2	9.241
	54.994	0.1126	0.07361	576.7	15.45	9.220
	54.998	0.12745	0.08316	576.7	17.4	11.791
	55.00	0.12745	0.08312	576.75	17.9	11.784
1295	55.015	0.14596	0.09505	577.1	19.2	15.432
	55.016	0.14595	0.09508	577.1	17.2	15.437
1290	54.97	0.1489	0.09713	576.2	18.2	16.088
	54.983	0.1491	0.09706	576.4	20.1	16.095
	54.992	0.16295	0.10648	576.46	16	19.3017
1295	55.02	0.16335	0.10638	577.1	19.1	19.332
1295	55.02	0.1634	0.10634	577.1	19.88	19.33
1300	55.026	0.1744	0.11321	577.2	22.54	21.96
	55.035	0.1744	0.11334	577.4	21.1	21.99
	55.02	0.1787	0.1160	577.2	22.7	23.06
	55.022	0.1787	0.1160	577.2	22.4	23.066
	55.048	0.1929	0.1251	577.7	23.7	26.84
	55.055	0.1928	0.12506	577.8	23	26.46
1295	55.002	0.19565	0.1268	576.8	24.5	27.60
1300	55.028	0.19565	0.12675	577.3	24.7	27.587
	55.04	0.2076	0.1343	577.5	26.1	31.14
	55.06	0.2074	0.13426	577.7	25	30.976
1305	55.07	0.2142	0.1385	577.9	25.8	33.012
	55.084	0.2142	0.13855	578	25.5	32.54
1310	55.095	0.2209	0.1428	578.4	25.8	35.096
	55.103	0.22085	0.1428	578.6	25.4	35.086

Data for 10-mil-diameter Test Sections (Cont'd.)

Observed Data				Computed Results		
P	R_T	$\Delta V_{x/20}$	ΔV_R	T_∞	θ	q" x 10^{-4}
	55.113	0.230	0.14854	578.8	26.6	38.005
1320	55.13	0.244	0.1578	580.9	23	42.837
	55.15	0.2444	0.1578	579.6	26.1	42.901
1325	55.17	0.250	0.16115	580	27.5	44.817
	55.19	0.260	0.16745	580.4	27.9	48.422
1330	55.206	0.26675	0.1717	580.7	28.37	50.95
1335	55.235	0.2772	0.17835	581.3	28.4	55.007
	55.255	0.2892	0.1858	581.7	29.2	59.79
1340	55.285	0.3072	0.19705	582.1	30.7	67.34
1350	55.33	0.31275	0.20055	583	30.2	69.774
1360	55.37	0.34905	0.22325	584	32.3	86.69
1365	55.40	0.351	0.2243	584.2	32.6	87.581
1360	55.36	0.3593	0.2294	583.8	34.4	91.69
1375	55.43	0.3943	0.2532	585.2	26.65	111.061
1385	55.50	0.4028	0.2546	586.3	43	114.08
1335	55.26	0.4259	0.2710	581.8	40.2	128.26
1330	55.20	0.4229	0.2705	580.6	35.8	127.25
	55.20	0.4623	0.2945	580.6	40.1	151.45
1345	55.28	0.4609	0.2945	582.2	35.1	150.99
1355	55.33	0.4790	0.3048	583.1	40.2	162.41
1360	55.42	0.4780	0.3048	584.8	33.1	162.07
1380	55.52	0.5044	0.315	586.6	56.4	176.75
2495	59.658	0.013903	0.0087	667.8	2.3	0.1345
	59.648	0.013904	0.0087	667.8	3.25	0.1345
	59.625	0.009532	0.005956	667.5	3	0.0631
2490	59.621	0.009533	0.005955	667.2	3.5	0.0631
2495	59.643	0.03352	0.02075	667.6	5	0.7737
2500	59.695	0.07379	0.04486	668.7	7	3.682
	59.666	0.07383	0.04489	668	7.5	3.687
	59.677	0.10199	0.06145	668.2	7.7	6.917
	59.682	0.10122	0.06145	668.4	8.4	6.919
	59.674	0.12118	0.07356	668.2	9.2	9.916
	59.663	0.14923	0.09059	668.0	11.3	15.039
	59.666	0.18525	0.1123	668.1	11.0	23.142
	59.674	0.2108	0.1274	668.2	13.6	29.87
	59.678	0.2109	0.1278	668.3	13.0	29.98

Test-section Length: 2.8125 in.

Data for 10-mil-diameter Test Sections (Cont'd.)

Observed Data				Computed Results		
P	R_T	$\Delta V_{x/20}$	ΔV_R	T_∞	θ	q" x 10^{-4}
2650	60.00	0.008072	0.008055	674.6	5.02	0.118
2685	60.17	0.03336	0.03325	678	3.08	2.019
2695	60.215	0.05402	0.05375	678.9	4.23	5.286
	60.217	0.08103	0.08039	678.9	7.69	11.86
	60.217	0.10913	0.10774	678.9	13.57	21.4
	60.218	0.13124	0.1330	678.9	9.55	31.05
2700	60.23	0.13662	0.13517	679.2	10.7	33.62
	60.246	0.13442	0.13378	679.5	3.33	32.7
	60.21	0.1505	0.14578	678.8	37	39.9
	60.24	0.1736	0.1725	679.4	5.35	54.51
2705	60.26	0.2548	0.1324	679.8	1235	61.41
2715	60.28	0.2086	0.1214	680.2	929.8	46.1
	60.27	0.2086	0.1216	680	926	46.18
2825	60.65	0.1691	0.1116	687.5	640.4	34.35
2705	60.257	0.1702	0.1117	679.7	659.7	34.61
2705	60.25	0.1382	0.1016	679.6	443.7	25.56
2700	60.22	0.09685	0.09635	679	4.33	16.98
	60.22	0.3095	0.14385	679	1601	81.05
2705	60.25	0.3098	0.1438	679.6	1605	81.1
2725	60.31	0.2442	0.12925	680.8	1181	57.46
2740	60.33	0.2438	0.1287	681.2	1188	57.12
2720	60.27	0.1817	0.1795	680	11.75	59.37
2740	60.491	0.00996	0.006007	683.3	1.13	0.0666
2790	60.495	0.009957	0.006	684.4	1.75	0.06646
	60.496	0.013756	0.00829	684.4	1.6	0.1268
2790	60.498	0.02058	0.01239	684.5	2.75	0.2836
	60.499	0.02056	0.012385	684.5	2.32	0.2833
	60.501	0.00991	0.00597	684.5	1.92	0.0658
2795	60.508	0.020375	0.01228	684.7	1.23	0.2783
	60.510	0.037285	0.02245	684.7	2.36	0.9312
	60.510	0.05704	0.03433	684.7	2.88	2.178
	60.510	0.07197	0.04328	684.7	3.81	3.466
2800	60.514	0.08991	0.05406	684.8	3.99	5.407
	60.518	0.10576	0.06362	684.9	3.4	8.785
	60.523	0.12261	0.07368	685	4.43	10.05

Data for 10-mil-diameter Test Sections (Cont'd.)

Observed Data				Computed Results		
P	R_T	$\Delta V_{x/20}$	ΔV_R	T_∞	θ	q" x 10^{-4}
	60.526	0.13393	0.08054	685	3.54	12.0
	60.534	0.15974	0.09599	685.2	4.35	17.056
2805	60.543	0.1818	0.1093	685.4	3.52	22.105
2810	60.562	0.1937	0.1162	685.7	5.75	25.04
2820	60.59	0.2478	0.1047	686.3	535	28.862
	60.60	0.302	0.1139	686.5	772	38.265
	60.62	0.3515	0.1215	686.9	980	47.509
	60.599	0.2617	0.1071	686.5	598	31.18
	60.61	0.23635	0.1022	686.7	491	26.92
	60.608	0.2175	0.09826	686.7	414	23.77
	60.607	0.1856	0.09057	686.6	286	18.7
	60.601	0.1467	0.08484	686.4	50	15.8
	60.593	0.11965	0.07177	686.4	5.3	9.553
2815	60.584	0.10264	0.06158	686.2	5.2	7.031
	60.574	0.08268	0.04962	686	4.9	4.594
2795	60.54	0.08266	0.04962	684.2	6.5	4.563
	60.542	0.1915	0.11495	684.2	6.6	24.49
2805	60.551	0.1782	0.10685	685.5	6.6	21.18
	60.556	0.1378	0.0826	685.6	6.85	12.66
	60.55	0.1062	0.06365	685.5	7.1	7.52
2795	60.544	0.0819	0.0492	684.3	5.6	4.483
2790	60.536	0.06735	0.04053	684.2	3.55	3.037
	60.52	0.02841	0.0163	684	3.1	0.576
2875	60.76	0.008695	0.00857	688.5	6.0	0.136
2890	60.763	0.00865	0.00856	689.8	9.8	0.135
	60.76	0.05202	0.05125	689.7	5.36	4.85
	60.755	0.05185	0.0512	689.6	2.68	4.83
	60.755	0.0872	0.0859	689.6	5.87	13.63
2890	60.757	0.11487	0.11293	689.6	7.99	23.61
	60.767	0.12636	0.1239	689.8	11	28.5
2895	60.78	0.1327	0.1305	690	7.5	31.53
	60.79	0.1331	0.1307	690.2	8.8	31.685
	60.795	0.1493	0.1464	690.3	10.7	39.78
	60.785	0.1836	0.120	690.2	658	40.11
	60.792	0.1846	0.1195	690.3	678	40.16
2900	60.798	0.1239	0.1033	690.4	229	23.3
2890	60.787	0.1243	0.1032	689.8	236	23.35
2900	60.786	0.1412	0.110	690.2	335	28.3

Data for 10-mil-diameter Test Sections (Cont'd.)

Observed Data				Computed Results		
P	R_T	$\Delta V_{x/20}$	ΔV_R	T_∞	θ	$q'' \times 10^{-4}$
	60.785	0.1402	0.1103	690.2	319	28.15
	60.785	0.09933	0.0911	690.2	96	16.47
2895	60.772	0.0978	0.09113	690.0	75	16.22
	60.770	0.09685	0.09113	689.9	62.4	16.07
	60.764	0.08246	0.08127	689.7	4.8	12.2
2890	60.755	0.08132	0.08025	688.6	8.4	11.88
2895	60.77	0.15415	0.15082	689.8	13.6	42.3
	60.80	0.1792	0.1309	690.4	444	42.7
2900	60.82	0.1794	0.1305	690.8	451	42.62
2910	60.83	0.1408	0.1144	691	267	29.32
	60.832	0.1411	0.1145	691.1	269	29.41
	60.84	0.1548	0.1206	691.2	334	34
3050	61.15	0.00867	0.0085	697.3	3.34	0.134
	61.16	0.008667	0.00848	697.4	6.05	0.134
3085	61.253	0.03532	0.03447	699.4	6.9	2.22
	61.258	0.064365	0.06275	699.5	8.3	7.35
3090	61.265	0.06395	0.062655	699.7	2.1	7.29
3095	61.269	0.09039	0.08027	699.8	129.3	13.21
3100	61.286	0.09001	0.08013	700	125	13.13
3090	60.26	0.00815	0.0081	689.8	4.65	0.12
3095	61.262	0.00817	0.00798	699.6	5.9	0.12
	61.262	0.04386	0.0429	699.6	4.2	3.42
	61.263	0.04382	0.04283	699.6	5.04	3.42
	61.263	0.05986	0.05856	699.6	3.95	6.38
	61.263	0.05984	0.05848	699.6	5.2	6.37
	61.263	0.06812	0.06644	699.6	7.6	8.24
	61.263	0.06812	0.06638	699.6	8.75	8.23
3095	61.263	0.07859	0.07635	699.6	12.5	10.9
	61.264	0.07853	0.07631	699.7	12.2	10.9
	61.264	0.08858	0.08474	699.7	31.6	13.65
	61.267	0.08767	0.08316	699.7	42.2	13.27
	61.274	0.11265	0.0911	699.8	266	18.7
3100	61.284	0.1152	0.090	700	320	18.9
	61.288	0.14195	0.09737	700	551	25.16
	61.298	0.14205	0.09679	700.2	564	25
3095	61.250	0.0723	0.06864	699.4	415	9.03
3090	61.250	0.0710	0.0683	699.4	24.9	8.827

Data for 10-mil-diameter Test Sections (Cont'd.)

Observed Data				Computed Results		
P	R_T	$\Delta V_{x/20}$	ΔV_R	T_∞	θ	q" x 10^{-4}
3095	61.256	0.1786	0.11023	699.5	772	35.838
3100	61.29	0.179	0.1098	700.2	785	35.778
3095	61.24	0.2185	0.1194	699.2	1074	47.492
3100	61.27	0.2202	0.120	699.8	1080	48.10
	61.29	0.2458	0.1263	700.1	1248	56.51
3120	61.34	0.247	0.1257	701.1	1277	56.52
3110	61.295	0.1657	0.1062	700.2	689	32.03
3115	61.31	0.1185	0.09121	700.5	344	19.676
	61.31	0.1179	0.09126	700.5	335	19.59
3110	61.302	0.14558	0.09591	700.4	449	23.1
3100	61.283	0.14549	0.09570	700	453	23.04
3110	61.30	0.212	0.11334	700.4	886	39.76
3125	61.337	0.2109	0.11365	701.1	866	39.67
3140	61.375	0.238	0.11845	701.9	1068	46.65
3150	61.396	0.2392	0.1181	702.3	1089	46.75
	61.403	0.2392	0.1178	702.4	1096	46.63
	61.402	0.1371	0.0933	702.4	390	21.17
3140	61.38	0.10094	0.0778	702	193	13.0
	61.377	0.10103	0.07797	701.9	192	13.04
	61.375	0.07831	0.06504	701.9	89.7	8.429
	61.386	0.07831	0.06508	702.1	88.6	8.434
3150	61.410	0.04565	0.04011	702.5	16.7	3.03
3160	61.43	0.02795	0.0248	703	4.2	1.147
3155	61.42	0.02796	0.0248	702.7	4.87	1.147
	61.416	0.01837	0.01633	702.7	2.2	0.496
3150	61.385	0.01418	0.01262	702.1	1.4	0.296
	61.404	0.02767	0.02457	702.4	3.8	1.125
	61.404	0.03924	0.03483	702.4	4.3	2.262
	61.396	0.03922	0.03482	702.3	4.2	2.26
3150	61.39	0.04944	0.0433	702.2	21	3.543
3140	61.387	0.06437	0.05522	702.1	47.3	5.883
	61.387	0.07769	0.06472	702.1	85.4	8.321
	61.39	0.09545	0.07529	702.1	160	11.893
	61.39	0.11842	0.08594	702.1	285	16.842

Data for 10-mil-diameter Test Sections (Cont'd.)

Observed Data				Computed Results		
P	R_T	$\Delta V_{x/20}$	ΔV_R	T_∞	θ	q" x 10^{-4}
	61.39	0.14537	0.0966	702.1	432	23.24
3150	61.403	0.1979	0.1096	702.4	800	35.89
	61.402	0.2246	0.1154	702.4	983	42.89
	61.40	0.0375	0.0332	702.4	7.55	2.06
3140	61.382	0.00935	0.00831	702	3.2	0.128
	61.376	0.03724	0.03305	701.8	5.2	2.04
	61.376	0.06578	0.05627	701.9	51.1	6.125
	61.379	0.07927	0.06567	701.9	93	8.615
3100	61.25	0.00863	0.00842	699.4	7.5	0.1322
	61.3	0.00863	0.00841	700	8.3	0.1321
3185	61.484	0.2432	0.0237	704	4.3	1.049
	61.487	0.03545	0.03433	704.1	12.0	2.215
3180	61.46	0.0353	0.03344	703.5	39.9	2.149
	61.46	0.04851	0.04643	703.6	27.1	4.1
3185	61.48	0.06777	0.06212	704	82.3	7.664
3180	61.44	0.08747	0.0757	703.2	162	12.05
3185	61.47	0.0563	0.05325	703.8	41.9	5.46
	61.47	0.0695	0.06368	703.8	83.1	8.06
	61.49	0.06933	0.06357	704.2	81.7	8.02
	61.48	0.11162	0.08649	704	330	17.57
3190	61.53	0.05186	0.04935	704.9	33.0	4.659
3185	61.50	0.150	0.09974	704.3	608	27.2
	61.49	0.1995	0.113	704.2	974	41.03
3190	61.51	0.251	0.1243	704.5	1359	56.8
3185	61.49	0.2038	0.11318	704.2	1025	42.0
3190	61.51	0.2040	0.11318	704.5	1027	42.0
3195	61.516	0.1195	0.08856	704.7	405	19.26
3190	61.515	0.8693	0.07433	704.6	178	11.76
3160	61.4	0.05198	0.04979	702.6	27	4.71
3185	61.512	0.02422	0.02358	704.6	4.9	1.04
	61.511	0.01683	0.01641	704.6	3.1	0.503
3000	60.80	0.00834	0.00816	690.3	13.2	0.1239
3180	61.48	0.06586	0.06056	704	78.2	7.26

Data for 10-mil-diameter Test Sections (Cont'd.)

Observed Data				Computed Results		
P	R_T	$\Delta V_{x/20}$	ΔV_R	T_∞	θ	q" x 10^{-4}
3210	61.485	0.1188	0.09085	711	345	19.65
3190	61.51	0.2808	0.1291	704.5	1615	66.0
	61.495	0.2258	0.11885	704.2	1174	48.85
3220	61.59	0.11177	0.0622	706.1	83.2	7.734
3225	61.60	0.1349	0.07165	706.3	146.5	10.75
3230	61.61	0.1648	0.0810	706.5	259	14.85
3225	61.59	0.1806	0.0850	706.1	327	17.08
	61.585	0.12406	0.06714	706.1	120	9.266
	61.592	0.10562	0.05936	706.1	69.5	6.974
	61.595	0.09217	0.0528	706.2	46.6	5.414
	61.60	0.07793	0.0453	706.3	26.6	3.927
3230	61.61	0.06315	0.03705	706.5	15.3	2.603
	61.61	0.05311	0.03135	706.5	8.01	1.852
3250	61.64	0.00844	0.0082	707.1	4.91	0.126
3245	61.62	0.03518	0.03408	706.7	8.9	2.18
3240	61.605	0.05594	0.05295	706.4	38.2	5.39
	61.591	0.09784	0.08079	706.1	228	14.39
	61.60	0.15365	0.1025	706.3	600	28.67
	61.606	0.06693	0.06143	706.4	78	7.48
	61.60	0.0188	0.01829	706.3	4	0.626
	61.60	0.2011	0.11275	706.3	998	41.28
3245	61.62	0.243	0.1205	706.7	1352	53.30
3250	61.63	0.10362	0.0818	706.9	297	15.43
3245	61.62	0.0335	0.0324	706.7	8.6	1.98
	61.616	0.01711	0.01665	706.6	3.4	0.519
3190	61.3	0.00852	0.0083	700.5	8.2	0.129
3320	61.801	0.1006	0.00592	710.3	4.7	0.0662
	61.796	0.1006	0.00592	710.2	5.8	0.0662
	61.796	0.014815	0.00872	710.2	4.5	0.1437
3315	61.792	0.02082	0.01225	710.1	5.05	0.284
	61.788	0.0266	0.01565	710.1	4.8	0.463

Test-section Length: 1.719 in.

Data for 10-mil-diameter Test Sections (Cont'd.)

Observed Data				Computed Results		
P	R_T	$\Delta V_{x/20}$	ΔV_R	T_∞	θ	q" x 10^{-4}
3270	61.715	0.009985	0.00589	708.7	3.4	0.0654
3285	61.726	0.02074	0.01223	708.9	3.6	0.282
3280	61.74	0.02659	0.01565	709.1	5.3	0.463
3360	61.72	0.0413	0.02428	708.7	7.8	1.116
3280	61.73	0.05415	0.03168	708.9	13.3	1.908
	61.73	0.07195	0.041605	708.9	27.9	3.33
3290	61.76	0.091525	0.05188	709.5	52.8	5.28
3280	61.745	0.09169	0.05195	709.2	54.3	5.305
3290	61.77	0.1159	0.06285	709.7	111.4	8.103
3295	61.78	0.1157	0.06286	709.9	110.8	8.08
3300	61.78	0.1652	0.07918	709.9	292	14.55
	61.795	0.1644	0.07917	710.2	284	14.48
3305	61.795	0.1913	0.08572	710.2	404	18.24
3310	61.806	0.1918	0.08573	710.4	408	18.29
	61.81	0.225	0.09264	710.5	562	23.187
	61.82	0.2215	0.09264	710.7	531	22.827
3315	61.825	0.259	0.09944	710.8	708	28.651
3320	61.84	0.2606	0.09944	711.1	721	28.828
3325	61.85	0.3371	0.11318	711.3	1031	42.44
	61.88	0.3375	0.11261	711.9	1049	42.279
3330	61.89	0.17735	0.08304	712	328	16.383
	61.886	0.1768	0.0830	712	360	16.324
3340	61.89	0.2583	0.1027	712.1	632	29.51
3345	61.92	0.261	0.101	712.7	688	29.32
3335	61.91	0.114	0.06197	712.5	105	7.86
	61.906	0.1139	0.06199	712.4	104	7.85
	61.905	0.0917	0.5178	712.3	55	5.28
3330	61.90	0.08512	0.4853	712.2	42.5	4.59
3335	61.897	0.06939	0.04007	712.2	26	3.093
3325	61.89	0.05025	0.2935	712.1	12.2	1.641
	61.885	0.02945	0.01730	712	5.2	0.567
3320	61.877	0.02946	0.01730	711.9	5.8	0.567
3380	61.8	0.00856	0.0083	710.7	3.8	0.1293
3390	61.93	0.03604	0.03453	712.9	16.5	2.265
	61.925	0.020	0.01935	712.8	4.4	0.7044
	61.924	0.05478	0.05164	712.8	37.1	5.15
	61.925	0.08352	0.0724	712.8	150	11.01

Test-section Length: 2.8125 in.

Data for 10-mil-diameter Test Sections (Cont'd.)

Observed Data				Computed Results		
P	R_T	$\Delta V_{x/20}$	ΔV_R	T_∞	θ	q" x 10^{-4}
3390	61.93	0.131	0.093	712.9	473	22.18
3395	61.938	0.1498	0.0981	713	631	26.75
	61.946	0.15198	0.09878	713.2	646	27.33
	61.942	0.05748	0.05354	713.1	52.2	5.60
3390	61.933	0.03502	0.03368	713	11.7	2.15
3385	61.926	0.02026	0.01958	712.8	5.76	0.722
	61.923	0.0748	0.0667	712.7	111	9.08
3395	61.936	0.202	0.11225	713	1015	41.28
3400	61.96	0.2427	0.12	713.5	1355	53.02
	61.95	0.01363	0.01318	713.3	4.6	0.327
3395	61.95	0.01363	0.01320	713.3	2.7	0.327
3625	62.1	0.00842	0.0081	716.9	7.42	0.124
3630	62.4	0.02472	0.02368	722.2	7.3	1.06
	62.447	0.03932	0.03744	723.2	13.9	2.68
	62.442	0.05631	0.05245	723.1	42.2	5.38
3625	62.437	0.0711	0.06393	723	89.1	8.27
	62.429	0.09164	0.0768	722.8	189	12.81
3620	62.416	0.12606	0.09229	722.6	408	21.18
3625	62.42	0.1495	0.0993	722.6	592	27.0
3630	62.44	0.1895	0.11136	723	863	38.4
3635	62.46	0.2307	0.1201	723.4	1186	50.4
3625	62.43	0.2544	0.1245	722.8	1379	57.65
	62.45	0.1252	0.0919	723.2	403	20.9
	62.436	0.0927	0.0775	723	192	13.08
	62.43	0.0744	0.0661	722.8	105	8.95
	62.42	0.043	0.0406	722.6	25.2	3.18
3615	62.2	0.024	0.02302	718.6	9.35	1.00
3610	62.0	0.017	0.01636	714.5	9.3	0.5063
3625	62.407	0.074	0.06615	722.4	97.6	8.91
	62.41	0.0467	0.04396	722.4	29.3	3.74
3630	62.44	0.2814	0.1303	723	1539	66.75
	62.45	0.04877	0.0457	723.2	34.3	4.06
	62.45	0.04882	0.04575	723.2	34.2	4.06

Test-section Length: 1.719 in.

Data for 10-mil-diameter Test Sections (Cont'd.)

Observed Data				Computed Results		
P	R_T	$\Delta V_{x/20}$	ΔV_R	T_∞	θ	q" x 10^{-4}
3930	62.868	0.00957	0.008295	731.6	4.31	0.131
3925	62.864	0.009515	0.00826	731.5	2.99	0.13
	62.862	0.00951	0.008253	731.5	3.01	0.1298
3930	62.87	0.02133	0.01845	731.6	7.27	0.65
	62.874	0.02132	0.018425	731.7	8.3	0.65
3920	62.873	0.03805	0.03271	731.7	16.9	2.05
	62.874	0.03804	0.03265	731.7	17	2.1
	62.854	0.05244	0.04446	731.3	33.1	3.85
	62.852	0.05242	0.0445	731.3	31.6	3.86
3925	62.852	0.0787	0.06359	731.3	97.3	8.28
	62.856	0.07869	0.06375	731.3	93.8	8.3
	62.856	0.09418	0.07291	731.3	158	11.37
3930	62.863	0.09405	0.07285	731.5	156	11.34
	62.867	0.11227	0.08167	731.5	252	15.1
	62.86	0.11237	0.08193	731.4	248	15.2
3925	62.86	0.13463	0.0904	731.4	385	20.1
	62.859	0.1354	0.09018	731.4	399	20.2
	62.856	0.1883	0.10493	731.3	757	32.7
3930	62.869	0.1850	0.1043	731.6	731	32.0
	62.875	0.2161	0.1111	731.7	952	39.7
3935	62.90	0.2174	0.1117	732.2	953	40.2
	62.902	0.1386	0.09191	732.3	406	21.1
3930	62.88	0.09255	0.07214	732	148	11.05
3935	62.873	0.09327	0.07205	731.6	160	11.1
	62.869	0.06623	0.05487	731.6	63.2	6.01
3930	62.861	0.06615	0.05486	731.4	62	6.0
3920	62.86	0.04962	0.04217	731.4	30	3.47
	62.86	0.04961	0.04217	731.4	29.6	3.47
	62.86	0.03849	0.033	731.4	18.7	2.11
	62.863	0.038495	0.0330	731.5	17.6	2.1
3925	62.863	0.02661	0.02295	731.5	11.1	1.02
	62.866	0.01898	0.01643	731.5	7.47	0.52
	62.866	0.009475	0.00821	731.5	5.15	0.13
3920	62.865	0.00948	0.008215	731.1	5.45	0.13
3925	62.865	0.03816	0.03276	731.5	16.9	2.05

Data for 10-mil-diameter Test Sections (Cont'd.)

Observed Data				Computed Results		
P	R_T	$\Delta V_{x/20}$	ΔV_R	T_∞	θ	q" x 10^{-4}
	62.866	0.03814	0.03268	731.5	19.4	2.05
	62.867	0.04835	0.04124	731.5	25.2	3.30
3930	62.874	0.04841	0.041225	731.7	27.1	3.3
	62.872	0.05818	0.049	731.7	41.6	4.72
	62.870	0.058	0.0489	731.6	39.9	4.695
	62.868	0.07924	0.0643	731.6	91.1	8.43
3925	62.866	0.0799	0.06424	731.5	104.2	8.495
	62.865	0.1488	0.09452	731.5	485	23.3
3930	62.881	0.14768	0.0952	731.8	457	23.3
3935	62.895	0.2374	0.11651	732.1	1076	45.8
3940	62.925	0.2346	0.116	732.7	1054	45
3930	62.890	0.2638	0.1205	732	1288	52.6
3940	62.922	0.2647	0.122	727	1259	53.4
	62.925	0.2624	0.1211	732.7	1255	52.6
	62.904	0.2853	0.1254	732.3	1413	59.2
3950	62.937	0.2846	0.1247	732.9	1422	58.7
3955	62.948	0.2847	0.1254	733.1	1404	59.1
3930	62.89	0.3057	0.1281	732	1580	64.8
3945	62.94	0.3051	0.1280	733	1575	64.6
3950	62.95	0.3035	0.12825	733.2	1548	64.4
	62.97	0.3161	0.131	733.6	1620	68.5
3965	63.01	0.31665	0.13115	734.4	1621	68.7
3915	62.84	0.3366	0.1347	731	1758	75
3920	62.85	0.335	0.1348	731.2	1736	74.7
	62.854	0.3351	0.1352	731.3	1724	75
	62.85	0.3344	0.1347	731.2	1732	74.5
3915	62.05	0.3371	0.1349	731.1	1758	75.2
	62.842	0.3357	0.1352	731	1733	75.1
	62.84	0.3351	0.1351	731	1728	74.9

Test-section Length: 1.891 in.

Data for $\frac{1}{4}$-in. Vertical Plate

Radiation Measurements

$\frac{1}{2}$	29.03	0.05564	0.1051	93.8	1425	0.553
	29.10	0.05534	0.1048	95	1418	0.5486
	29.30	0.06657	0.1178	98.6	1580	0.7418
	29.48	0.04509	0.09207	102	1247	0.3927
	29.64	0.04510	0.0919			

Data for $\frac{1}{4}$-in. Vertical Plate (Cont'd.)

Radiation Measurements

P	R_T	$\Delta V_{x/20}$	ΔV_R	T_∞	θ	$q'' \times 10^{-4}$
	29.695	0.03854	0.0835	105.5	1125	0.3044
	29.73	0.03096	0.073715	106.3	956	0.2159
	29.69	0.02409	0.063975	105.5	786	0.1458
	29.68	0.01755	0.05369	105.4	598	0.0892
	29.65	0.01084	0.04108	104.8	368	0.0421
	28.80	0.010755	0.04095	89.7	378	0.0417
	28.71	0.004423	0.02347	88.0	121	0.00982
	28.67	0.001383	0.00871	87.3	20.6	0.00114
	29.60	0.0703	0.1215	104	1589	0.808
	29.64	0.07076	0.122	104.5	1594	0.8166
$\frac{1}{2}$	29.69	0.07775	0.1297	105.5	1682	0.9538
	29.73	0.07773	0.12965	106.3	1681	0.9533
	29.48	0.0043	0.02282	102	95.2	0.00928
	29.43	0.001387	0.00862	101	4.61	0.0011
	29.45	0.08373	0.1362	101.3	1756	1.079
	29.53	0.0962	0.1426	102.7	1819	1.209
	29.68	0.09656	0.1499	105.4	1891	1.369
	29.80	0.10435	0.158	107.5	1968	1.559
	30.06	0.11296	0.1666	112.2	2050	1.78
	30.20	0.12213	0.1755	114.7	2138	2.028
	30.38	0.125	0.1785	118	2157	2.112
	30.85	0.1375	0.19055	126	2260	2.478
	31.00	0.13735	0.1904	129	2256	2.474
	61.51	0.00301	0.008904	704.5	17.1	0.00254
	61.54	0.006335	0.0183	705.1	46.5	0.011
	61.58	0.01567	0.04061	705.9	194	0.0602
	61.61	0.02975	0.0656	706.5	457	0.1846
	61.68	0.04236	0.08405	707.9	662	0.3368
	61.71	0.047935	0.0915	708.5	745	0.4149
	61.73	0.05935	0.1061	708.9	899	0.596
	61.76	0.07132	0.1202	709.5	1050	0.811
	61.75	0.003055	0.00899	709.3	18.9	0.0026
	61.73	0.0053275	0.01551	708.9	32.8	0.00782

Data for $\frac{1}{4}$-in. Vertical Plate (Cont'd.)

Radiation Measurements

Observed Data				Computed Results		
P	R_T	$\Delta V_{x/20}$	ΔV_R	T_∞	θ	$q'' \times 10^{-4}$
	61.72	0.0807	0.13095	708.7	1156	0.9997
	61.74	0.0926	0.14395	709.1	1283	1.261
	61.77	0.09957	0.1512	709.7	1356	1.424
	61.785	0.116085	0.1684	710	1509	1.849
	61.80	0.1261	0.1781	710.3	1605	2.125
	61.70	0.00387	0.0091	708.3	17.7	0.00265
	61.60	0.003083	0.009125	706.3	14.7	0.00266
0.001 x 0.250 x 2.078-in. Test Section						
	27.803	0.001377	0.00888	72	10	0.00116
	27.802	0.00181	0.011525	71.5	22.5	0.00198
	27.802	0.0109	0.04283	72	350.5	0.0442
	27.802	0.010885	0.04252	72	355	0.0438
	27.805	0.03105	0.07345	72	944	0.2158
	27.84	0.05618	0.10395	73	1455	0.551
	27.90	0.082865	0.1334	73.5	1813	1.046
0.001 x 0.250 x 2.078-in. Test Section						

Nucleate and Film Boiling Measurements

1.5	30.207	0.00519	0.01319	115.2	1.9	0.0125
	30.2176	0.0136	0.0359	115	4.2	0.0918
	30.221	0.01417	0.03567	114.8	7.6	0.09217
	30.221	0.0171	0.0354	114.8	9.1	0.0923
	30.221	0.01749	0.04402	114.8	9.3	0.1404
	30.235	0.02695	0.06689	115.3	18	0.3287
	30.25	0.03823	0.09369	115.5	25.8	0.6531
	30.256	0.05616	0.1339	115.6	43.5	1.371
	30.242	0.0792	0.1853	115.4	50	2.676
	30.235	0.1278	0.29695	115.3	68	6.920
	30.25	0.10525	0.2448	115.5	50	4.698
	30.236	0.1279	0.3012	115.3	59.5	10.25
	30.154	0.1549	0.36225	114.7	175	10.23
	30.192	0.161	0.364	114.9	220	10.98
	30.243	0.1632	0.3643	115.4	350	11.17
0.001 x 0.125 x 2.218-in. Test Section						

Data for $\frac{1}{4}$-in. Vertical Plate (Cont'd.)

Nucleate and Film Boiling Measurements

Observed Data				Computed Results		
P	R_T	$\Delta V_{x/20}$	ΔV_R	T_∞	θ	$q'' \times 10^{-4}$
42	38.792	0.0158	0.04151	270.7	5.5	0.0674
	38.795	0.0157	0.04149	270.7	4.4	0.0673
	38.797	0.013885	0.05448	270.75	6.2	0.116
	38.833	0.021875	0.085605	271.4	8.5	0.2872
	38.836	0.03922	0.15251	271.5	17	0.9175
	38.872	0.0563	0.2183	271.7	19.4	1.234
	38.89	0.08384	0.3237	272.5	21.5	4.163
	38.93	0.12611	0.4791	273.2	31.5	9.268
	38.98	0.1260	0.477	274.1	36.1	9.221

0.001 x 0.250 x 2.5625-in. Test Section

Data for $\frac{1}{8}$-in. Vertical Plate

2440	59.48	0.1293	0.1211	664.4	13	4.106
	59.486	0.12904	0.12105	664.5	14.2	4.094
	59.484	0.00885	0.00841	664.5	0.5	0.0195
	59.477	0.02029	0.01921	664.3	3.1	0.1022
	59.474	0.03727	0.03512	664.3	8.5	0.3432
	59.46	0.06839	0.0643	664	11	1.153
	59.454	0.09824	0.09228	663.9	12	2.376
	59.48	0.1415	0.1328	664.4	13.2	4.926
2470	59.64	0.1919	0.1795	667.5	14	9.031
	59.66	0.192	0.1795	667.9	15	9.033
2450	59.51	0.2816	0.2632	665	17	19.43
2460	59.58	0.28115	0.2628	666	16	19.367
2800	60.484	0.0089	0.00831	684.2	0.6	0.0196
	60.492	0.0277	0.02562	684.4	4	0.186
	60.505	0.048	0.04432	684.6	5	0.5578
	60.515	0.0478	0.04417	684.8	3.35	0.5535
	60.530	0.07112	0.06565	685.1	4.5	1.224
2810	60.542	0.09105	0.08408	685.3	3.9	2.01
	60.538	0.113475	0.10473	685.3	5.2	3.115
	60.538	0.1411	0.130275	685.3	4.5	4.82
	60.542	0.14101	0.13017	685.3	4.4	4.81
2800	60.510	0.1758	0.1627	684.7	4.5	7.50

Data for $\frac{1}{8}$-in. Vertical Plate (Cont'd.)

Nucleate and Film Boiling Measurements

Observed Data				Computed Results		
P	R_T	$\Delta V_{x/20}$	ΔV_R	T_∞	θ	$q'' \times 10^{-4}$
	60.520	0.1755	0.16195	684.9	5.5	7.45
2810	60.54	0.2233	0.2063	685.3	4.6	12.08
2815	60.58	0.25915	0.2386	686.1	6.1	16.21
2825	60.61	0.2813	0.259	686.7	7.5	19.10
2810	60.54	0.29215	0.269	685.3	8.5	20.6
2825	60.60	0.36465	0.21575	686.5	730	20.62
2830	60.64	0.4051	0.2274	687.3	875	24.14
	60.65	0.3428	0.221	687.5	640	18.1
0.0005 x 0.125 x 1.50-in. Test Section						
2990	61.01	0.009579	0.0083	694.6	1.8	0.0417
2995	61.00	0.00956	0.00829	694.5	3	0.0416
2995	61.06	0.03825	0.03305	695.1	3.7	0.6636
	61.05	0.0384	0.03309	695	4.3	0.667
	61.05	0.1545	0.1318	695.1	8.2	10.47
	61.03	0.1674	0.1433	694.8	12	12.15
3000	61.05	0.183	0.129	695.4	280	9.25
3005	61.065	0.1857	0.131	695.6	300	10.95
	61.075	0.178	0.172	695.8	222	8.7
3010	61.081	0.712	0.125	696	165	8.1
	61.075	0.167	0.121	695.8	65	6.9
3025	61.063	0.1107	0.1554	697	9	2.92
	61.095	0.01758	0.02507	697	1.3	0.0803
	61.089	0.0394	0.05583	697	3.6	0.401
	61.083	0.0754	0.1064	697	7.25	1.465
	61.081	0.1095	0.15405	697	8.2	3.07
	61.081	0.1385	0.19497	697	8.4	4.92
	61.082	0.18263	0.2569	697	9.3	8.56
	61.088	0.21315	0.25175	697	245	9.75
3030	61.11	0.232	0.26275	697.5	310	11.1
3035	61.13	0.2461	0.2715	698	320	11.25
	61.155	0.18345	0.2281	698.5	170	7.62
	61.170	0.1649	0.21165	698.5	135	6.34
	61.172	0.164	0.2108	699	125	6.25
	61.173	0.1111	0.1561	699	8.3	3.06

Data for $\frac{1}{8}$-in. Vertical Plate (Cont'd.)

Nucleate and Film Boiling Measurements

Observed Data				Computed Results		
P	R_T	$\Delta V_{x/20}$	ΔV_R	T_∞	θ	$q'' \times 10^{-4}$
	61.11	0.00605	0.00854	697.5	1.3	0.0094
	61.09	0.01086	0.01531	697	0.4	0.0303
	61.083	0.1743	0.2453	697	8.9	7.7
3100	61.312	0.26945	0.03775	700.6	2.4	0.1855
	61.312	0.00616	0.00866	700.6	0.45	0.00973
	61.311	0.03913	0.05485	700.6	4	0.3914
	61.312	0.059	0.08275	700.6	5.8	0.8903
	61.314	0.0819	0.1150	700.6	8.1	1.717
3120	61.333	0.10905	0.15285	701	9.3	3.04
	61.34	0.1403	0.18575	701.1	8.7	4.752
3125	61.35	0.1802	0.2236	701.4	170	7.34
	61.37	0.17935	0.2230	701.7	167	7.29
3130	61.40	0.2422	0.2656	702.3	361	11.73
3125	61.35	0.2522	0.2717	701.4	392	12.49
	61.38	0.1976	0.2371	701.9	220	8.54
	61.32	0.18325	0.22625	700.8	178	7.56
3130	61.395	0.2724	0.2817	702.2	464	14
	61.38	0.31175	0.2994	701.9	606	17.02
3160	61.40	0.007525	0.0106	702.4	0.2	0.0145
3170	61.467	0.00754	0.010615	703.7	0.3	0.0145
	61.472	0.01726	0.0243	703.8	1.8	0.0763
	61.468	0.00619	0.008695	703.7	0.4	0.0098
	61.455	0.02662	0.0373	703.4	4	0.1811
	61.45	0.019	0.02668	703.3	3	0.0924
	61.454	0.031565	0.0442	703.4	5	0.2544
	61.462	0.03942	0.05518	703.6	5.22	0.3967
	61.455	0.046645	0.06519	703.4	6.9	0.5545
	61.458	0.05955	0.08334	703.5	7.1	0.905
	61.4585	0.07385	0.1033	703.5	8.2	1.391
	61.455	0.08935	0.12385	703.4	20.7	2.018
	61.456	0.1147	0.15625	703.5	42.5	3.268
	61.46	0.140	0.1858	703.5	76	4.743

Data for $\frac{1}{8}$-in. Vertical Plate (Cont'd.)

Nucleate and Film Boiling Measurements

Observed Data				Computed Results		
P	R_T	$\Delta V_{x/20}$	ΔV_R	T_∞	θ	$q'' \times 10^{-4}$
3175	61.47	0.1776	0.2216	703.7	160	7.177
	61.476	0.21315	0.24835	703.8	262	9.65
3180	61.475	0.1879	0.2307	703.8	183	7.905
	61.49	0.2702	0.2781	704.1	470	13.7
3185	61.50	0.313	0.2979	704.3	622	1.70
3180	61.485	0.2122	0.2475	704.1	260	9.58
3175	61.46	0.01794	0.025135	703.6	3.8	0.0822
3170	61.45	0.0061	0.00856	703.4	1.4	0.0095
3205	61.54	0.00605	0.00849	705.1	0.1	0.00937
	61.54	0.006068	0.008502	705.1	0.6	0.0094
3210	61.583	0.006083	0.008523	706	0.08	0.00945
	61.582	0.00609	0.008523	706	1	0.00946
	61.560	0.010337	0.014465	705.5	1.8	0.0272
	61.551	0.07495	0.1046	705.4	7.2	1.43
	61.557	0.07472	0.10393	705.5	11	1.416
	61.562	0.07442	0.10367	705.6	9.3	1.407
	61.558	0.005996	0.0840	705.5	0.4	0.0092
	61.56	0.11325	0.1545	705.5	31	3.191
	61.561	0.11302	0.1539	705.6	34	3.172
	61.57	0.13985	0.1855	705.7	37	4.731
	61.565	0.01466	0.02058	705.6	2.2	0.055
	61.557	0.0262	0.03665	705.5	4.2	0.175
	61.55	0.0396	0.05535	705.3	5.6	3.997
3205	61.543	0.05312	0.0742	705.2	6.5	0.7187
	61.538	0.06815	0.0949	705.1	10.3	1.179
	61.533	0.08776	0.12168	705	15.2	1.947
	61.546	0.1397	0.18513	705.2	75	4.716
3210	61.562	0.1395	0.18486	705.6	71	4.702
	61.562	0.1052	0.1440	705.6	31	2.762
	61.560	0.17665	0.22275	705.5	140	7.175
3215	61.59	0.3079	0.2962	706.1	500	16.63
3210	61,57	0.21305	0.2505	705.7	240	9.732
3195	61.52	0.02685	0.037545	704.7	5.5	0.1838
	61.515	0.007227	0.01013	704.6	0.5	0.01335

Data for $\frac{1}{8}$-in. Vertical Plate (Cont'd.)

Nucleate and Film Boiling Measurements

Observed Data				Computed Results		
P	R_T	$\Delta V_x/_{20}$	ΔV_R	T_∞	θ	q" x 10^{-4}
3255	61.67	0.00616	0.008625	707.7	.5	0.00969
3260	61.68	0.01273	0.0178	707.9	2.85	0.0413
3255	61.675	0.027	0.03773	707.8	5.7	0.1857
3260	61.678	0.0405	0.0564	707.9	9.5	0.4165
	61.68	0.0528	0.07364	707.9	8.5	0.709
	61.68	0.0675	0.09383	707.9	12.6	1.155
	61.68	0.0895	0.12375	707.9	19.3	2.02
	61.68	0.11196	0.1524	707.9	39	3.111
	61.69	0.1407	0.18615	708.1	76	4.776
3255	61.67	0.2202	0.2527	707.1	281	10.15
3260	61.683	0.1751	0.220	707.9	146	7.025
3265	61.69	0.3133	0.29605	708.1	632	16.91
	61.562	0.1395	0.18486	708.3	899	22.13
3270	61.73	0.40415	0.3247	708.9	1009	23.93
3400	62.018	0.0057	0.01052	714.6	1.25	0.0145
	62.015	0.01823	0.02535	714.6	2.1	0.0842
	62.008	0.02711	0.0376	714.4	5.4	0.1859
	61.998	0.0407	0.05642	714.2	8.8	0.419
	61.996	0.06185	0.08536	714.2	13.7	0.962
	61.996	0.08275	0.1139	714.2	18.9	1.719
	61.996	0.11135	0.1506	714.2	41	3.058
	62.00	0.1458	0.1910	714.2	83	5.078
	62.01	0.1855	0.2275	714.5	174	7.695
3410	62.03	0.3208	0.300	714.9	647	17.55
	62.01	0.23115	0.25735	714.5	324	10.85
3415	62.04	0.393	0.3253	715.1	927	23.31
3400	61.97	0.00684	0.0095	713.7	1.9	0.01185
3420	62.06	0.4734	0.3497	715.5	1240	30.19
3390	61.964	0.039915	0.05525	713.6	11.5	0.4021
3425	62.10	0.511	0.361	716.3	1379	33.64
	62.09	0.0767	0.1058	716.1	14	1.48

Data for $\frac{1}{8}$-in. Vertical Plate (Cont'd.)

Nucleate and Film Boiling Measurements

Observed Data				Computed Results		
P	R_T	$\Delta V_{x/20}$	ΔV_R	T_∞	θ	$q'' \times 10^{-4}$
3630	62.561	0.00618	0.008545	725.4	0.7	0.00963
	62.55	0.02768	0.03827	725.2	2.1	0.193
	62.536	0.047315	0.0651	725	7.8	0.562
3625	62.524	0.0688	0.09448	724.7	11.1	1.185
	62.515	0.09123	0.1245	724.5	19.1	2.071
3625	62.512	0.1449	0.18925	724.5	77	5.00
3620	62.510	0.1129	0.15185	724.4	38	3.126
3625	62.515	0.1868	0.2294	724.5	162	7.814
3630	62.525	0.2567	0.2717	724.7	400	12.718
3635	62.57	0.3732	0.3188	725.6	839	21.695
3630	62.55	0.5068	0.3638	725.2	1319	33.62
3640	62.46	0.0833	0.1134	723.4	23.4	1.72
3620	62.43	0.01804	0.02505	722.8	0.5	0.0824
3615	62.41	0.006065	0.00839	722.4	2.5	0.00928

0.001 x 0.125 x 2.218-in. Test Section

APPENDIX C

PHYSICAL PROPERTIES

The graphical plots of Nowak[72,73] based on experimental data were interpolated to evaluate the specific heat, thermal conductivity, and viscosity of water in regions near the critical pressure where no data are available.

Values and predictions of surface tension for saturated liquid water are plotted in Figure 41. The curve due to Volyak[95] was used in evaluating equation (2) due to Kutateladze.[54] The curve due to Sato[85] was used in evaluating the correlation of Nishikawa.[71] Note that the prediction of Macleod[60] agrees quite well with all the data. This prediction (dashed line in Figure 41) was used for all other surface tension values.

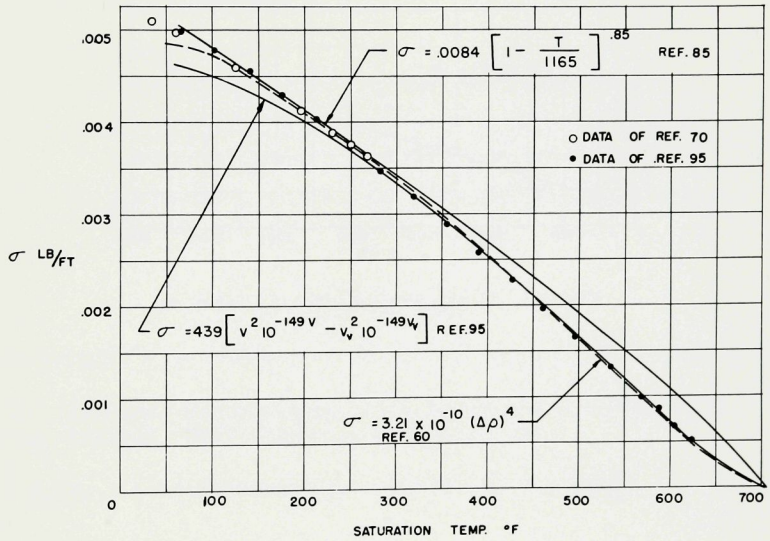

Fig. 41. Surface Tension of Saturated Liquid Water

The result of the qualitative investigation of the electrical conductivity of saturated liquid water is indicated in Figure 42. No data were found for water above 150°F, and the curve was plotted from the following equation[21,38,39,70]:

$$\text{Electrical Conductivity} = (\Lambda_H + \Lambda_{OH})\,\rho\,\sqrt{K}/1000 \text{ ohm cm}^{-1} \quad . (27)$$

The equivalent conductance Λ and the ionization constant K were obtained from reference 21, p. 374-380; reference 39, p. 646; and reference 38, p. 2608. The density ρ is for the saturated liquid water.

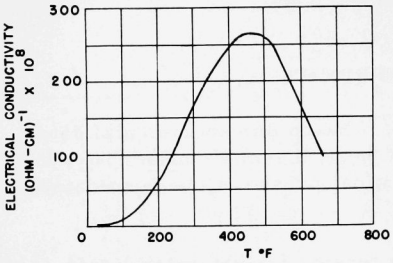

Fig. 42

Predicted Electrical Conductivity of Pure Saturated Liquid Water

The values of emissivity for platinum that were used in the computations were taken from the curve in Figure 43.

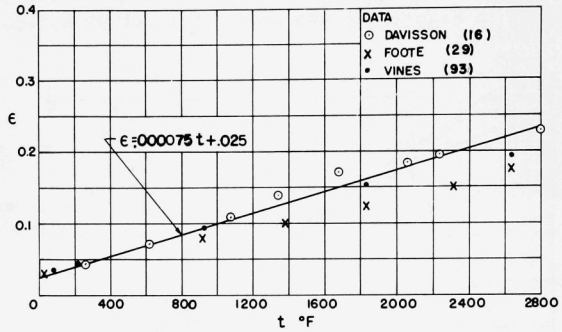

Fig. 43. Total Emissivity of Platinum

APPENDIX D

LIST OF EQUIPMENT

Control

Pressure vessel: 1 ea. modified American Instrument Company #41-6130 type 316 stainless steel, cold tested at 8325 psi, Serial No. D 5514

Vacuum pump: 1 ea. Central Scientific Co. Hyvac, Serial No. EF 6931

Powerstat transformers: Superior Electric Co.

3 ea. 220-volt, 7.5 kva

3 ea. 110-volt, 2 kva

2 ea. 110-volt, 1 kva

Direct-current power supply:

13 ea. 6-volt storage batteries, 100 amp-hour rating

1 ea. Westinghouse Elect. Corp. 1.5-hp, 220-volt induction motor, Serial No. 138/36339

1 ea. Bendix Corp. aviation generator, model 31, 30-volt, 50-amp, Serial No. 432004

Measurement

Mueller bridge: 1 ea. Minneapolis Honeywell Corp. #1551, Serial No. 106272

Platinum resistance thermometer: 1 ea. Leeds and Northrup #8163, Serial No. 1331403. NBS calibration tabulated from:

$$R_t/R_0 = 1 + 0.00392609\, t\, [1 + 0.014916\{1 - (t/100)\}]$$

where

R_0 = 25.554 abs ohms at 0°C

t = temperature, °C

Temperature recorder: 1 ea. Leeds and Northrup Co. Micromax 6-point recorder, Serial No. 575566.

Kelvin bridge: 1 ea. Otto Wolff, Berlin, Serial No. 3614.

Potentiometer: Leeds and Northrup Co.

1 ea. Type K-2, Serial No. 72301

1 ea. Type 8662, Serial No. 671025

Volt box: 1 ea. Leeds and Northrup Co., #7591, multiplies two to 500 times, $\pm$ 0.04%, Serial No. 767110

Pressure gauge: 1 ea. Heise Corp. 0-4000 psi, Serial No. H-22875C.

Dead-weight tester: 1 ea. Ashcroft 0-5000 psi within 1 psi, Type 13053-50, Serial No. 1 DX 24456.

Galvanometer: 1 ea. Leeds and Northrup Co., #2430-A, 14-ohm coil, Serial No. 1546459.

Water cooled resistors: Forsythe, Central Scientific Co.

1 ea. 25 amp, 5.5 ohms

1 ea. 50 amp, 1.5 ohms

Standard resistances: Leeds and Northrup Co.

1 ea. 0.01006 ohm abs. #4222, Serial No. 761432

1 ea. 0.10005 ohm abs. #4221, Serial No. 761430

1 ea. 1.0001 ohms abs., Serial No. 1054826

1 ea. 0.0009949 ohm abs. Weston 50-amp, 50-mv shunt

Panel Meters: Triplett 3-in. size

2 ea. 50 amp DC

2 ea. 50-volt DC

1 ea. 150 ma DC

1 ea. 50 ma DC

1 ea. 10 ma DC

Thermocouple Switches: Leeds and Northrup Co.

3 ea. DPDT-plated switch

1 ea. 10-point selector switch

Resistors: 7 ea. 10-ohm, 200-watt

Latching Relays: 7 ea. Potter and Brumfield 10-amp contacts, 110 v.

Equiphase triple-point temperature reference cell: 1 ea. Transonics Corp. Type 130, Serial No. 21935, triple point temperature, 0.01°C.

Synthetic sapphire: Linde Air Products Co., ends optically finished.

3 ea. 5/16-in. dia by 7-in.-long rods

2 ea. 3/4-in. dia by 1/2-in. cylinders

Cathetometer: 1 ea. Gaertner Scientific Co. Serial No. 8-0-A

Capacitor discharge: 1 ea. Unitek Corp. Weldmatic, Model 1016 B welder, Serial No. 16 B 1248.

Resistance welder: Eisler Engineering Co. Serial No. 7998-93 RA.

APPENDIX E

Method of Calibration and Measurement

The reference resistance of the test section at 32°F was obtained by the method used in the following example:

1) First, the bulk fluid pressure and temperature desired for the particular test were achieved (for example, 14.7 psia and 212°F).

2) A calibration current of approximately 100 ma was passed through the 10-mil-diameter test section.

3) The following readings were taken:

   a) thermometer resistance R_T = 35.5925 ohms

   b) Kelvin bridge reading = 194.6

   c) standard resistance voltage drop ΔV_R = 0.011767 volt

   d) test-section voltage drop ΔV_x = 0.022901 volt

   e) pressure = atmospheric

4) The following calculations were performed:

   a) $R_T/R_0 = 35.5925/25.554 = 1.39283$,

   where the resistance of the thermometer at 0°C was 25.554 ohms.

   b) the test-section resistance as measured with the Kelvin bridge was

$$R_x = \frac{\text{bridge reading} \times R_{std}}{\text{fixed-arm resistance}}$$

$$= \frac{194.6\ (1.0005)}{100}$$

$$= 0.1947 \text{ ohm}$$

   c) the test-section resistance as determined from voltage measurements was

$$R_x = \frac{\Delta V_x}{I} = \frac{\Delta V_x R_{std}}{\Delta V_R} = \frac{(0.022901)(0.10005)}{0.011767}$$

$$= 0.19472 \text{ ohm.}$$

d) Assuming that the temperature of the fluid and the test section are the same,

$$R_x/R_0 = 1.39283 = 0.19472/R_0$$

or

$$\underline{\underline{R_0 = 0.1398}} \text{ ohm, resistance of the test section at } 0°C.$$

This reference resistance obtained from measurements was checked by packing the test section in pure flaked ice and measuring its resistance. Also, the resistivity at 0°C was calculated and compared with tabulated values for platinum as an additional check. For the case just calculated,

$$\rho_0 = R_0 A_x/L = \frac{0.1398(0.7854)2.54}{2\frac{13}{16} \times 10^4}$$

$$= 9.92 \times 10^{-6} \text{ ohm-cm} \quad ,$$

which compared favorably with typical values of resistivity.(93)

It was concluded that the most representative value for the reference resistance of the test section at 0°C was obtained from the measurements made at the particular test conditions. Also, the NBS calibration report of tabulated resistance ratios for the resistance thermometer was found to be applicable for the purpose of this investigation.

Method of Computation

The data tabulated in Appendix B were expressed in terms of the heat flux q" and the temperature difference θ by the procedure illustrated in the following example:

1) measured data -

$R_T = 35.5920$ ohms

$\Delta V_x = 20\ (0.11475) = 2.295$ volts (volt box multiplier = 20)

$\Delta V_R = 0.11277$ volts

P = atmospheric

2) calculated results -

a) fluid temperature -

$R_T/R_0 = 35.592/25.554 = 1.39281$ from the NBS resistance thermometer calibration:

$$t = 6{,}155.636 - 1{,}536.802\sqrt{15.8775 - 2.3425\left(\frac{R_T}{R_0} - 1\right)} \tag{28}$$

$$t = 212.1°F$$

b) test-section temperature -

$R_0 = 0.1398$ ohm, from previous section

$$\frac{R_x}{R_0} = \frac{\Delta V_x R_{std}}{\Delta V_R R_0} = \frac{2.295\ (0.010006)}{0.11277\ (0.1398)}$$

$$= 1.45661$$

$t = 241.9°F$ from equation (28)

c) heat flux q" -

$$q" = \frac{3.413\ \Delta V_x\ \Delta V_R}{A R_{std}} = \frac{3.413\ (2.295)\ (0.11277)}{0.0006136\ (0.010006)}$$

$$= 1.438 \times 10^5\ BTU/(hr)\,(ft^2)$$

d) temperature difference θ -

$$\theta = T_w - T_\infty = 241.9 - 212.1 = 29.8°F.$$

e) heat transfer coefficient h -

$$h = q"/\theta = 1.438 \times 10^5/29.8$$

$$= 4830\ BTU/(hr)\,(ft^2)\,(°F).$$

The data were reduced by this procedure with the aid of the Purdue University Datatron 204 computer. The measured data were recorded directly on computer work sheets in the form required for card punching.

Error Analysis

The approximate accrued error in the determination of the heat transfer rates and temperature differences was estimated by considering two specific cases. The first case was for one of the lower nucleate boiling heat fluxes, and the second case was for one of the higher nucleate

boiling heat fluxes. Both cases were taken for 2800 psia, at which the smallest temperature differences were measured; thus, measurements made at other pressures should be subject to less error.

The per cent error in heat flux determination was calculated by considering

$$q'' = 3.413 \frac{V_x I}{A} = 3.413 \frac{V_x}{A} \frac{V_R}{R_{std}} .$$

$$\left|\frac{\Delta q''}{q''}\right| = \left|\frac{\Delta V_x}{V_x}\right| + \left|\frac{\Delta V_R}{V_R}\right| + \left|\frac{\Delta R}{R_{std}}\right| + \left|\frac{\Delta A}{A}\right|$$

+ voltage-tap conduction losses.

For 2800 psia with $q'' = 2 \times 10^3$ BTU/(hr)(ft^2),

$$\left|\frac{\Delta q''}{q''}\right| < 0.001 + 0.001 + 0.0001 + 0.01 + 0.01 = \underline{2.21\%}.$$

For 2800 psia with $q'' = 10^5$ BTU/(hr)(ft^2),

$$\left|\frac{\Delta q''}{q''}\right| < 0.001 + 0.001 + 0.0001 + 0.01 + 0.02 = \underline{3.21\%}.$$

The per cent error in the determination of the temperature difference was calculated by considering

$$\left|\frac{\Delta\theta}{\theta}\right| = \left|\frac{\Delta T_w - \Delta T_\infty}{T_w - T_\infty}\right| = \left|\frac{\Delta T_w}{\theta}\right| + \left|\frac{\Delta T_\infty}{\theta}\right| .$$

For 2800 psia with $q'' = 2 \times 10^3$ BTU/(hr)(ft^2),

$$\left|\frac{\Delta\theta}{\theta}\right| < \frac{0.1 + 0.05}{3.5} = 4.3\%.$$

For 2800 psia with $q'' = 10^5$ BTU/(hr)(ft^2),

$$\left|\frac{\Delta\theta}{\theta}\right| < \frac{0.15 + 0.05}{5.4} = 3.7\%.$$

Note that some of the errors estimated above were constant throughout a particular test and did not contribute to data scatter. Also, the errors were estimated for the most unfavorable pressure. The measurements of film boiling temperature differences were subject to a smaller per cent error than calculated for the nucleate boiling cases considered above.